U.S. Department
of Commerce

Volume 120
Number 3–4
July–October 2022

Fishery Bulletin

Pacific Islands Fisheries
Science Center Library

Received on: 1/23

U.S. Department of Commerce

Gina M. Raimondo
Secretary

National Oceanic and Atmospheric Administration

Richard W. Spinrad
Administrator

National Marine Fisheries Service

Janet Coit
Assistant Administrator
for Fisheries

Fishery Bulletin

Scientific Editor
José I. Castro
National Marine Fisheries Service, NOAA
263 13th Avenue South
Saint Petersburg, Florida 33701

Managing Editor
Kathryn Dennis
Scientific Publications Office
National Marine Fisheries Service, NOAA
1845 Wasp Boulevard, Building 176
Honolulu, Hawaii 96818

Associate Editor
Cara Mayo
Scientific Publications Office
National Marine Fisheries Service, NOAA
7600 Sand Point Way NE
Seattle, Washington 98115-0070

Editorial Board

Henry L. Bart Jr.	Tulane University, New Orleans, Louisiana
Katherine E. Bemis	National Systematics Laboratory, Washington, DC
Matthew D. Campbell	National Marine Fisheries Service, Pascagoula, Mississippi
William B. Driggers III	National Marine Fisheries Service, Pascagoula, Mississippi
Gretchen L. Grammer	South Australian Research and Development Institute, Adelaide, Australia
Richard Langton	National Marine Fisheries Service, Walpole, Maine (retired)
J. Fernando Márquez-Farías	Universidad Autónoma de Sinaloa, Mazatlán, México
Richard S. McBride	National Marine Fisheries Service, Woods Hole, Massachusetts
Richard L. Merrick	National Marine Fisheries Service, Falmouth, Massachusetts (retired)
Richard D. Methot	National Marine Fisheries Service, Seattle, Washington
Lisa J. Natanson	National Marine Fisheries Service, Narragansett, Rhode Island (retired)
Mark S. Peterson	University of Southern Mississippi, Ocean Springs, Mississippi
André E. Punt	University of Washington, Seattle, Washington
Joseph M. Quattro	University of South Carolina, Columbia, South Carolina
John F. Walter III	National Marine Fisheries Service, Miami, Florida

***Fishery Bulletin* website: https://spo.nmfs.noaa.gov/fb.htm**

Fishery Bulletin (ISSN 0090-0656) is published quarterly by the Scientific Publications Office, National Marine Fisheries Service, NOAA, 7600 Sand Point Way NE, Seattle, WA 98115-0070.

Although the contents of this publication have not been copyrighted and may be reprinted entirely, reference to source is appreciated.

The Secretary of Commerce has determined that the publication of this periodical is necessary according to law for the transaction of public business of this Department. Use of funds for printing of this periodical has been approved by the Director of the Office of Management and Budget.

For Sale by the Superintendent of Documents, U.S. Government Publishing Office, Washington, DC 20401. Subscription price per year: $32.00 domestic and $44.80 foreign. Cost per single issue: $19.00 domestic and $26.60 foreign. **See back for order form.**

Fishery Bulletin carries original research reports on investigations in fishery science, engineering, and economics. It began as the Bulletin of the United States Fish Commission in 1881; it became the Bulletin of the Bureau of Fisheries in 1904 and the *Fishery Bulletin* of the U.S. Fish and Wildlife Service in 1941. Separates were issued as documents through volume 46; the last document was no. 1103. Beginning with volume 47 in 1931 and continuing through volume 62 in 1963, each separate appeared as a numbered bulletin. A new system began in 1963, with volume 63, in which papers are bound together in a single issue. Beginning with volume 70, number 1, January 1972, *Fishery Bulletin* became a periodical, issued quarterly. In this form, it is available by subscription from the Superintendent of Documents, U.S. Government Publishing Office, Washington, DC 20401. It is also available free in limited numbers to libraries, research institutions, and state and federal agencies and in exchange for other scientific publications.

U.S. Department of Commerce
Seattle, Washington

Volume 120
Number 3–4
July–October 2022

Fishery Bulletin

Contents

Articles

195–204 **Marcus A. Zokan, David M. Wyanski, D. Byron White, and George R. Sedberry**

Life history of the spotted moray (*Gymnothorax moringa*) off the Atlantic coast of the southeastern United States: age, growth, and reproduction

205–217 **J. Fernando Márquez-Farías, L. Daniel Carrillo-Colín, Allan Rosales-Valencia, Raúl E. Lara-Mendoza, and Oscar G. Zamora-García**

Bayesian estimation of the age and growth of the round stingray (*Urobatis halleri*) in the Gulf of California in Mexico

218–233 **Kelly S. Boyle, Crystal L. Hightower, and Sean P. Powers**

Evaluation of factors contributing to postrelease mortality of greater amberjack (*Seriola dumerili*) in the northern Gulf of Mexico with depth and acceleration data from acoustic tags

Note

234–239 **Andrew T. Chin, Morgan H. Bond, and Thomas P. Quinn**

Life history differences between 2 anadromous populations of the northern form of the Dolly Varden (*Salvelinus malma malma*) in Bristol Bay in southwestern Alaska

Articles

240–251 **Cameron T. Hodgdon, Noah S. Khalsa, Mackenzie D. Mazur, and Yong Chen**

Climate-driven changes in growth and size at maturity of Gulf of Maine lobster stocks: implications for stock assessment models

The National Marine Fisheries Service (NMFS) does not approve, recommend, or endorse any proprietary product or proprietary material mentioned in this publication. No reference shall be made to NMFS, or to this publication furnished by NMFS, in any advertising or sales promotion that would indicate or imply that NMFS approves, recommends, or endorses any proprietary product or proprietary material mentioned herein or that has as its purpose an intent to cause directly or indirectly the advertised product to be used or purchased because of this NMFS publication.

The NMFS Scientific Publications Office is not responsible for the contents of the articles.

252–267 **Amy Zimney and Tracey Smart**

Effects of incomplete sampling and standardization on indices of abundance from a fishery-independent trawl survey off the Atlantic coast of the southeastern United States

268–276 **Tu T. C. Phan, Albert V. Manuel, Naoaki Tsutsui, and Takao Yoshimatsu**

Effects of salinity and turbidity on development of bamboo sole (*Heteromycteris japonicus*)

277 **Acknowledgment of reviewers**

279–282 **Guidelines for authors**

National Marine Fisheries Service
NOAA

Fishery Bulletin
established in 1881

Spencer F. Baird
First U.S. Commissioner of Fisheries and founder of *Fishery Bulletin*

Bayesian estimation of the age and growth of the round stingray (*Urobatis halleri*) in the Gulf of California in Mexico

J. Fernando Márquez-Farías[1]
L. Daniel Carrillo-Colín[2]
Allan Rosales-Valencia[1]
Raúl E. Lara-Mendoza[3]
Oscar G. Zamora-García (contact author)[4]

Email address for contact author: ozamora@sirbaa.com

[1] Facultad de Ciencias del Mar
Universidad Autónoma de Sinaloa
Paseo Claussen s/n
Colonia Los Pinos
82000 Mazatlán, Sinaloa, Mexico

[2] Posgrado en Ciencias del Mar y Limnología
Universidad Nacional Autónoma de Mexico
Avenida Ciudad Universitaria 3000
04510 Coyoacán, Ciudad de Mexico, Mexico

[3] Dirección General Adjunta de Investigación Pesquera en el Atlántico
Instituto Nacional de Pesca y Acuacultura
Secretaría de Agricultura y Desarrollo Rural
Avenida Mexico 190
Colonia Del Carmen
04100 Coyoacán, Ciudad de Mexico, Mexico

[4] Servicios Integrales de Recursos Biológicos, Acuáticos y Ambientales
Avenida Macarela 3302
Edificio Cardones I-104
Palmilla Grand Residencial
82112, Mazatlán, Sinaloa, Mexico

Abstract—Life-history studies of species discarded in fisheries are a low priority, particularly those of age and growth estimation. Consequently, almost everything is unknown about such species despite their having been caught as bycatch over the long term. In this study, age estimates were obtained by using the vertebrae of round stingrays (*Urobatis halleri*). We fitted 3 different growth models (von Bertalanffy, Gompertz, and logistic) to length-at-age data. Bayesian estimation of the various growth parameters was done by using the Markov chain Monte Carlo algorithm. Prior distributions of the parameters disc width at birth (DW_0) and the theoretical maximum disc width (DW_∞) were included and considered informative. The priors for the growth coefficient (k) and the completion growth parameter (k_2) were set as noninformative (k for the von Bertalanffy growth function and k_2 for the Gompertz and logistic growth models). Results of our analyses indicate that growth bands are annual and that the round stingray lives up to 8 years. According to the Watanabe–Akaike information criterion for model selection, the von Bertalanffy growth function for sexes combined was selected as the best model. The mean values of marginal posteriors were as follows: DW_0=9.52 cm (95% credible interval [CI]: 9.25–9.79), DW_∞=32.50 cm (95% CI: 30.60–34.46), and k=0.114 year^{-1} (95% CI: 0.101–0.129).

Manuscript submitted 28 January 2022.
Manuscript accepted 9 June 2022.
Fish. Bull. 120:205–217 (2022).
Online publication date: 8 July 2022.
doi: 10.7755/FB.120.3-4.2

The views and opinions expressed or implied in this article are those of the author (or authors) and do not necessarily reflect the position of the National Marine Fisheries Service, NOAA.

The geography and oceanographic characteristics of the Gulf of California (GOC) provide a highly productive area that supports some of the largest fisheries in Mexico. As a result, the GOC is one of the most productive regions for elasmobranchs. According to official fisheries statistics, in 2018, ~59% and ~39% of the landings of sharks and rays (batoids), respectively, came from the GOC (CONAPESCA[1]).

Both the industrial and artisanal fisheries of the GOC contribute to the landings of batoids (Márquez-Farías, 2002; Bizzarro et al., 2009). In addition to the current exploitation by industrial and artisanal ray fisheries, elasmobranch populations have been affected by the shrimp-trawl fishery that has been operating in the GOC since 1921 (Lluch-Cota et al., 2007).

The most important species in the landings of the ray fishery belong to the families Rhinobatidae, Dasyatidae, Myliobatidae, and Gymnuridae (Saldaña-Ruíz et al., 2016). In addition, because the fishing grounds of the artisanal ray fishery are inshore, the landings frequently include juveniles and pregnant females of many species (Márquez-Farías and Blanco-Parra, 2006; Bizzarro et al., 2009).

The composition of ray species in landings varies depending on the type of fishery, essentially because of the seasonal migrations of individuals, the habitat they occupy, and their susceptibility to capture. Given this situation and

[1] CONAPESCA (Comisión Nacional de Acuacultura y Pesca). 2018. Anuario estadístico de acuacultura y pesca 2018, 277 p. Comisión Nacional de Acuacultura y Pesca, Mazatlán, Mexico. [Available from website.]

the magnitude of the exploitation of elasmobranchs, the research priorities in the Mexican national plan of action for sharks focus on the more abundant species in the catch (CONAPESCA-INP, 2004). Considering the time series of historical catch of rays, the mixed-species fisheries, and the disadvantages of the low biological productivity of elasmobranchs (Musick, 1999), the negative effect of multiple fisheries on ray populations is presumably high.

A recent study of species composition and fishing dynamics revealed the effect of the industrial shrimp fishery on the elasmobranch populations of the GOC (Garcés-García et al., 2020). Results from that study confirm the importance of American round rays (family Urotrygonidae) as bycatch. The round stingray (*Urobatis halleri*) is the most abundant fish species in the bycatch of the industrial shrimp fishery in the GOC (López-Martínez et al., 2010; Rábago-Quiroz et al., 2011). Unfortunately, up to 95% of the bycatch volume of the shrimp fishery in the GOC is discarded at sea because of its low commercial importance (Zamora-García, 2015), limiting the study of the life history of the round stingray and other species.

The round stingray is distributed from California (in the United States) to Ecuador. It is a benthic and small (maximum disc width [DW]: 30.8 cm) batoid inhabiting soft mud or sand bottoms and is usually found in nearshore waters less than 15 m deep but can occur at depths down to 91 m (McEachran and Notarbartolo-di-Sciara, 1995). Aggregations are modulated by water temperature (>17°C) (Ebert, 2003; Hoisington and Lowe, 2005). Its food preferences include benthic invertebrates, bivalves, and small fishes. It is a viviparous species, and brood size ranges from 1 to 6 pups per season, depending on the size of the female (Babel, 1967), after 3 months of gestation (Nordell, 1994).

Differences in life-history traits in some elasmobranch species, such as the shovelnose guitarfish (*Pseudobatos productus*) and Pacific angel shark (*Squatina californica*), have been documented between populations in California and those farther south on the western coast of Baja California and in the GOC in Mexico (Márquez-Farías, 2007, 2020). The growth characteristics of round stingrays have been estimated for only the California population and are unknown for the GOC population (Hale and Lowe, 2008). The round stingray is categorized as a species of least concern in the IUCN Red List of Threatened Species (Lyons et al., 2015). From a regional perspective, populations of the round stingray and other rays likely have been affected by the shrimp-trawl fishery, given its intensity for more than 70 years in the GOC.

In this study, we report the results of Bayesian analyses used to investigate the age and growth of the round stingray in the GOC for the first time. First, using standard aging protocols, we used sectioned vertebrae to interpret and count the growth bands and to test the accuracy of band counts by readers. Then, we fitted 3 nonlinear growth models to age–length data pairs to estimate growth. Selection of the model that best explained and predicted the length-at-age data was based on the Watanabe–Akaike information criterion (WAIC), an appropriate approach for Markov chain Monte Carlo numerical integration. Growth parameters are presented as posterior probabilities that summarize the information of data and the prior probability of the parameters. The results of this study provide insight into key population characteristics necessary to model the demography of the round stingray and to test its potential resilience to fishing mortality.

Material and methods

Data and sample collection

Specimens of the round stingray were collected monthly during 2007–2012 as bycatch from trawl surveys conducted by the artisanal shrimp fishery in Teacapan, Sinaloa, Mexico (22°32′N, 105°45′W). We recorded the sex of each specimen and measured the DW (in centimeters) in a straight line, avoiding the curvature of the body. In addition, a section of 8–10 cervical vertebrae was extracted from each specimen to prevent intravertebral variability of band pairs (Natanson et al., 2018). Finally, the samples were labeled and frozen at −20°C at lab facilities for subsequent analysis.

Sample processing

Excess tissue and neural arches were removed from the vertebral segments manually. Each centrum was removed and mounted onto a flat piece of wood with synthetic resin. The vertebral diameters (VDs) were measured sagittally (to the nearest 0.05 mm) by using a Wixey[2] WR100 digital vernier (Barry Wixey Development, Seattle, WA). Using an IsoMet Low-Speed Saw (Buehler Ltd., Lake Bluff, IL), with twin blades separated by 0.24 mm, we cut each vertebra in a sagittal plane through the focus. Each vertebral section was mounted on a slide and photographed by using transmitted light with an Olympus SZ61 stereoscopic microscope (Olympus Corp., Tokyo, Japan) equipped with an Infinity*1-2* digital camera (Teledyne Lumenera, Ottawa, Canada). We created an image bank for the interpretation and counting of growth bands.

Size frequency and the relationship of size to vertebral diameter

We prepared DW–frequency histograms for comparison of size between the sexes. We used a *t*-test to determine whether there was a difference in the mean size between the male and female specimens. The relationship between VD and DW was assessed by using linear regression.

[2] Mention of trade names or commercial companies is for identification purposes only and does not imply endorsement by the National Marine Fisheries Service, NOAA.

Age estimation

In the vertebral sections of round stingrays, growth-band pairs appear opaque and translucent under transmitted light (Cailliet et al., 2006). Age estimates were made by counting band pairs along the corpus calcareum after identifying the birthmark, which can be seen as a change in the angle close to the focus. After establishing the aging criteria, 3 independent readers counted the growth bands.

Aging bias and precision

Reproducibility of counts of growth bands was assessed by using the index of average percent error (IAPE) (Equation 1) and the coefficient of variation (CV) (Equation 2). Next, the accuracy was evaluated by using the precision index (D) (Equation 3) for estimates from the 3 readers together and between readers (Chang, 1982; Goldman and Musick, 2006). Finally, the consensus of growth-band counts was visually evaluated by using age-bias plots (Campana et al., 1995). The following equations were used:

$$IAPE = 100\left[\frac{1}{N}\sum_{j=1}^{N}\left(\frac{1}{R}\sum_{i=1}^{R}\frac{\left|x_{ij}-\bar{x}_j\right|}{\bar{x}_j}\right)\right]; \quad (1)$$

$$CV = 100\left[\frac{1}{N}\left(\sqrt{\sum_{i=1}^{R}\frac{(x_{ij}-\bar{x}_j)^2}{R}}\right)\right]; \text{and} \quad (2)$$

$$D = \left[100\left(\frac{A}{B}\right)\right], \quad (3)$$

where N = the number of individuals aged;
R = the number of readers;
x_{ij} = the age estimate i for individual j;
$\bar{x}_j$ = the mean age calculated for individual j;
A = the number of agreements; and
B = the number of readings done.

For further analyses, we considered only age estimates on which at least 2 readers agreed; otherwise, the reading was discarded (Goldman et al., 2012). After growth bands were counted, the radius (distance from the focus to the edge) of a vertebra and each band's thickness were recorded by using Image-Pro Plus image analysis software (vers. 6.0, Media Cybernetics Inc., Rockville, MD).

Periodicity of band formation

The periodicity of growth-band formation in round stingrays was assessed through centrum edge analysis (CEA) and marginal increment analysis (MIA) following Cailliet (2015). First, we categorized the edge type of each section of a vertebra as *opaque* or *translucent*. Then, the relative frequency of each edge type was tabulated in bimesters (2-month intervals). The MIA (Equation 4) was conducted bimonthly by using the ages 2–8 years, following Natanson et al. (1995). Bimesters with mean marginal increment (MI) values close to 1 were interpreted to be the time of year when the growth cycle is about to be completed (Cailliet et al., 2006):

$$MI = \left(\frac{VR - r_n}{r_n - r_{n-1}}\right), \quad (4)$$

where VR = the vertebral radius;
r_n = the distance from the focus to the last band pair; and
r_{n-1} = the distance from the focus to the penultimate band pair.

One-way analysis of variance (ANOVA) was used to assess both the strength of the difference in total band counts between each pair of readers and the differences in the MI among bimesters (Gerrodette, 2011; Carrillo-Colín et al., 2021).

A Bayesian approach was used for the t-test, the linear regression, and the ANOVA described above. The Bayes factor (BF_{10}) was used to measure the weight of the evidence of the alternative hypothesis (H_1) against the null hypothesis (H_0) (Kass and Raftery, 1995; Rouder et al., 2009):

$$BF_{10} = H_1 / H_0. \quad (5)$$

The null hypothesis corresponds to the effect size (δ) of 0, and the alternative hypothesis was specified as a Cauchy prior with location and scale parameters of 0.000 and 0.707, respectively (Jeffreys, 1961).

All statistical treatments were done under the Bayesian approach by using the programs JAGS (vers. 4.3.0; Plummer, 2003) and JASP (vers. 0.15; JASP Team, 2021), statistical software R, vers. 4.0.5 (R Core Team, 2021), and the BayesFactor R package (vers. 0.9.12-4.2; Morey and Rouder, 2018). We relied on the guidelines proposed by Jeffreys (1961) for interpreting BF_{10}.

Growth modeling

To maximize the accuracy of the length-at-age predictions for both sexes of round stingrays and to contrast different hypotheses about growth, we used the von Bertalanffy, Gompertz, and logistic growth models (Katsanevakis and Maravelias, 2008). Growth models included in this study were those versions that incorporate disc width at birth (DW_0), as recommended for rays (Smart et al., 2016):

von Bertalanffy growth function (VBGF),

$$DW_t = DW_\infty - (DW_\infty - DW_0)e^{-kt}; \quad (6)$$

Gompertz growth model,

$$DW_t = DW_0 e^{-\log\left(\frac{DW_0}{DW_\infty}\right)\left(1-e^{-k_2 t}\right)}; \text{and} \quad (7)$$

logistic growth model,

$$DW_t = \frac{DW_\infty DW_0 e^{k_2 t}}{DW_\infty + DW_0 e^{k_2 t-1}}, \quad (8)$$

where DW_t = the estimated disc width (in centimeters) at a given age t (in years);
DW_∞ = the theoretical maximum disc width (in centimeters);
k = the growth coefficient (year^{-1}); and
k_2 = the completion growth parameter (year^{-1}).

Model fitting was done by using the Bayesian approach, which requires an initial probability distribution (prior) for each model parameter. We conducted a meta-analysis based on growth parameters published in the literature for round stingrays (Table 1). The mean and standard deviation of published growth parameters were used to set the parameters of the prior distributions (informative). The priors for the parameters k and k_2 were chosen to be relatively noninformative as the uniform distribution, with a minimum of 0 and maximum of 10 to avoid negative values and let the model acquire the needed curvature (Smart and Grammer, 2021). The prior for DW_∞ was informative and set as a normal distribution (ND): the population mean equal to 33.05 (standard deviation [SD] 10.07). The prior for DW_0 was also informative with an ND (population mean=7.32, σ=0.29). The prior of the residual σ was uniform, with a minimum of 0 and a maximum of 100.

The posterior distribution for the parameters of the 3 growth models (Equations 6–8) was computed by using the Bayes theorem (Gelman et al., 2003). With the actual growth parameters substituted into the Bayes formula and the terms simplified, the equation is as follows:

$$P(DW_\infty, k_n, DW_0 | d) = \frac{P(d|DW_\infty, k_n, DW_0)P(DW_\infty, k_n, DW_0)}{\int P(d|DW_\infty, k_n, DW_0)P(DW_\infty, k_n, DW_0)\partial\theta}, \quad (9)$$

where P = the probability;
k_n = the growth parameter of the n model;
d = the data; and
$\partial\theta$ = the partial derivate for each parameter θ.

The complexity of this multiparameter equation requires numerical integration. Therefore, we used a Markov chain Monte Carlo algorithm to obtain the posterior probability distribution by drawing random samples from the vector of all parameters of each model. For this purpose, we used JAGS, assuming an additive error. To assess the posterior distribution convergence, 4 Markov chains were simulated, with 100,000 iterations, a burn-in of 5000 runs, and a thinning of 1 iteration (Carrillo-Colín et al., 2021). Trace plots were assessed visually (Gelman and Rubin, 1992).

Model selection

To decide which model best explained and predicted the growth of round stingrays with Markov chain Monte Carlo numerical integration, we used the WAIC. This Bayesian criterion considers the entire parameter's likelihood matrix (Watanabe, 2009). First, model selection was made after comparing the WAIC values of the 3 competing models, and the one with the lowest WAIC value was selected. After that, the selected model, including the version with

Table 1

Reported growth parameters for male (M) and female (F) round stingray (*Urobatis halleri*) or for both sexes combined from other studies. These published means for disc width at birth (DW_0), theoretical maximum disc width (DW_∞), and the growth coefficient (k) were used in this study to set the parameters of the prior distributions and to compare the von Bertalanffy growth function (VBGF) and the Gompertz growth model for round stingray in the southern Gulf of California in Mexico. A single asterisk (*) indicates a value of DW_∞ determined through the transformation of the theoretical maximum total length (TL_∞) of 47.2 cm with the equation DW=1.33+0.53(TL) obtained in this study. A double asterisk (**) indicates values for the completion growth parameter from the Gompertz growth model. A dash indicates that the k value was not provided by the author.

Model	Sex	DW_∞ (cm)	DW_0 (cm)	k (year^{-1})	Location of study	Source
VBGF	F	31.00	7.50	–	Seal Beach, California	Babel (1967)
	M	25.00	7.50	–		
VBGF	Both	26.35*	4.72	0.27	Gulf of California, Mexico	Morales-Azpeitia et al. (2013)
VBGF	F	22.45	7.60	0.15	Seal Beach, California	Hale and Lowe (2008)
	M	28.56	7.50	0.09		
Gompertz	F	46.56	7.00	0.16**	Southern Gulf of California, Mexico	Diliegros-Valencia (2019)
	M	30.75	7.00	0.26**		

sex variation, was fitted, and the WAIC was computed. The WAIC values of the selected model for both sexes (reduced model) and its version that includes sex variation (full model) were then compared to decide if there was evidence of differences in growth between sexes.

Results

In total, 244 round stingrays were examined (99 females and 145 males). We found weak evidence (BF_{10}=1.00) in the mean differences in DW between sexes, where males were 1.01 cm (SD 0.50) larger than females (95% credible interval [CI]: 0.03–2.01). The size range for sexes combined was 7.8–24.5 cm DW (mean: 14.36 cm DW [SD 3.87]) (Fig. 1). We found conclusive evidence (BF_{10}>100) of a positive linear correlation between DW and VD (coefficient of determination [r^2]=0.87) with regression coefficients a and b of 18.43 (95% CI: 12.04–24.74) and 55.26 (95% CI: 52.62–58.03), respectively, described by the equation DW=18.43+55.26(VD) for sexes combined (Fig. 2).

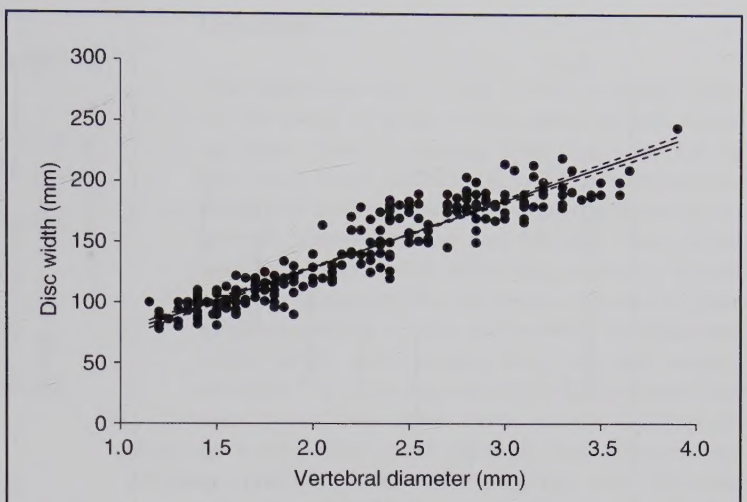

Figure 2

Relationship between vertebral diameter and disc width for round stingrays (*Urobatis halleri*) sampled during 2007–2012 in the southern Gulf of California in Mexico (for sexes combined). Dashed lines indicate the 95% credible interval.

Growth-band counts ranged from 0 to 8. The 3 readers agreed on 38% of the counts. When just 2 readers agreed (62% of cases), their count differed by 1 band in 59% of cases and by 2 bands in 3% of cases. The indicators of bias and precision for the total sample were as follows: IAPE=20%, CV=27%, and D=56%. Visual inspection of the age-bias plots between each pair of readers revealed minimal variation around the 1:1 ratio (Fig. 3, A–C). The results of the post hoc tests done as part of the ANOVA provide anecdotal evidence that the mean counts between readers 1 and 2 were different (BF_{10}=2.02). In contrast, for the mean counts between readers 1 and 3 (BF_{10}=0.27) and readers 2 and 3 (BF_{10}=0.17), the evidence of difference was null (Fig. 3D).

Results from the CEA indicate that the highest frequency of opaque edges occurred in the summer months, likely the time when deposition of growth bands began. Results from the MIA indicate that growth-band deposition appears close to being completed in November–December when the maximum MI was reached (Fig. 4). The lower MI estimated in the fourth bimester (July–August) was probably caused by the low sample size. However, we found substantial evidence in the mean differences in MI between bimester 2 (March–April) and bimester 4 (July–August), bimester 3 (May–June) and bimester 4 (July–August), and bimester 5 (September–October) and bimester 6 (November–December) (Suppl. Table) (online only). Results from both CEA and MIA indicate that every growth band was formed annually.

The estimated ages for sexes combined ranged from 0 to 8 years. The mean age of all the samples was 2.27 years (SD 1.87), with 23.8% and 17.6% of individuals aged at 0 and 1 years, respectively. As it is with many elasmobranchs, overlap in size at age increased with age for our specimens of the round stingray, which can be seen in the size-at-age key in Table 2.

The model selected according to the WAIC as the best fit to the data was the VBGF (Table 3). When sex was included in the VBGF, the WAIC increased by 6.46 units (from 804.47 to 810.93). Given the loss of parsimony by including sex as

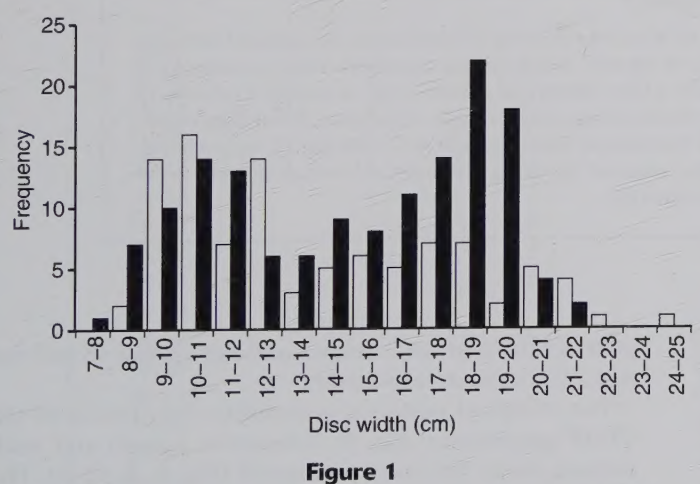

Figure 1

Length–frequency distributions for female (white bars) and male (black bars) round stingrays (*Urobatis halleri*) sampled during 2007–2012 in the southern Gulf of California in Mexico (number of rays=244).

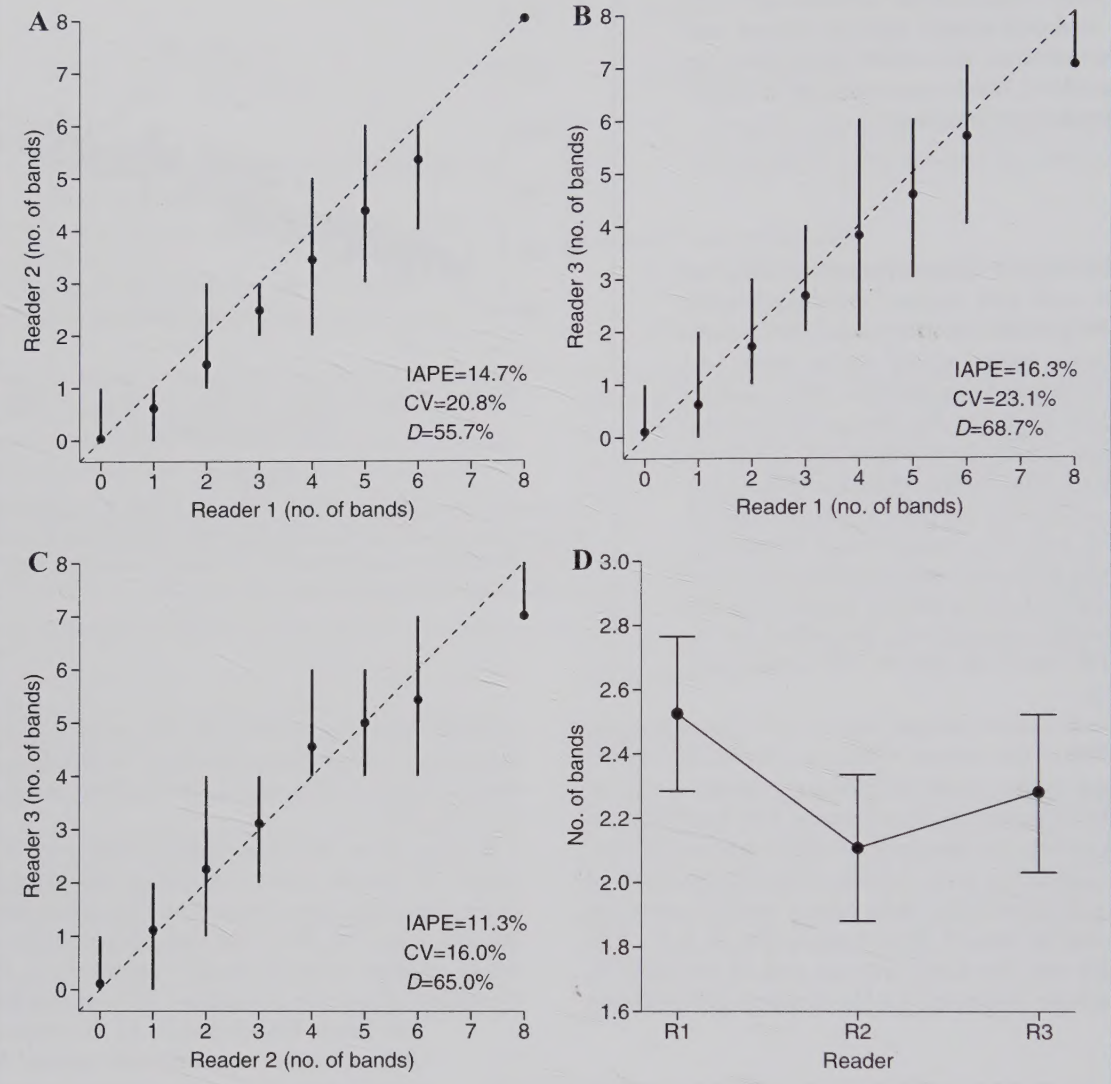

Figure 3

Age-bias plots of counts of growth bands on vertebrae of round stingrays (*Urobatis halleri*) sampled between 2007 and 2012 in the southern Gulf of California in Mexico. Black circles represent mean counts (**A**) of reader 2 (R2) relative to reader 1 (R1), (**B**) of reader 3 (R3) relative to reader 1, (**C**) of reader 3 relative to reader 2, and (**D**) between readers 1–3 from ad hoc Bayesian one-way analysis of variance. Error bars represent the range of band counts assigned by readers. The dashed line in panels A–C indicate 1:1 equivalence. Reproducibility and precision of age estimates were assessed by using the index of average percent error (IAPE), coefficient of variation (CV), and precision index (*D*).

a factor, we selected the VBGF fitted with data for the sexes combined. The mean values of marginal posteriors from the VBGF were as follows: DW_0=9.52 cm (95% CI: 9.25–9.79), DW_∞=32.50 cm (95% CI: 30.60–34.46), and k=0.114 year^{-1} (95% CI: 0.101–0.129). The growth curve is monotonic as expected. However, because the sample size decreased with age, the model lost accuracy at ages 6 and 8 (Fig. 5). The VBGF for the round stingray predicts growth from the birth size of 9.52 cm DW to 11.92 cm DW for age 1 and to 14.21 cm DW for age 2. Therefore, the growth rate from age 0 to age 1 and age 2 was 2.48 cm/year and 2.21 cm/year, respectively.

The marginal posterior probability distribution of the VBGF parameters (Fig. 6) indicates a smooth and well-defined shape for every parameter (Fig. 6, A, C, E). The relationship of DW_∞ to k is typically inverse (Fig. 6B). Similarly, the relationship of k to DW_0 is inverse but with a slope that is less steep (Fig. 6F), whereas the relationship of DW_0 to DW_∞ is dispersed and centered without correlation (Fig. 6D).

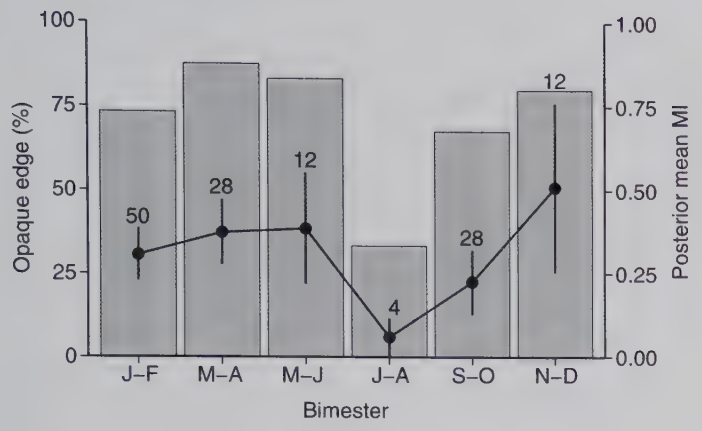

Figure 4

The periodicity of band formation was assessed by using marginal increment (MI) analysis and edge percentage analysis for round stingrays (*Urobatis halleri*) sampled during 2007–2012 in the southern Gulf of California in Mexico. The black circles represent the posterior mean marginal increments, and the error bars indicate the 95% credible intervals. The gray columns represent the percentages of opaque edges. Numerals above the circles indicate number of rays. Results of analyses are shown for each bimester (2-month interval): January–February, March–April, May–June, July–August, September–October, and November–December.

Discussion

The maximum age of the round stingray found in this study (8 years) is the same as that found by Babel (1967) but lower than that reported by Hale and Lowe (2008) (14 years). Furthermore, the latter authors found statistical differences in growth between males and females. This difference could be related to the size structure of both samples. Although the size range obtained in this study is similar to that in the study by Hale and Lowe (2008), their sample was composed mainly of males (71%), and our sample did not have such bias in sex proportion (59% males). Differences in availability could produce the phenomenon of apparent change in the growth rate like gear selectivity can (Walker et al., 1998). Also, the difference in conclusions between the studies could be a result of the use of the different statistical approach in our study (Gerrodette, 2011).

Compared to other members of the family Urotrygonidae, the round stingray has a maximum age that is similar to that of the Panamic stingray (*Urotrygon aspidura*) from the Pacific coast of Columbia (Torres-Palacios et al., 2019) but is shorter than that reported for the

Table 2

Age–size key for round stingrays (*Urobatis halleri*) sampled between 2007 and 2012 in the southern Gulf of California in Mexico (for sexes combined). In the center of the table are the numbers of individuals that correspond to each disc width (DW) class and age class. In the margin of the table, the total number of stingrays (n) and the mean and standard deviation (SD) for each DW class and age class are presented.

	Age (years)											
DW (cm)	0	1	2	3	4	5	6	7	8	n	Mean (years)	SD
7–8	1									1	0.0	–
8–9	9									9	0.0	–
9–10	22	2								24	0.1	0.28
10–11	21	9								30	0.3	0.47
11–12	4	13	3							20	1.0	0.60
12–13	1	12	7							20	1.3	0.57
13–14		4	5							9	1.6	0.53
14–15		3	8	3						14	2.0	0.68
15–16			8	6						14	2.4	0.51
16–17			5	10	1					16	2.8	0.58
17–18			1	12	7		1			21	3.4	0.81
18–19				4	15	8	2			29	4.3	0.80
19–20				1	8	7	4			20	4.7	0.86
20–21					3	4	2			9	4.9	0.78
21–22					1	3	2			6	5.2	0.75
22–23						1				1	5.8	–
24–25									1	1	8.0	–
n	58	43	37	36	35	23	11		1	244		
Mean (cm)	9.7	11.7	14.0	16.6	18.5	19.4	19.4		–	14.4	2.3	
SD	0.89	1.19	1.55	1.32	0.95	1.20	1.17		–	3.96		1.87

Table 3

Comparison of the von Bertalanffy, Gompertz, and logistic growth models fit to length-at-age data for round stingrays (*Urobatis halleri*) sampled between 2007 and 2012 in the southern Gulf of California in Mexico. The parameters are disc width at birth (DW_0, in centimeters), theoretical maximum length (DW_∞, in centimeters), and the growth coefficient (k, year^{-1}) for the von Bertalanffy growth function and the completion growth coefficient (k_2, year^{-1}) for the Gompertz and logistic growth models. Posterior values and 95% credible intervals (lower quartile: 2.5%; upper quartile: 97.5%) are provided from the fit of the growth models with a Markov chain Monte Carlo algorithm to data pooled for both sexes. The Watanabe–Akaike information criterion (WAIC) was used in model selection. The deviance information criterion (DIC) is reported to facilitate comparison of parameter estimates with those from previous studies in which the frequentist approach was used. SD=standard deviation; SE=standard error.

				Credible interval			
Model	Parameter	Mean	SD	2.5%	97.5%	DIC	WAIC (SE)
von Bertalanffy						805.20	804.47 (20.3)
	DW_0	9.52	0.14	9.25	9.79		
	DW_∞	32.55	0.97	30.60	34.46		
	k	0.11	0.01	0.10	0.13		
	SD	1.25	0.06	1.15	1.37		
Gompertz						824.10	820.77 (21.1)
	DW_0	9.80	0.13	9.55	10.06		
	DW_∞	33.64	1.03	31.65	35.70		
	k_2	0.17	0.01	0.15	0.18		
	SD	1.30	0.06	1.19	1.42		
Logistic						898.30	897.75 (21.5)
	DW_0	11.71	0.17	11.38	12.04		
	DW_∞	34.82	1.01	32.84	36.77		
	k_2	0.15	0.01	0.14	0.16		
	SD	1.52	0.07	1.30	1.66		

blotched stingray (*Urotrygon chilensis*) (14 years) in the Mexican Pacific Ocean (Guzmán Castellanos, 2015). This new information about the maximum age of the round stingray has considerable implications for studies of population dynamics.

The evidence of a relationship between VD and DW supports the use of vertebrae for aging (Goldman et al., 2012). The precision values (IAPE, CV, D) for samples in our study are within the expected interval for this group of species (Campana, 2001) and agree with the readings that have been done for the family Urotrygonidae (Mejía-Falla et al., 2014; Guzmán Castellanos, 2015; Santander Neto, 2015; Diliegros-Valencia, 2019).

Results from both the CEA and MIA support the assumption of an annual pattern of growth-band formation, and annual formation has also been reported for round stingrays in California (Hale and Lowe, 2008) and in the southeastern

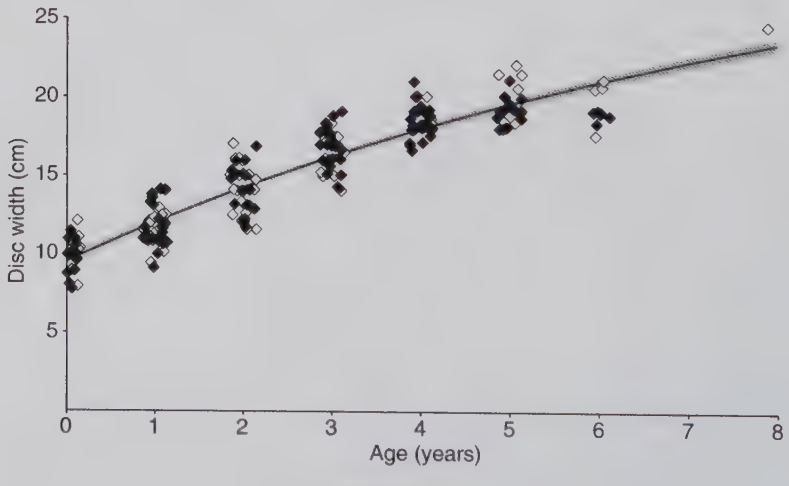

Figure 5

Estimated von Bertalanffy growth curve for round stingrays (*Urobatis halleri*) in the southern Gulf of California in Mexico (for sexes combined). The black (male) and open (female) diamonds represent observed lengths at age for stingrays sampled during 2007–2012. The gray shaded area indicates the 95% credible interval.

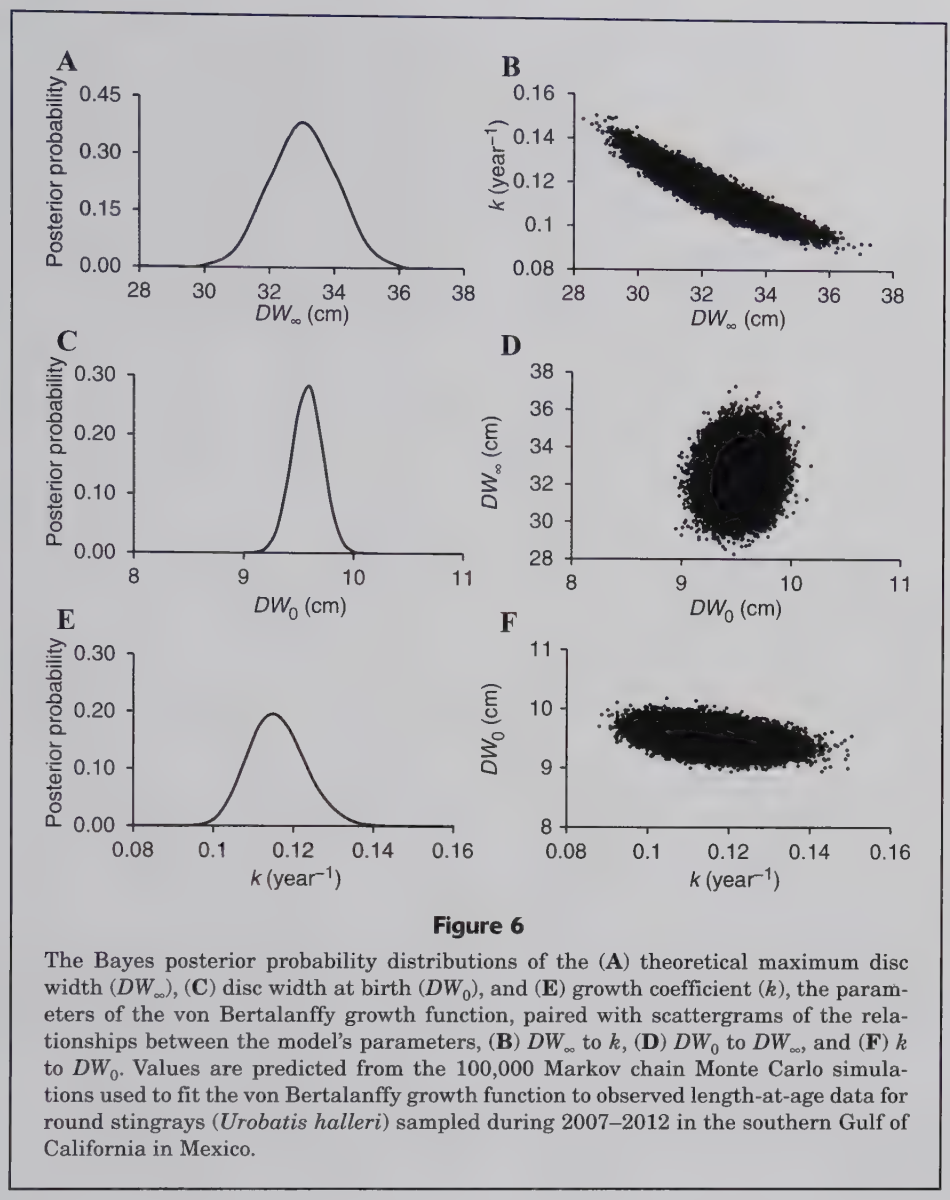

Figure 6

The Bayes posterior probability distributions of the (**A**) theoretical maximum disc width (DW_∞), (**C**) disc width at birth (DW_0), and (**E**) growth coefficient (k), the parameters of the von Bertalanffy growth function, paired with scattergrams of the relationships between the model's parameters, (**B**) DW_∞ to k, (**D**) DW_0 to DW_∞, and (**F**) k to DW_0. Values are predicted from the 100,000 Markov chain Monte Carlo simulations used to fit the von Bertalanffy growth function to observed length-at-age data for round stingrays (*Urobatis halleri*) sampled during 2007–2012 in the southern Gulf of California in Mexico.

GOC (Diliegros-Valencia, 2019). The opaque bands were deposited in the summer months. They are broad and represent rapid growth, and the translucent bands formed in winter are thinner and reflect slower growth (Cailliet et al., 1986; Cailliet and Goldman, 2004). Evidence of variability between individuals in the number of band pairs has been documented for the round stingray (James and Natanson, 2020), and such a source of bias was prevented in this study by using just the cervical vertebrae for all round stingrays. Also, band-pair counts without validation need to be taken with caution. Although there are more direct methods for validating the periodicity of growth bands of aquatic organisms, CEA and MIA are advantageous because they yield reliable and comparable results (Campana, 2001; Carrillo-Colín et al., 2021). Although new methods and approaches will rise to overcome the current controversies in age studies for batoids (James and Natanson, 2020), our statistical approach and results set a baseline for the age and growth of the round stingray in the tropical region of the Pacific Ocean.

In this study, we explored 3 conceptually different models that include DW_0, an appropriate parameter for viviparous chondrichthyans (Cailliet et al., 2006). We avoided exploring other models with more parameters because the WAIC penalizes them or because they do not have any biological significance (Richards, 1959; Katsanevakis, 2006). The continuous growth pattern observed in this study (as indicated by parameter estimates from the VBGF) and the representativeness of most age groups indicate that the round stingray completes its life cycle in the study area (Bergstad et al., 2021). Interestingly, the round stingray has been reported to segregate by size and life stage (Silva-Garay and Lowe, 2021), but there are no signs of segregation in our data set. Size segregation and

length selectivity of fishing gears can bias growth data to indicate a discontinuous pattern (Walker et al., 1998) that can favor more flexible models (with an inflection point) or even 2-phase growth models arguing investment in reproductive processes (Torres-Palacios et al., 2019).

The round stingray is not commercially targeted in the GOC artisanal fisheries (Bizzarro et al., 2009). However, the low sample size for large individuals (>6 years and >22 cm DW) might indicate an effect of fishing mortality on its population due to being caught as bycatch of shrimp trawlers (Garcés-García et al., 2020), as implied by the difference between the observed maximum DW (24.50 cm) and the estimated mean DW_∞ (32.50 cm). Fortunately, the statistical framework used in this study allowed us to estimate DW_∞ by combining the prior information and support of data considering the parameter's uncertainty in a probabilistic manner.

Size selectivity does not seem to be an explanation for the absence of large individuals because the maximum DW obtained during this study is very similar to those of other studies (27.00 cm; Hale and Lowe, 2008), and such a minimal difference in maximum DW does not indicate a significant difference in swimming speeds or turning ability. The latter may be true for species with higher swimming ability and size, such as the golden cownose ray (*Rhinoptera steindachneri*), the eagle rays (*Myliobatis* spp.), or those of the genus *Hypanus*, which are more likely to outswim the relatively slow shrimp trawls. In contrast, the poor mobility of round stingrays limits their ability to escape, and their flattened shape restricts size selection through the trawl. Consequently, fishing mortality is likely to affect the size range of the round stingrays available in the fishing area and susceptible to being captured by the trawlers. Although our surveys were conducted with small trawl nets used in the artisanal shrimp fishery, the size range sampled was convenient for this study and included individuals in all classes for both sexes. Furthermore, similar sizes for the round stingray were recently reported from fishery-independent surveys conducted with large vessels and in different areas, depths, and seasons in the GOC (Garcés-García et al., 2020).

In this study, we investigated the round stingray's age and growth and developed a fully Bayesian approach for estimation of all quantities. In contrast, leaving the model fitting to the data alone could produce misleading estimates of parameters, especially when the observed data do not follow the expected pattern, are incomplete, or are biased. The stochastic approach in which Monte Carlo simulation is used can be advantageous for remedying the lack of fit. However, it also requires assigning a probability distribution to the parameters without weighting them with the data to produce the final distributions of the parameters (Neer et al., 2005). Alternatively, the Bayesian approach in this study relies on the explicit use of uncertainty for the growth parameters. A parameter's uncertainty is expressed as a probability distribution and combined with the information contained in the data (likelihood) throughout the Bayes theorem (Equation 9); it is possible to obtain an enriched marginal posterior probability distribution (Fig. 6) of each parameter (Gelman et al., 2003). This fact is essential in age and growth studies when parameters can be informative based on the knowledge of the life history of a species, as is the case for DW_0 (Carrillo-Colín et al., 2021; Smart and Grammer, 2021).

Neither Monte Carlo simulation nor the Bayesian approach can correct for biases in the data caused by length-selective fishing mortality. Troynikov and Walker (1999) stated that the influence of length-selective mortality on determining growth parameters is not easily explained because it is a combination of 2 overlapping effects on lengths for different age classes. These authors proved that a growth pattern can be affected by an apparent change in growth rate due to length-selective fishing mortality.

Reporting the parameters as probability distributions (and their credible intervals) is not only fundamentally different from classical (frequentist) estimation but also useful as inputs in further quantitative demographic analysis or stock assessment for elasmobranchs (Cortés, 2002). However, the philosophy of measuring the statistical support of each growth parameter when fitting the model goes beyond the scope of our work described here (Gerrodette, 2011).

In our study, we used the Bayes factor in the *t*-test and ANOVA to evaluate the size of the effects, and we used the WAIC for the selection of the best growth models. The WAIC is convenient for more complex stochastic numerical approximations.

The convergence of the growth parameters DW_∞, k, and DW_0 was satisfactorily achieved on the basis of their marginal posterior distributions (Carrillo-Colín et al., 2021). The informative prior distribution for DW_0 favored model fitting because it helped in the selection of realistic birth size values (Rolim et al., 2020; Smart and Grammer, 2021). The k value (from the VBGF) we obtained in our study ranged between 0.11 and 0.13 $year^{-1}$ and is close to the range of 0.2–0.5 $year^{-1}$ that has been reported for species of the families Rhinobatidae, Torpedinidae, and Urotrygonidae (Cailliet and Goldman, 2004). However, it must be noted that this broad difference in k values can also be related to sample size, aging method, and verification, validation, and growth model fitting techniques (Cailliet and Goldman, 2004).

Conclusions

In the GOC, chondrichthyan populations have long been affected by fisheries that trawl for teleost and shrimp species. Capture as bycatch in those fisheries causes significant mortality for species of no commercial value, including for the round stingray and other demersal small rays (Garcés-García et al., 2020). Variations in life-history characteristics among populations can be expected in chondrichthyan species because of the following: 1) cold-water species tend to grow larger and

probably live longer than tropical water species; 2) differences in food availability, habitat type, and environmental conditions affect their growth rate; and sample distribution can be biased 3) by the effects of migration and segregation and 4) by the length selectivity of fishing gears (Walker, 1998; Walker et al., 1998). In this study, we estimated growth parameters by using the counts of growth bands in vertebrae taken from sampled round stingrays. We found a maximum age of 6 or 8 years, a remarkably short life span for a chondrichthyan species, indicating that the round stingray has a short intrinsic generation time and, therefore, a high intrinsic rate of population increase (King and McFarlane, 2003). Stock assessment and ecological risk analyses require inputs from age, growth, and reproductive rate studies. The Bayesian estimation of this study can be used in future quantitative analyses to gain the advantage of considering uncertainty in the estimation of parameters (Punt and Hilborn, 1997).

Resumen

Los estudios sobre la historia de vida de las especies descartadas en pesquerías son de baja prioridad, especialmente aquellos sobre estimaciones de edad y crecimiento. En consecuencia, se desconoce casi todo sobre estas especies, a pesar de haber sido capturadas de forma incidental por mucho tiempo. En este estudio, las estimaciones de edad se obtuvieron utilizando las vértebras de la raya redonda (*Urobatis halleri*). Se ajustaron 3 diferentes modelos de crecimiento (von Bertalanffy, Gompertz y logístico) a datos de longitud a la edad. La estimación Bayesiana de los distintos parámetros de crecimiento se realizó mediante el algoritmo cadenas de Markov de Monte Carlo. Se incluyeron y consideraron distribuciones previas informativas de los parámetros ancho del disco al nacer (DW_0) y ancho del disco máximo teórico (DW_∞). Las distribuciones previas para el coeficiente de crecimiento (k) y el parámetro de terminación del crecimiento (k_2) se establecieron como no informativas (k para la función de crecimiento de von Bertalanffy y k_2 para los modelos de crecimiento Gompertz y logístico). Los resultados de nuestros análisis indican que las bandas de crecimiento son anuales y que la raya redonda vive hasta 8 años. Según el criterio de información de Watanabe–Akaike para la selección del modelo, la función de crecimiento de von Bertalanffy para sexos combinados fue seleccionada como el mejor modelo. Los valores promedio de las posteriores marginales fueron los siguientes: DW_0=9.52 cm (intervalo de credibilidad [IC] al 95%: 9.25–9.79), DW_∞=32.50 cm (IC 95%: 30.60–34.46), y k =0.114 año^{-1} (IC 95%: 0.101–0.129).

Acknowledgments

We express our gratitude to T. Walker for his constructive review and recommendations. This research was funded by Universidad Autónoma de Sinaloa through the projects PROFAPI-UAS (81-2010) and PROFAPI-UAS (101-2011).

Literature cited

Babel, J. S.
1967. Reproduction, life history and ecology of the round stingray *Urolophus halleri* Cooper. Calif. Dep. Fish Game, Fish Bull. 137, 104 p.

Bergstad, O. A., R. H. Hunter, N. J. Cousins, D. M. Bailey, and T. Jørgensen.
2021. Notes on age determination, size and age structure, longevity and growth of co-occurring macrourid fishes. J. Fish Biol. 99:1032–1043.

Bizzarro, J. J., W. D. Smith, J. F. Márquez-Farías, J. Tyminski, and R. E. Hueter.
2009. Temporal variation in the artisanal elasmobranch fishery of Sonora, Mexico. Fish. Res. 97:103–117.

Cailliet, G. M.
2015. Perspectives on elasmobranch life-history studies: a focus on age validation and relevance to fishery management. J. Fish Biol. 87:1271–1292.

Cailliet, G. M., and K. J. Goldman.
2004. Age determination and validation in chondrichthyan fishes. *In* Biology of sharks and their relatives (J. C. Carrier, J. A. Musick, and M. R. Heithaus, eds.), p. 399–447. CRC Press, Boca Raton, FL.

Cailliet, G. M., R. L. Radtke, and B. A. Welden.
1986. Elasmobranch age determination and verification: a review. *In* Indo-Pacific fish biology: proceedings of the second international conference on Indo-Pacific fishes (T. Uyeno, R. Arai, T. Taniuchi, and K. Matsuura, eds.), p. 345–360. Ichthyol. Soc. Jpn., Tokyo, Japan.

Cailliet, G. M., W. D. Smith, H. F. Mollet, and K. J. Goldman.
2006. Age and growth studies of chondrichthyan fishes: the need for consistency in terminology, verification, validation, and growth function fitting. Environ. Biol. Fishes 77:211–228.

Campana, S. E.
2001. Accuracy, precision and quality control in age determination, including a review of the use and abuse of age validation methods. J. Fish Biol. 59:197–242.

Campana, S. E., M. C. Annand, and J. I. McMillan.
1995. Graphical and statistical methods for determining the consistency of age determinations. Trans. Am. Fish. Soc. 124:131–138.

Carrillo-Colín, L. D., J. F. Márquez- Farías, R. E. Lara-Mendoza, and O. G. Zamora-García.
2021. Bayesian estimation of the age and growth of the golden cownose ray (*Rhinoptera steindachneri*) in the southern Gulf of California in Mexico. Fish. Bull. 119:10–20.

CONAPESCA-INP (Comisión Nacional de Acuacultura y Pesca-Instituto Nacional de la Pesca).
2004. Plan de acción nacional para el manejo y conservación de tiburones, rayas y especies afines en México, 80 p. Com. Nac. Acuac. Pesca and Inst. Nac. Pesca, Secr. Agric. Ganad. Desarro. Rural Pesca Aliment., Mazatlán, Mexico. [Available from website.]

Cortés, E.
2002. Stock assessment of small coastal sharks in the U.S. Atlantic and Gulf of Mexico. Southeast Data Assess. Rev., SEDAR 13-DW-13, 133 p. [Available from website.]

Diliegros-Valencia, M.
2019. Edad y crecimiento de la raya redonda *Urobatis halleri* (Cooper, 1863) en el Sur de Sinaloa y Norte de Nayarit,

México. Bachelor's thesis, 69 p. Univ. Veracruzana, Tuxpan, Veracruz, Mexico.

Ebert, D. A.
2003. Sharks, rays and chimaeras of California, 297 p. Univ. Calif. Press, Berkeley, CA.

Garcés-García, K. C., J. Tovar-Ávila, B. Vargas-Trejo, D. A. Chávez-Arrenquín, T. I. Walker, and R. W. Day.
2020. Elasmobranch bycatch by prawn trawls in the Gulf of California: first comprehensive analysis and the effect of fish escape devices. Fish. Res. 230:105639.

Gelman, A. D., and D. B. Rubin.
1992. Inference from iterative simulation using multiple sequences. Stat. Sci. 7:457–472.

Gelman, A., J. B. Carlin, H. S. Stern, and D. B. Rubin.
2003. Bayesian data analysis, 2nd ed., 668 p. Chapman and Hall/CRC, London.

Gerrodette, T.
2011. Inference without significance: measuring support for hypotheses rather than rejecting them. Mar. Ecol. 32:404–418.

Goldman, K. J., and J. A. Musick.
2006. Growth and maturity of salmon sharks (*Lamna ditropis*) in the eastern and western North Pacific, and comments on back-calculation methods. Fish. Bull. 104:278–292.

Goldman, K. J., G. M. Cailliet, A. H. Andrews, and L. J. Natanson.
2012. Assessing the age and growth of Chondrichthyan fishes. *In* Biology of sharks and their relatives, 2nd ed. (J. C. Carrier, J. A. Musick, and M. R. Heithaus, eds.), p. 423–451. CRC Press, Boca Raton, FL.

Guzmán Castellanos, A. B.
2015. Historia de vida de la raya chilena *Urotrygon chilensis* (Günther, 1872) en el sureste del Pacífico mexicano. Ph.D. diss., 133 p. Cent. Investig. Biol. Noroeste, La Paz, Mexico. [Available from website.]

Hale, L. F., and C. G. Lowe.
2008. Age and growth of the round stingray *Urobatis halleri* at Seal Beach, California. J. Fish Biol. 73:510–523.

Hoisington, G., IV, and C. G. Lowe.
2005. Abundance and distribution of the round stingray, *Urobatis halleri*, near a heated effluent outfall. Mar. Environ. Res. 60:437–453.

James, K. C., and L. J. Natanson.
2020. Positional and ontogenetic variation in vertebral centra morphology in five batoid species. Mar. Freshw. Res. 72:887–898.

Jeffreys, H.
1961. Theory of probability, 3rd ed., 447 p. Oxford Univ. Press, Oxford, UK.

JASP Team.
2021. JASP. Computer software, vers. 0.15. [Available from website, accessed September 2021.]

Katsanevakis, S.
2006. Modelling fish growth: model selection, multi-model inference and model selection uncertainty. Fish. Res. 81:229–235.

Katsanevakis, S., and C. D. Maravelias.
2008. Modelling fish growth: multi-model inference as a better alternative to a priori using von Bertalanffy equation. Fish Fish. 9:178–187.

Kass, R. E., and A. E. Raftery.
1995. Bayes factors. J. Am. Stat. Assoc. 90:773–795.

King, J. R., and G. A. McFarlane.
2003. Marine fish life history strategies: applications to fishery management. Fish. Manag. Ecol. 10:249–264.

López-Martínez, J., E. Herrera-Valdivia, J. Rodríguez-Romero, and S. Hernández-Vázquez.
2010. Peces de la fauna de acompañamiento en la pesca industrial de camarón en el Golfo de California, México. Rev. Biol. Trop. 58:925–942.

Lluch-Cota, S. E., E. A. Aragón-Noriega, F. Arreguín-Sánchez, D. Aurioles-Gamboa, J. J. Bautista-Romero, R. C. Brusca, R. Cervantes-Duarte, R. Cortés-Altamirano, P. Del-Monte-Luna, A. Esquivel-Herrera, et al.
2007. The Gulf of California: review of ecosystem status and sustainability challenges. Prog. Oceanogr. 73:1–26.

Lyons, K., D. A. Ebert, and C. G. Lowe.
2015. *Urobatis halleri*. The IUCN Red List of Threatened Species 2015:e.T60108A80677446. [Available from website accessed January 2021].

Márquez-Farías, J. F.
2002. The artisanal ray fishery in the Gulf of California: development, fisheries research and management issues. Shark News 14:12–13.
2007. Reproductive biology of shovelnose guitarfish *Rhinobatos productus* from the eastern Gulf of California México. Mar. Biol. 151:1445–1454.
2020. Length at maturity of the Pacific angel shark (*Squatina californica*) in the artisanal elasmobranch fishery in the Gulf of California in Mexico. Fish. Bull. 118:359–364.

Márquez-Farías, J. F., and M. P. Blanco-Parra.
2006. Rayas. *In* Sustentabilidad y pesca responsable en México: evaluación y manejo (F. A. Sánchez, L. B. Moreno, I. M. Gómez-Humarán, R. S. Sansores, and C. R. Dávalos, eds.), p. 303–321. Inst. Nac. Pesca, Mexico City, Mexico.

McEachran, J. D., and G. Notarbartolo-di-Sciara.
1995. Peces Batoideos. *In* Guía FAO para la identificación de especies para los fines de la pesca. Pacifico centro-oriental. Volumen 2: vertebrados—parte 1 (W. Fischer, F. Krupp, W. Schneider, C. Sommer, K. E. Carpenter, and V. H. Niem, eds.), p. 745–792. FAO, Rome.

Mejía-Falla, P. A., E. Cortés, A. F. Navia, and F. A. Zapata.
2014. Age and growth of the round stingray *Urotrygon rogersi*, a particularly fast-growing and short-lived elasmobranch. PLoS ONE 9(4):e96077.

Morales-Azpeitia, R., J. López-Martínez, C. H. Rábago-Quiroz, M. O. Nevárez-Martínez, and E. Herrera-Valdivia.
2013. Growth and mortality rates of *Pseudupeneus grandisquamis* and *Urobatis halleri* bycatch species in the shrimp fishery. Hidrobiológica 23:386–393.

Morey, R. D., and J. N. Rouder.
2018. BayesFactor: computation of Bayes factors for common designs. R package, vers. 0.9.12-4.2. [Available from website, accessed December 2020.]

Musick, J. A.
1999. Ecology and conservation of long-lived marine animals. Am. Fish. Soc. Symp. 23:1–10.

Natanson, L. J., J. G. Casey, and N. E. Kohler.
1995. Age and growth estimates for the dusky shark, *Carcharhinus obscurus*, in the western North Atlantic Ocean. Fish. Bull. 93:116–126.

Natanson, L. J., G. B. Skomal, S. L. Hoffmann, M. E. Porter, K. J. Goldman, and D. Serra.
2018. Age and growth of sharks: do vertebral band pairs record age? Mar. Freshw. Res. 69:1440–1452.

Neer, J. A., B. A. Thompson, and J. K. Carlson.
2005. Age and growth of *Carcharhinus leucas* in the northern Gulf of Mexico: incorporating variability in size at birth. J. Fish Biol. 67:370–383.

Nordell, S. E.
1994. Observations of the mating behavior and dentition of the round stingray, *Urolophus halleri*. Environ. Biol. Fishes 39:219–229.

Plummer, M.
2003. JAGS: a program for analysis of Bayesian graphical models using Gibbs sampling. *In* Proceedings of the 3rd international workshop on distributed statistical computing (DSC 2003); Vienna, 20–22 March (K. Hornik, F. Leisch, and A. Zeileis, eds.), 10 p. [Available from website.]

Punt, A. E., and R. Hilborn.
1997. Fisheries stock assessment and decision analysis: the Bayesian approach. Rev. Fish Biol. Fish. 7:35–63.

R Core Team.
2021. R: a language and environment for statistical computing. R Foundation for Statistical Computing, Vienna, Austria. [Available from website, accessed April 2021.]

Rábago-Quiroz, C. H., J. López-Martínez, J. E. Valdez-Holguín, and M. O. Nevárez-Martínez.
2011. Distribución latitudinal y batimétrica de las especies más abundantes y frecuentes en la fauna acompañante del camarón del Golfo de California, México. Rev. Biol. Trop. 59:255–267.

Richards, F. J.
1959. A flexible growth function for empirical use. J. Exp. Bot. 10:290–300.

Rouder, J. N., P. L. Speckman, D. Sun, R. D. Morey, and G. Iverson.
2009. Bayesian *t* tests for accepting and rejecting the null hypothesis. Psychon. Bull. Rev. 16: 225–237.

Rolim, F. A., Z. A. Siders., F. P. Caltabellotta, M. M. Rotundo, and T. Vaske-Júnior.
2020. Growth and derived life-history characteristics of the Brazilian electric ray *Narcine brasiliensis*. J. Fish Biol. 97:396–408.

Saldaña-Ruíz, L. E., O. Sosa-Nishizaki, Z. Ramírez-Mendoza, M. A. Pérez-Miranda, F. I. Rocha-González, and M. C. Rodríguez-Medrano.
2016. Reconstrucción de capturas por especie de la pesca artesanal de rayas del Golfo de California, 1997–2014. Cienc. Pesq. 24:81–96.

Santander Neto, J.
2015. Dinâmica populacional da raia *Urotrygon microphthalmum* Delsman, 1941 no nordeste do Brasil. Ph.D. diss., 142 p. Univ. Fed. Pernambuco, Recife, Brazil. [Available from website.]

Silva-Garay, L., and C. G. Lowe.
2021. Effects of temperature and body-mass on the standard metabolic rates of the round stingray, *Urobatis halleri* (Cooper, 1863). J. Exp. Mar. Biol. Ecol. 540:151564.

Smart, J. J., and G. L. Grammer.
2021. Modernising fish and shark growth curves with Bayesian length-at-age models. PLoS ONE 16(2):e0246734.

Smart, J. J., A. Chin, A. J. Tobin, and C. A. Simpfendorfer.
2016. Multimodel approaches in shark and ray growth studies: strengths, weaknesses and the future. Fish Fish. 17:955–971.

Torres-Palacios, K., P. A. Mejía-Falla, A. F. Navia, V. H. Cruz-Escalona, R. Félix-Uraga, and C. Quiñonez-Velázquez.
2019. Age and growth parameters of the Panamic stingray (*Urotrygon aspidura*). Fish. Bull. 117:169–179.

Troynikov, V. S., and T. I. Walker.
1999. Vertebral size-at-age heterogeneity in gummy shark harvested off southern Australia. J. Fish Biol. 54:863–877.

Walker, T. I.
1998. Can shark resources be harvested sustainably? A question revisited with a review of shark fisheries. Mar. Freshw. Res. 49:553–572.

Walker, T. I., B. L. Taylor, R. J. Hudson, and J. P. Cottier.
1998. The phenomenon of apparent change of growth rate in gummy shark (*Mustelus antarcticus*) harvested off southern Australia. Fish. Res. 39:139–163.

Watanabe, S.
2009. Algebraic geometry and statistical learning theory, 284 p. Cambridge Univ. Press, Cambridge, UK.

Zamora-García, O. G.
2015. Identificación de un punto de referencia para el cierre de temporada con base en la captura incidental de la pesquería industrial de camarón del Alto golfo de California. M.S. thesis, 120 p. Univ. Nac. Aut. Mex., Mexico City, Mexcio. [Available from: website.]

National Marine
Fisheries Service
NOAA

Fishery Bulletin
established in 1881

Spencer F. Baird
First U.S. Commissioner
of Fisheries and founder
of *Fishery Bulletin*

Evaluation of factors contributing to postrelease mortality of greater amberjack (*Seriola dumerili*) in the northern Gulf of Mexico with depth and acceleration data from acoustic tags

Kelly S. Boyle (contact author)
Crystal L. Hightower
Sean P. Powers

Email address for contact author: ksboyle@uno.edu

School of Marine and Environmental Sciences
University of South Alabama and
Dauphin Island Sea Lab
101 Bienville Boulevard
Dauphin Island, Alabama 36528
Present address for contact author: Department of Biological Sciences
University of New Orleans
2000 Lakeshore Drive
New Orleans, Louisiana 70148

Abstract—Management of recreational fishing for greater amberjack (*Seriola dumerili*) in the Gulf of Mexico involves size regulations and closed seasons. Water temperature, salinity, fight and handling times, and barotrauma can influence survival of released fish. We examined postrelease mortality and behavior by using acoustic telemetry of the movements of 78 fish, monitored for up to 58 d across 3 sampling efforts in 2018, 2019, and 2020 over a depth gradient of 29–64 m. To assess descender devices as a mitigation tool, we assigned fish to 2 treatments: surface release without swim bladder venting and release with a descender device. Cox proportional hazards models were used to assess the effects of site depth, release treatment, bait type (jigging or live bait), fishing injury, tagging injury, fight and handling times, surface and bottom temperatures, and fish length. We found neither a positive association between mortality risk and site depth, as might be expected from barotrauma, nor increased survivorship for fish released with a descender device. The best-supported model considered only fish length as a factor in postrelease mortality; legal-size fish (≥864 mm in fork length) had a mortality risk 20 times greater than that of smaller fish. Our results indicate that sublegal-size fish released because of size restrictions face much lower mortality risk than legal-size fish.

Manuscript submitted 14 February 2022.
Manuscript accepted 7 July 2022.
Fish. Bull. 120:218–233 (2022).
Online publication date: 29 July 2022.
doi: 10.7755/FB.120.3-4.3

The views and opinions expressed or implied in this article are those of the author (or authors) and do not necessarily reflect the position of the National Marine Fisheries Service, NOAA.

The greater amberjack (*Seriola dumerili*) is a cosmopolitan tropical and temperate predatory fish taken in recreational and commercial fisheries (Smith-Vaniz, 2002). In the Gulf of Mexico, the greater amberjack is considered overfished and currently experiencing overfishing (SEDAR, 2020). Past amendments to the Gulf of Mexico Fishery Management Council fishery management plan included requirements for the use of non-stainless-steel circle hooks with natural baits, an increase in the recreational minimum size from 762 mm (30 in) to 864 mm (34 in) in fork length (FL), and seasonal closures during open recreational seasons for red snapper (*Lutjanus campechanus*) and other reef fish species (SEDAR, 2020). These factors make it likely that more greater amberjack will be caught at sublegal sizes (<864 mm FL at the time of the study) and out of season and then released. Therefore, there is a need to gain a better understanding of factors that contribute to discard mortality.

Greater amberjack discarded in recreational fisheries face several potential sources of mortality. These sources include the following: 1) at-vessel mortality (AVM), meaning a death after a fish is hooked but before landing; 2) capture and handling mortality (CHM), meaning a lethal event during capture and handling after landing that prevents successful release; and 3) postrelease mortality (PRM).

Several factors have been predicted to affect discard mortality associated with recreational fishing for greater amberjack. Swim bladder barotrauma is associated with increased PRM risk for some reef fishes (Curtis et al., 2015; Runde and Buckel, 2018). Swim bladders in acanthomorph fishes, like the greater amberjack, lack a pneumatic connection to the gut and are termed physoclistous (Lagler et al., 1962). Physoclistous fishes cannot expel gas from the swim bladder lumen through the pharynx and as a result must resorb gas into the blood stream through the oval (Woodland, 1913). Therefore, depth-related pressure changes from rapid fishing ascents may cause injury to swim bladder tissues, increase stress,

and make descent to deeper habitats difficult for fish after release. Results from a previous study of red snapper indicate that barotrauma is associated with both immediate discard mortality (AVM in our study) and delayed mortality (PRM in our study) (up to 72 h postrelease) and that barotrauma can be mitigated by venting the swim bladder or using a descender device to recompress the swim bladder and then releasing the fish at depth (Curtis et al., 2015).

Other factors may contribute to AVM and PRM in reef fishes like the greater amberjack. Fight time during fishing may raise risk of AVM and PRM by increasing stress (Mohan et al., 2020), depleting energy, and elevating predation risk. In addition, fight time may increase with fish size and fishing depth, and the combined factors may contribute to mortality. Water temperature, salinity, and dissolved oxygen may also be additional sources of physiological stress.

Biotelemetry was used to assess PRM in greater amberjack at artificial reefs off the coast of Alabama (Jackson et al., 2018). Using depth-logging acoustic tags to study fish that were vented and released, Jackson et al. (2018) found a PRM estimate (18.8%) similar to the estimate for 1 of 3 modeled PRM scenarios in a stock assessment from the same time (SEDAR, 2014). In our study, we caught greater amberjack in the northern Gulf of Mexico using common recreational angling techniques in 2018, 2019, and 2020. We used direct observation to calculate AVM and CHM and used data from acceleration- and depth-logging acoustic tags to estimate PRM of fish released at the surface or with a descender device. The main study objectives were 1) to estimate survivorship and associated PRM of discarded greater amberjack and 2) to evaluate the following factors as potential predictors of PRM risk: fish size, fight and handling times, use of a descender device, site depth, capture method (live bait or jigging), observed fishing and tagging injuries, and water temperature at the surface and on the bottom.

Materials and methods

Receiver deployment

Vemco VR2AR[1] acoustic receivers (Innovasea Systems Inc., Boston, MA) were deployed at 16 sites on artificial reefs before each study period in 2018, 2019, and 2020. Artificial reefs were steel and concrete pyramids, sunken boats, a barge, an oil rig jacket, a fuel tank, a grain hopper, and a submarine (Suppl. Table 1) (online only). One or 2 receivers were placed near each site (Suppl. Table 1) (online only). For deployment, VR2AR receivers were attached to cement moorings with approximately 2 m of polypropylene line attached to the detachable lug, and a midline swivel was present between the mooring and lug to prevent twisting. Two non-compressible 20-cm (8-in) trawl floats were attached to the receiver collar with 3.5-m of polypropylene line with a midline swivel to provide buoyancy. Each assembled receiver, along with its moorings and floats, was deployed at the sea surface and released with the manufacturer's acoustic release function with a Vemco VHTx-69k transponding hydrophone (Innovasea Systems Inc.) and VR100 receiver (Innovasea Systems Inc.) at the end of each study period.

Fish collection and tagging

Tagging took place on 16–17 and 23–24 August 2018, on 30 April and 13–14 May 2019, and on 17–18 and 21–22 August 2020. These dates were chosen on the basis of the availability of personnel and vessels and the aim to provide an opportunity to examine mortality under different water temperatures and at different fish sizes, which varied among the 3 study periods.

Greater amberjack were caught and tagged by following common recreational fishing methods on chartered boats (FV *Lady Ann* and FV *Escape*). Fish were caught by using 2 methods opportunistically, either with live bait (11/0 or 12/0 circle hooks, 340–450-g weights, and a 36.3–45.4-kg test monofilament leader with a swivel tied to the mainline) or with artificial lures (140–170-g jig heads with soft plastic lures). A data recorder on board, using a stopwatch, noted the time from when an angler first had a fish on the line to when the fish was landed (fight time, in seconds) and the time from the landing to the release of a fish (handling time, in seconds). Upon their landings, fish were immediately measured and ventilated with a saltwater hose. Standard, fork, natural total, and stretch total lengths were recorded to the nearest millimeter. Injuries to fish were noted prior to release, and all dead fish prior to landing (AVM events) were recorded.

Fishing release treatment (surface or descender device) was alternated in the order that fish were landed. Before fishing began each day, we randomly chose the starting release treatment. For the release treatment in which a descender device was used, a SeaQualizer Descending Device (standard model, SeaQualizer, Davie, FL) was attached to the fish's lower jaw and set to the deepest possible release depth (increments of 15.2 m, 30.5 m, and 45.7 m) at each site, requiring a release depth less than the site depth. The fish and descender device were lowered with approximately 2.3 kg of weight attached to a fishing rod along with a digital video camera (Hero5 Black Edition, GoPro Inc., San Mateo, CA) for observing potential predation.

Results from a previous study (Jackson et al., 2018) indicate that the observed "release condition" of a fish was indicative of PRM risk. We assigned a number for the release condition (Patterson et al., 2001; Jackson et al., 2018) of fish released at the surface as follows: 1, fish immediately oriented and swam downward rapidly; 2, fish appeared disorientated and swam down slowly; 3, fish appeared disoriented and remained at the surface for several minutes; and 4, fish was dead and unresponsive at the surface. It was not possible to assess release condition for fish released with a descender device because fish drifted out of the view of the camera in most cases.

[1] Mention of trade names or commercial companies is for identification purposes only and does not imply endorsement by the National Marine Fisheries Service, NOAA.

Fish were tagged with Vemco V9AP depth and accelerometry acoustic transmitters (Innovasea Systems Inc.) coded with the following parameters: activity algorithm, triaxial root mean square of acceleration, 5 samples/s, 20–40-s delay, accelerometer range of ±4.9 m/s, high power setting, a slope (resolution) of 0.3 m for depth, depth range of 68 m, and acceleration-to-depth transmission ratio of 1:1. We initially attached transmitters externally on fish rather than intraperitoneally to avoid inadvertent swim bladder venting that could result from surgical implantation and that might interfere with testing of barotrauma effects. In 2018, acoustic transmitters were attached externally on a second external dart tag (Floy FH-69 stainless-steel dart tag, Floy Tag Inc., Seattle, WA), with the tag attached to the dart with a 68-kg monofilament line. Dart tags were inserted and locked to interneurals (pterygiophores) below the spiny dorsal fin on the left side. Prior to tagging, acoustic transmitters were attached to tags with marine epoxy and 2 zip ties, with the transmitter's longitudinal axis parallel to the external tag. A second dart tag (FIM-96 nylon dart tag, Floy Tag Inc.), with a unique tag ID, phone number, and website URL on it, was placed caudally to the stainless-steel dart tag on the fish's left side.

Because of acoustic transmitter shedding (see the "Results" section) in 2018, we modified the tagging procedure for 2019 and 2020. Vemco V9AP accelerometer transmitters were placed intraperitoneally through a small incision, just wide enough to pass the transmitter. The incision was made in the left abdomen, just dorsal (1–2 cm) and anterior (1–2 cm) to the cloaca. The swim bladder was not visible in any tagging surgeries, and no evidence of venting was observed. After tag implantation, incisions were closed with 2 interrupted sutures by using monofilament suture thread. In addition to acoustic transmitters, fish received a dart tag with ID and contact information as described above: FIM-96 tags were used in 2019, and FH-69 tags were used in 2020.

Postrelease fate inferred from acoustic telemetry

We used depth and acceleration data from tagging of fish to infer their fate (Whitney et al., 2016). We tabulated raw depth and acceleration data from receivers by time and examined graphs of all raw data. We plotted raw data over an approximately 5-d period (if available) at the end of the detection period for each fish or, in the cases of suspected mortality or tags that had been shed (see the "Postrelease fate based on acoustic telemetry" subsection in the "Results" section), over the time period of suspected death or tag shedding. Fish were determined to be dead when transmissions indicated that the tag was on the bottom and acceleration had ceased. Rapid onset of high acceleration values were predicted to indicate possible predation or carcass scavenging.

Survivorship

We estimated overall survivorship, accounting for all sources of discard mortality (AVM, CHM, and PRM); at-vessel survivorship, accounting for AVM and CHM; and postrelease survivorship, accounting for PRM. Survivorship ($\hat{S}$) and its standard error (SE) were estimated from acoustic telemetry (see the "Results" section) and data on recapture of fish by using equations 17 and 18 of Pollock and Pine (2007):

$$\hat{S} = \frac{x}{n}, \tag{1}$$

$$SE(\hat{S}) = \sqrt{\frac{\hat{S}(1-\hat{S})}{n}}, \tag{2}$$

where x = the number of surviving fish; and

n = the number of fish: in the context of this equation, total number of fish caught or dead prior to landing for estimates of overall survivorship, number of fish landed for at-vessel survivorship, or number of fish released for postrelease survivorship.

We produced Cox proportional hazards models (Cox, 1972) to test for the contribution of factors (i.e., fishing related variables, abiotic conditions, release treatment, and fish size) to postrelease mortality. Cox models were produced by using the survival package (vers. 3.2-13; Thernau, 2021) in R (vers. 4.1.1; R Core Team, 2021). For all models, we report the statistic from the likelihood ratio test in which models were compared to a null model and the P-values for each test and their associated model predictors. Separate models were run for externally tagged fish and internally tagged fish because many fish in the former group shed their transmitters. Only some fish were recaptured, and because it is not possible to determine death events after acoustic tags ceased to transmit data for fish that were not recaptured, we restricted the observation period of our Cox models and survivorship curves to the period when acoustic tags were transmitting and receivers were deployed. This restricted observation period did not change model outcomes but limited the duration of survivorship curves to <60 d. All 9 recaptured fish had transmitters that were detected until the end of predicted transmitter battery life or receiver retrieval, but 4 of these fish were externally tagged fish that shed their acoustic tags. Acceleration and depth data from the tags attached to these 4 fish indicate that tags were shed within range of receivers while they were still transmitting (see the "Results" section).

We initially considered the following potential predictors: FL (in millimeters); fight and handling times; release treatment (categorical, fish released at surface or with descender device); site depth; bait type (categorical, live bait or jigging); fishing injury (categorical, no injury versus visible injury from fishing gear before handling and tagging); tagging injury (categorical, no injury versus visible bleeding from site of external tagging); surface, mid-depth, and bottom water temperatures; surface, mid-depth, and bottom salinities; and surface, mid-depth, and bottom dissolved oxygen. Barotrauma injuries (e.g., expanded swim bladders and bulging eyes) were not included in models because they were never observed, although internal tissue damage may have been present. Release condition

was not tested because that information was not available for fish released with a descender device. Before including predictors in Cox models, we tested for correlation among predictors with Spearman rank correlation tests (Kneebone et al., 2021) (Suppl. Table 2) (online only). Many abiotic variables (e.g., temperature, salinity, and dissolved oxygen) were highly correlated (Suppl. Table 2) (online only); therefore, we reduced the analysis to include bottom and surface temperature as the only abiotic variables. Several additional correlations were observed among other predictors included in initial Cox models (e.g., fight time and fish length; Suppl. Table 2 [online only]), and these correlations are considered in our interpretation of results.

The internal placement of tags in fish in 2019 and 2020 may have caused additional handling stress, and although attempts were made to not vent the swim bladder, we inadvertently may have partially vented it. Therefore, we used separate Cox models to analyze fish with transmitters placed externally (in 2018) and those with transmitters placed intraperitoneally (in 2019 and 2020). Stepwise model selection was conducted with the stepAIC function from the package MASS (vers. 7.3-54; Venables and Ripley, 2002) in R, and both forward and backward selections were attempted to select the model with the lowest Akaike information criterion (AIC). We used the AIC with correction for small sample sizes (AICc) (Burnham and Anderson, 2002) and considered models with a difference in AICc from that of the best model (ΔAICc) of 2 units or less to have comparable support, unless the model with more variables differed by addition of a single parameter, indicating a potentially spurious variable (Burnham and Anderson, 2002).

Predictor data were missing for several fish: fight time (1 fish from 2018), handling time (1 fish from 2018), bottom temperature (14 fish from 2019 and 2020), and fight and handling times (6 fish from 2019 and 2020). Therefore, to explore all factors, we began with full models for the subset of fish with available predictor data and completed stepwise AICc model selection. In one instance, for internally tagged fish with bottom temperature data available, the full model was overparameterized and did not converge. We ran exploratory models with single predictors and removed predictors with the highest AICc before running the stepwise procedure on the fullest model that would converge. We then ran separate procedures for stepwise AICc model selection on the complete data sets (externally tagged fish from 2018 [number of fish (n)=23] and internally tagged fish from 2019 and 2020 [n=55]) that did not include the predictors that were missing for some fish.

Kaplan–Meier survival function curves were generated for variables informed by Cox models by using the survfit function in the survival package in R and were plotted with the survminer package (vers. 0.4.9; Kassambra et al., 2021) in R.

Results

We tagged 78 greater amberjack at 15 artificial reef sites that ranged in depth from 29 to 64 m during separate efforts in 2018, 2019, and 2020 (Table 1). Three fish died before successful release (Table 1). Fish D1 died on the boat and was bleeding severely from the hook site (classified as a CHM). Fish D2 died from a propeller injury, and fish D3 died from predation by a shark before landing (both considered an AVM). All other fish released at the surface had a release condition of 1. In underwater video from the descender rig, fish were usually out of view because of a long leader between the camera and fish. Therefore, fish released with a descender device near the bottom were rarely observed, and it was not possible to determine their release condition. Further, no predation or potential predators (e.g., carcharhinid sharks) were observed on video.

Fourteen acoustically tagged fish were detected on receivers at reefs where they were not originally tagged (Table 1). Three of these 14 fish, fish 118, 120, and 121, were detected on 2 reefs at close proximity (0.5 km apart) throughout the study. Six fish tagged in 2020 (fish 53, 58, 104, 105, 107, 115) were not detected on the first day after being tagged and released (Table 1).

Postrelease fate based on acoustic telemetry

Patterns of acceleration and depth over time were distinct among fish determined to have died versus lived. Seven fish acoustically tagged during 2018–2020 were inferred to have died (Fig. 1, Table 2). Profiles from tags of dead fish indicate only brief depth changes and acceleration oscillations greater than 2 m/s^2 (Fig. 1, Table 2). Fish 22, 31, 51, 117, and 119 were dead very soon after release (≤2 h), and fish 23 and 47 remained alive longer (Fig. 1, Table 2). In contrast, fish inferred to have lived had strong and consistent depth and acceleration oscillations until the end of predicted transmitter battery life or deployments of acoustic receiver arrays, until they emigrated from receiver arrays, or in the case of some fish with externally placed transmitters (as was done in 2018), until their tag was shed (Fig. 2, Table 2, Suppl. Figs. 1 and 2, Suppl. Table 2 [online only]).

Acceleration and depth profiles indicate that 13 of 23 fish tagged in 2018 shed their tags, and information on the recapture of fish by anglers confirms this outcome in 4 instances (Table 1); secondary external tags were not shed. Results of analysis of the carcass of a recaptured fish indicate that the stainless-steel dart remained in place but that the monofilament line attachment point broke on the dart, perhaps as a result of drag on the tag or the fish actively scraping the tag off. No tags that were intraperitoneally placed in 2019 or 2020 were shed. Telemetry profiles for fish inferred to have shed tags indicate relatively consistent depth and acceleration oscillations that abruptly ended at the time of the presumed tag shedding (Fig. 2, Table 2, Suppl. Figs. 1 and 2, Suppl. Table 3 [online only]). The tag records for fish inferred to have shed tags differed from the tag records of fish presumed to have died; for fish that died, acceleration and depth variation was evident but less consistent during the brief period before their apparent death (Fig. 1). Ten fish were detected briefly (<4 h)

Table 1

Summary of tagging effort and the fork lengths (FLs) and fates for greater amberjack (*Seriola dumerili*) caught on charter boats in the northern Gulf of Mexico during 2018–2020. Tagged fish were released either at the surface (S) or with a descender device (DC). In 2018, fish had an acoustic tag attached to a primary external tag (Ex.), and in 2019 and 2020, fish had an acoustic transmitter placed intraperitoneally (In.), in addition to a secondary external tag. Symbols after the last detection date indicate if the tag was shed (st) or if the fish was recaptured (†). Fish <864 mm FL were of sublegal size. Either jigging (J) or live bait (L) was used to catch fish. Fates of fish include alive (A), dead (D), lived until recaptured (R), emigrated outside of detection range during the life of the transmitter battery and before receivers were retrieved (E), moved between sites with receivers (M), and unknown because the fish spent <68 h in the receiver array (U). Symbols in the "Fate" column indicate that the external tag was shed, either determined from acceleration and depth data (*) or confirmed from angler recapture (**). Fish D1 was dead before release, fish D2 died from a propeller injury before landing, and fish D3 died of predation before landing. UK=unknown because no data were taken.

Fish ID	Release type	Tag type	Site depth (m)	Tagging date	Detection date		FL (mm)	Bait type	FT (s)	HT (s)	Fate
					First	Last					
01	S	Ex.	30.5	16-Aug-2018	16-Aug-2018	23-Aug-2018[st]	950	L	99	146	A*
02	DC	Ex.	33.2	16-Aug-2018	16-Aug-2018	16-Aug-2018	1006	L	172	126	U
03	S	Ex.	33.2	16-Aug-2018	16-Aug-2018	1-Aug-2019[†]	750	L	73	137	R**
04	DC	Ex.	37.0	16-Aug-2018	16-Aug-2018	5-Jun-2019[†]	995	L	250	155	R**
05	S	Ex.	37.0	16-Aug-2018	16-Aug-2018	17-Sep-2018[st]	630	J	145	135	A*
06	DC	Ex.	37.0	16-Aug-2018	16-Aug-2018	12-Sep-2018[st]	527	J	54	UK	A*
07	S	Ex.	37.0	16-Aug-2018	16-Aug-2018	23-Aug-2018[st]	1100	L	UK	22	A*
08	DC	Ex.	45.0	16-Aug-2018	16-Aug-2018	21-Aug-2018[st]	895	L	141	159	A*
09	S	Ex.	45.0	16-Aug-2018	16-Aug-2018	16-Aug-2018	930	L	108	72	U
10	DC	Ex.	45.0	16-Aug-2018	16-Aug-2018	19-Sep-2018[†]	940	L	173	107	R**
11	S	Ex.	45.0	16-Aug-2018	16-Aug-2018	16-Aug-2018[st]	900	L	171	58	A*
12	DC	Ex.	49.0	16-Aug-2018	16-Aug-2018	8-Oct-2018	855	L	117	151	A
13	S	Ex.	52.4	17-Aug-2018	17-Aug-2018	17-Aug-2018	984	L	134	98	AE
14	DC	Ex.	52.4	17-Aug-2018	17-Aug-2018	17-Aug-2018	1029	L	185	75	U
15	S	Ex.	52.4	17-Aug-2018	17-Aug-2018	17-Aug-2018	986	L	167	93	U
16	DC	Ex.	38.0	17-Aug-2018	17-Aug-2018	17-Aug-2018	896	L	170	117	AE
17	S	Ex.	38.0	17-Aug-2018	17-Aug-2018	17-Aug-2018[st]	917	J	269	62	U*
18	DC	Ex.	38.0	17-Aug-2018	17-Aug-2018	17-Aug-2018	905	L	99	210	U
19	S	Ex.	38.0	17-Aug-2018	17-Aug-2018	17-Aug-2018[st]	966	J	260	58	AE*
20	DC	Ex.	38.0	17-Aug-2018	17-Aug-2018	17-Aug-2018[st]	919	L	154	93	A*
21	S	Ex.	33.2	23-Aug-2018	23-Aug-2018	5-Jun-2019[†]	836	L	98	129	R**
22	DC	Ex.	33.2	23-Aug-2018	23-Aug-2018	23-Aug-2018	779	L	100	157	D
23	S	Ex.	37.0	23-Aug-2018	23-Aug-2018	26-Aug-2018	540	J	55	70	D
24	DC	In.	29.1	30-Apr-2019	30-Apr-2019	25-Jun-2019	835	J	UK	UK	A
25	S	In.	29.1	30-Apr-2019	30-Apr-2019	23-May-2019	736	L	UK	UK	AE
26	DC	In.	29.1	30-Apr-2019	30-Apr-2019	6-Jan-2020[†]	730	L		UK	R
27	S	In.	29.1	30-Apr-2019	30-Apr-2019	15-Oct-2021[†]	730	L		UK	R
28	DC	In.	64.0	30-Apr-2019	30-Apr-2019	2-Aug-2019[†]	829	L		UK	R
29	S	In.	64.0	30-Apr-2019	30-Apr-2019	23-May-2019	825	L		UK	AE
30	DC	In.	64.0	30-Apr-2019			1030	L	156	318	U
31	S	In.	64.0	30-Apr-2019	30-Apr-2019	30-Apr-2019	983	L	374	278	D
32	DC	In.	32.3	13-May-2019	13-May-2019	25-Jun-2019	718	J	99	320	AM
33	S	In.	32.3	13-May-2019	13-May-2019	25-Jun-2019	735	L	10	219	A
34	DC	In.	32.3	13-May-2019	13-May-2019	31-May-2019	707	J	112	228	AE
35	S	In.	32.3	13-May-2019	13-May-2019	25-Jun-2019	720	L	90	136	AM
36	DC	In.	36.9	13-May-2019	13-May-2019	25-Jun-2019	634	J	90	285	A
37	S	In.	36.9	13-May-2019	13-May-2019	25-Jun-2019	703	L	60	189	A
38	DC	In.	64.0	14-May-2019	14-May-2019	22-Jun-2019	650	J	96	534	AE
39	S	In.	64.0	14-May-2019	14-May-2019	22-Jun-2019	809	L	115	355	AE
40	DC	In.	64.0	14-May-2019	14-May-2019	24-May-2020[†]	705	L	120	430	R
41	S	In.	64.0	14-May-2019	14-May-2019	25-Jun-2019	800	J	165	394	A
42	DC	In.	64.0	14-May-2019	14-May-2019	22-Jun-2019	734	L	108	538	AE
43	S	In.	29.1	14-May-2019	14-May-2019	25-Jun-2019	656	L	47	248	A
44	DC	In.	29.1	14-May-2019	14-May-2019	27-May-2019	716	J	100	445	AE
45	S	In.	29.1	14-May-2019	14-May-2019	27-May-2019	705	J	130	548	A
47	DC	In.	37.0	17-Aug-2020	17-Aug-2020	27-Aug-2020	961	L	177	324	D

(*Continued on next page*)

Table 1 (*continued*)

Fish ID	Release type	Tag type	Site depth (m)	Tagging date	Detection date		FL (mm)	Bait type	FT (s)	HT (s)	Fate
					First	Last					
48	S	In.	37.0	17-Aug-2020	17-Aug-2020	18-Aug-2020	601	L	73	243	UME
49	DC	In.	37.0	17-Aug-2020	17-Aug-2020	14-Sep-2020	1050	L	170	286	AME
50	S	In.	36.1	17-Aug-2020	17-Aug-2020	21-Aug-2020	920	L	117	223	AME
51	DC	In.	36.1	17-Aug-2020	17-Aug-2020	17-Aug-2020	1064	L	358	241	D
52	S	In.	34.8	18-Aug-2020	18-Aug-2020	1-Oct-2020	785	L	87	203	A
53	DC	In.	34.8	18-Aug-2020	25-Aug-2020	23-Sep-2020	804	L	285	175	AME
54	S	In.	34.8	18-Aug-2020			895	L	45	152	U
55	DC	In.	34.8	18-Aug-2020	18-Aug-2020	18-Aug-2020	800	L	367	165	U
56	S	In.	34.8	18-Aug-2020	30-Aug-2020	1-Oct-2020	780	L	386	234	A
57	DC	In.	34.8	18-Aug-2020	18-Aug-2020	1-Oct-2020	773	L	411	149	A
58	S	In.	34.8	18-Aug-2020	28-Aug-2020	1-Oct-2020	715	L	332	146	A
59	DC	In.	34.8	18-Aug-2020	18-Aug-2020	1-Oct-2020	810	L	295	281	A
101	S	In.	34.8	18-Aug-2020			980	L	341	155	U
103	DC	In.	34.8	18-Aug-2020			845	L	175	225	U
104	DC	In.	34.8	18-Aug-2020	28-Aug-2020	14-Sep-2020	845	L	115	225	AE
105	S	In.	34.8	18-Aug-2020	30-Aug-2020	1-Oct-2020	785	L	264	198	A
106	DC	In.	34.8	18-Aug-2020	18-Aug-2020	1-Oct-2020	787	L	424	196	A
107	S	In.	38.0	18-Aug-2020	29-Aug-2020	26-Sep-2020	800	L	113	207	AE
108	DC	In.	38.0	18-Aug-2020	18-Aug-2020	1-Oct-2020	515	L	28	172	AM
109	S	In.	38.0	18-Aug-2020	18-Aug-2020	1-Oct-2020	751	L	130	185	AM
110	DC	In.	38.0	18-Aug-2020	18-Aug-2020	18-Aug-2020	520	J	75	125	U
111	S	In.	38.0	18-Aug-2020	18-Aug-2020	15-Sep-2020	491	J	112	124	AME
112	DC	In.	38.0	18-Aug-2020			476	J	100	121	U
113	S	In.	38.0	18-Aug-2020	18-Aug-2020	26-Aug-2020	824	L	126	159	AE
114	DC	In.	38.0	18-Aug-2020	18-Aug-2020	1-Oct-2020	750	L	146	243	AM
115	S	In.	36.1	21-Aug-2020	22-Aug-2020	24-Aug-2020	959	L	202	188	UME
116	S	In.	36.1	21-Aug-2020	21-Aug-2020	14-Sep-2020	1004	L	331	151	AE
117	S	In.	36.1	21-Aug-2020	21-Aug-2020	21-Aug-2020	945	L	125	171	D
118	DC	In.	47.8	22-Aug-2020	22-Aug-2020	25-Sep-2020	774	L	116	157	AE
119	S	In.	47.8	22-Aug-2020	22-Aug-2020	22-Aug-2020	641	L	57	177	D
120	DC	In.	47.8	22-Aug-2020	22-Aug-2020	1-Oct-2020	865	L	147	105	R
121	DC	In.	47.8	22-Aug-2020	22-Aug-2020	22-Aug-2020	476	L	37	472	U
D1	–	–	37.0	16-Aug-2018	–	–	510	J	29	–	D
D2	–	–	37.0	23-Aug-2018	–	–	1023	L	243	–	D
D3	–	–	33.2	16-Aug-2018	–	–	UK	L	180	–	D

(Fig. 3). Few detections occurred for these fish, but the depth and acceleration values were similar to fish that lived (Fig. 3, Table 2). Five fish were never detected by any receivers (Table 1).

Among released fish that died, 4 greater amberjack (57%) were released at the surface and 3 fish (43%) were released with a descender device. For externally tagged fish for which PRM was not observed, the length of time during which their tags were detected in 2018 was variable (median: 7.8 d; 1st quartile: 2.8 d; 3rd quartile: 33.0 d) because some fish shed their transmitters and were not recaptured and some likely emigrated away from reefs with acoustic receivers. For internally tagged fish, the length of time during which their tags were detected in 2019 and 2020 were longer (median: 38.9 d; 1st quartile: 14.1 d; 3rd quartile: 43.8 d). Eight fish were captured 90 d or later (maximum: 899 d) after tagging.

Recapture rate and postrelease survivorship

The fish recapture rate from recreational and commercial angling (fishing mortality rate) was 11.5%. In 2018, acoustic tags were placed externally. Postrelease mortality was inferred from acceleration and depth data for 2 fish in 2018, 1 fish in 2019, and 4 fish in 2020, or 9% of fish tagged in all 3 years combined.

We estimated survivorship with data for all fish in the study except fish that either were never recaptured or were detected acoustically for less than 68 h, the latest observed PRM event (Fig. 1). Overall survivorship after accounting for all sources of discard mortality, AVM, CHM, and PRM (i.e., including the 3 fish that died before release), was moderate ($\hat{S}$=84.6% [SE 4.1]). At-vessel survivorship following AVM and CHM was 94.8% (SE 4.4), and postrelease survivorship was 88.7% (SE 4.2).

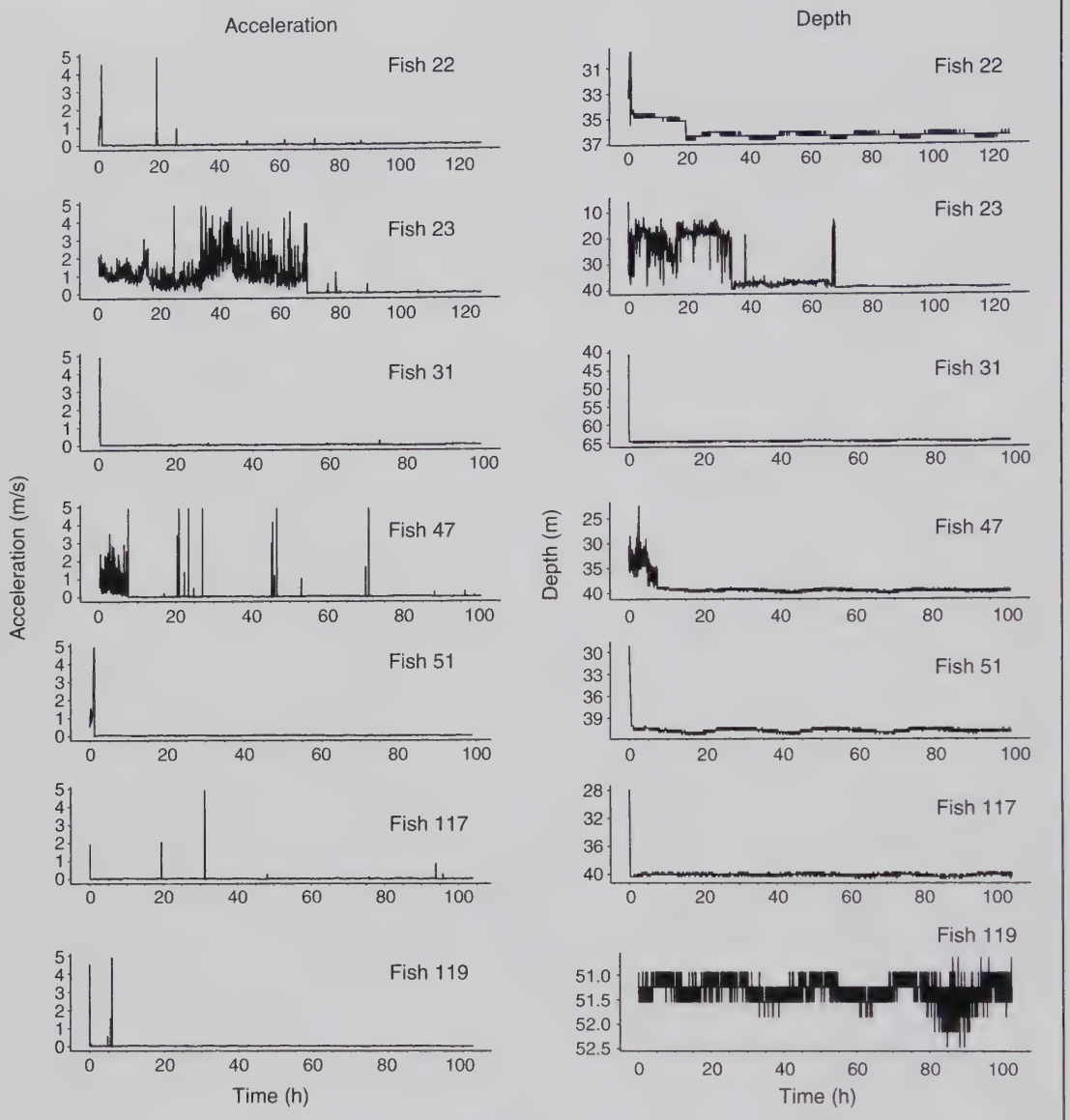

Figure 1

Acceleration and depth profiles from acoustic telemetry for tagged greater amberjack (*Seriola dumerili*) in the northern Gulf of Mexico inferred to have died after release. Table 2 provides the rationale for the fate and time of inferred death of each fish. Fish were caught and tagged on charter boats during 2018–2020.

Cox proportional hazards models: factors of postrelease mortality

The 2 best models used to examine PRM of fish tagged with external transmitters in 2018 received comparable support (ΔAICc: 0.86), and both included bait type and surface temperature as predictors (Table 3). In the second-best model, bait type and surface temperature were significant predictors (Table 3); however, the very small hazard ratios associated with these predictors indicate a tiny decrease in mortality associated with fish caught on a jig and an even smaller decrease in mortality with each 1°C increase in surface temperature. No predictors were significant in the best model, which also included fishing injury as a variable (Table 3). Effects of fight and handling times were tested by using a subset of data from 2018 for fish for which these values were available, and these factors were not significant predictors of mortality in any of the models used in this study (Suppl. Tables 4–6) (online only). The Kaplan–Meier survivorship curve for fish tagged externally in 2018 (Fig. 4) indicates that survival probability dropped to 94.7% 2 h postrelease and to 88.8% 68 h postrelease and then remained at that level throughout the rest of the period of acoustic monitoring.

Table 2

Fates of 25 greater amberjack (*Seriola dumerili*) tagged and released between 2018 and 2020 in the northern Gulf of Mexico, inferred with depth and acceleration data from acoustic tags. Fates include alive (A), alive and detected on 2 separate reef sites before emigrating away from the receiver array (AME), alive and emigrated (AE), alive and shed tag (AST), alive but detected for <68 h (U), alive and detected on 2 separate reef sites for 68 h (UM), and dead (D). Also noted for each fish are the figure (Fig.) showing acceleration and depth data that were recorded before and continued to be recorded until the last acoustic detection or fate assignment and either the time from release to fate assignment determined from acoustic telemetry data (alive, dead, or shed tag) or the date the fish was recaptured.

Fish ID	Fate	Rationale for fate assignment	Fig.	Time to fate (h) or recapture date
22	D	Brief acceleration activity and little depth variation indicates fish remained near bottom (at depth of ~36.5 m) and ventured up to a depth of only 30 m. Appears to have died within 2 h postrelease. Movement seen in slightly deeper water 20 h after first detection consistent with movement of carcass by scavengers or of tag by currents.	1	2.00
23	D	Appears near bottom from 34 to 67 h postrelease, but acceleration indicates fish still moving vigorously. Makes one last foray to shallow water (depths of 38.5–15.5 m) ~67 h postrelease (perhaps dragged by a predator and dropped). Tag remains on bottom after 68 h.	1	67.97
31	D	Brief, strong acceleration quickly ceases. Depth values drop quickly, indicating that fish is dead on the bottom.	1	0.28
47	D	Acceleration stops suddenly at time of death with additional brief peaks (~20, ~45, and ~70 h postrelease) not associated with depth changes but consistent with movement of carcass by scavengers or of tag by currents.	1	7.62
51	D	Acceleration stops suddenly, and fish is at the bottom (depth of ~39 m) within 1.20 h postrelease.	1	1.20
117	D	Detected on the bottom (depth of ~40 m), and acceleration stopped within 0.20 h postrelease. Additional, isolated accelerations at ~20, 30, and 94 h postrelease consistent with movement of carcass by scavengers or of tag by currents.	1	0.20
119	D	Appears dead within 1 min of release. Only one acceleration transmission indicative of fish movement and first depth detections occur on bottom at depth of ~51.5 m. Additional movement ~6 h postrelease is consistent with movement of carcass by scavengers or of tag by currents.	1	0.02
01	AST	Tag shed (inferred) 166 h postrelease. Consistent variation of acceleration and depth and an immediate cessation of movement when tag is on bottom, at a depth of ~33 m. Note similarity to depth and acceleration profiles of fish 03, 08, and 10 in Figure 2.	2	166.38
03	AST	Tag shed, confirmed from recapture by angler. Tag appears to have been shed 164 h postrelease. Note similarity to fates of fish 01, 08, and 10.	2	1-Aug-2019
08	AST	Tag shed (inferred) 116 h postrelease. Note similarity to fates of fish 01, 03, and 10.	2	115.95
10	AST	Tag shed, confirmed from recapture by angler during acoustic monitoring period. Tag appears to have been shed 86 h postrelease. Note similarity to fates of fish 01, 03, and 08 in Figure 2. Data was right-censored at 800.50 h postrelease in Cox proportional hazards models.	2	19-Sept-2018
27	A	Remains alive and emigrates, confirmed by angler recapture. Note the large gaps in detection of tag transmissions at ~765–770 h, ~815–820 h, and ~840–850 h postrelease.	2	15-Oct-2021
29	AE	Appears alive until it leaves acoustic receiver array.	2	543.17
118	A	Appears alive through the end of tag transmissions.	2	813.00
120	A	Appears alive through the end of tag transmissions.	2	960.98
02	U	Very few detections, but fish appears alive when last detected.	3	0.60
09	U	Only 3 acceleration and 2 depth detections, but fish appears to have been alive when last detected.	3	3.07
14	U	Very few detections, but fish appears to have been alive when last detected.	3	1.72
15	U	Very few detections, but fish appears to have been alive when last detected.	3	1.22
18	U	Only 3 acceleration and 5 depth detections, but fish appears to have been alive when last detected.	3	0.28
48	UM	Few detections. Fish is detected at a second site after emigrating from first site. Fish appears alive when last detected.	3	11.70
50	AME	Fish is detected at a second site after emigrating from first site. Fish appears alive after leaving receiver array.	3	93.83
55	U	Very few detections, but fish appears to have been alive when last detected.	3	3.50
115	U	Very few detections, but fish appears to have been alive when last detected.	3	67.23
121	U	Very few detections, but fish appears to have been alive when last detected.	3	0.45

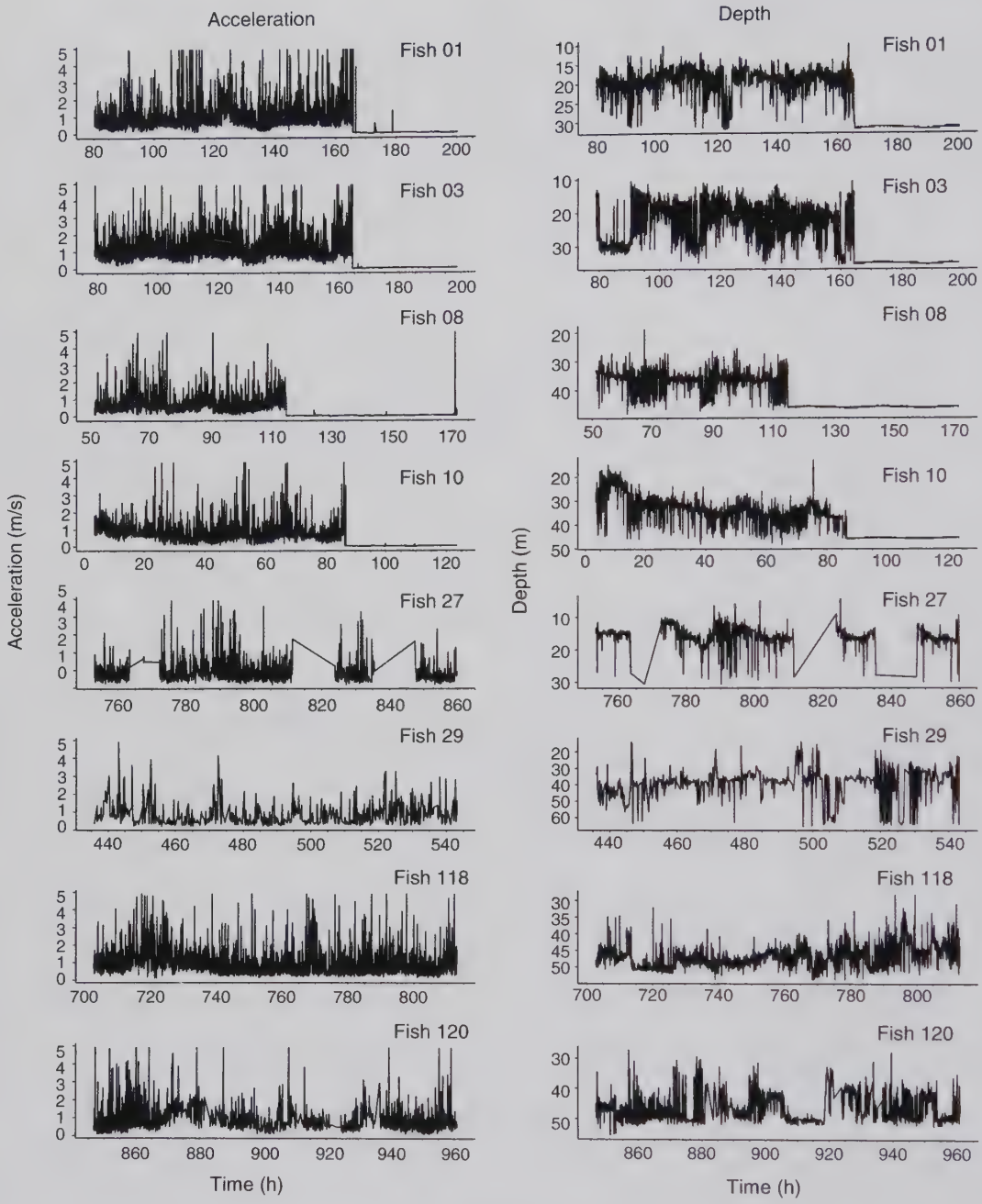

Figure 2

Acceleration and depth profiles from acoustic telemetry for tagged greater amberjack (*Seriola dumerili*) in the northern Gulf of Mexico inferred to have lived after release until the end of the battery life for their transmitters, until they emigrated from the detection range of the acoustic receiver at their release site, or until they shed their tag. Table 2 provides the rationale for the fate of each fish. Fish were caught and tagged on charter boats during 2018–2020.

For fish internally tagged in 2019 and 2020, fish length was the best predictor of survivorship, with PRM risk increasing with fish length (Table 4). The second-best model (ΔAICc: 0.67) included fishing injury in addition to fish length (Table 4). With legal length (≥864 mm FL) considered a categorical predictor, the estimated hazard ratio indicates 20 times greater PRM risk for fish of legal lengths (Table 4, Fig. 5). Legal-size fish had an estimated survival probability of 55.6% 7.6 h postrelease, and sublegal-size fish had a survival probability of 97.6% from

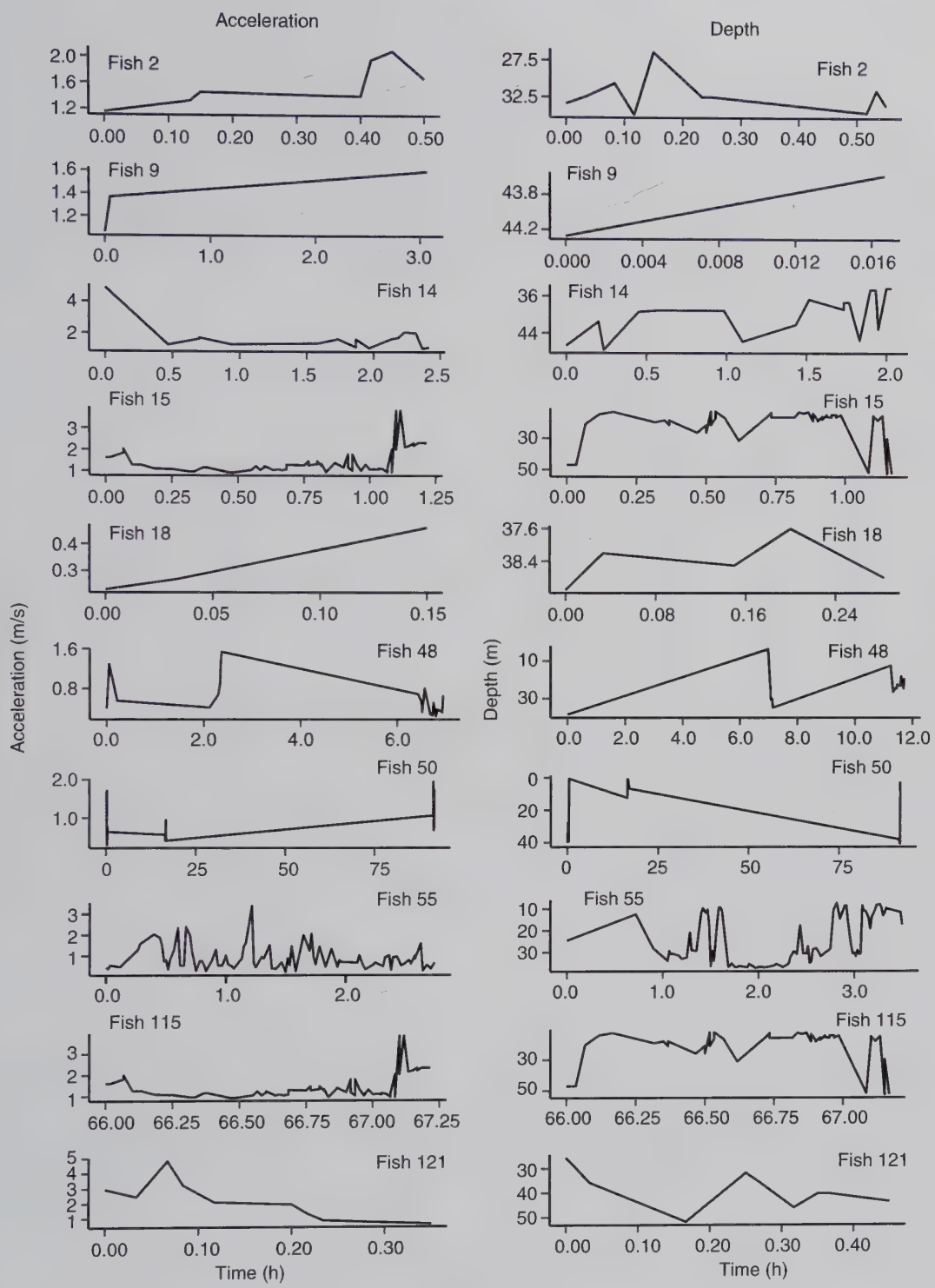

Figure 3

Acceleration and depth profiles from acoustic telemetry for tagged greater amberjack (*Seriola dumerili*) that were briefly detected with receiver arrays deployed at 16 artificial reef sites in the northern Gulf of Mexico. Fish were caught and tagged on charter boats during 2018–2020. All acceleration and depth data through the last detection of each fish are shown. The fish were inferred to be alive at the time of the last detection. All fish for which data are depicted in this figure, except fish 50, had a fate classified as *unknown* because their tags were detected for less than 68 h (the longest time observed in a case of postrelease mortality).

Table 3

Results from analysis with the Cox proportional hazards models fit to data for a subset of greater amberjack (*Seriola dumerili*) tagged with external acoustic transmitters in 2018 in the northern Gulf of Mexico (number of fish [*n*]=23). In the full model, the following predictors (P) are considered: fork length (FL); use of a descender device or not (DC); bait type (BJ), live bait or jigging; fishing injury (FI), an injury attributed to fishing gear; tagging injury (TI), an injury associated with the tagging procedure; surface temperature (ST); site depth (D); and bottom temperature (BT). Stepwise model selection based on Akaike information criterion (AIC) scores was used to determine the model with the most support. For each model, the AIC corrected for small sample sizes (AICc), the difference in AICc between the model and the best model (ΔAICc), and the likelihood ratio test statistic used to determine support of each model relative to a null model are provided. For each predictor in each model, the beta coefficient (β) and its standard error (SE) and the hazard ratio and its 95% confidence interval (95% CI) are provided. An asterisk (*) indicates that the predictor or model is significant (P<0.05).

AICc	ΔAICc	P	β	SE	Hazard ratio	Hazard ratio 95% CI	*P*	Likelihood ratio statistic	df	Overall *P*
Full model										
26.29	19.02							11.4	8	0.200
		FL	−0.18	43.32	0.837	1×10^{-37}–6×10^{36}	0.997			
		DC	−9.13	30,010	11,000	~0 to ∞	~1			
		D	−2.72	3232	0.066	~0 to ∞	0.999			
		BJ	−85.0	17,330	1.2×10^{-37}	~0 to ∞	0.996			
		FI	−46.9	1.2×10^{5}	4.2×10^{-21}	~0 to ∞	~1			
		TI	−3.05	1.6×10^{5}	21.2	~0 to ∞	~1			
		ST	−57.6	23,560	0.7×10^{-26}	~0 to ∞	0.998			
		BT	−31.3	81,380	2.5×10^{-14}	~0 to ∞	~1			
Second-best model										
8.13	0.86							7.9	2	0.020*
		BJ	−21.1	1.44	6.8×10^{-10}	4×10^{-11}–1×10^{-8}	<0.001*			
		ST	−76.7	5.13	5.2×10^{-34}	2×10^{-38}–1×10^{-29}	<0.001*			
Best model										
7.26	0.00							11.3	3	0.010*
		BJ	−61.3	12,170	1.2×10^{27}	~0 to ∞	0.996			
		FI	−41.7	52,850	7.7×10^{-19}	~0 to ∞	0.999			
		ST	−148	25,950	5.7×10^{-65}	~0 to ∞	0.995			
Null model										
11.30	4.17									

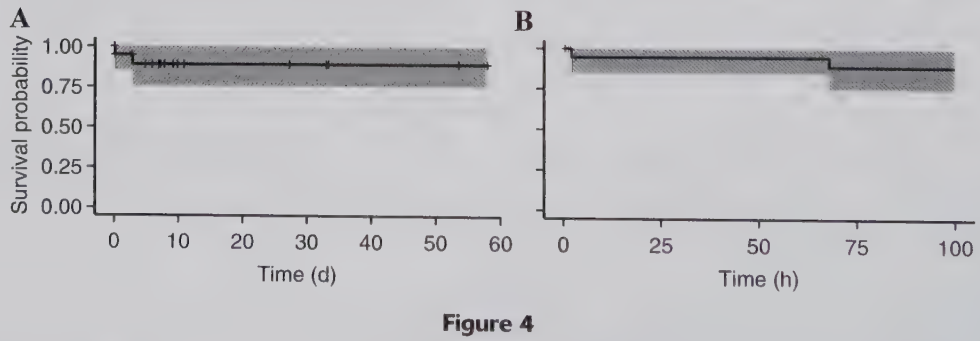

Figure 4

The Kaplan–Meier survivorship curve for greater amberjack (*Seriola dumerili*) with external acoustic tags in the northern Gulf of Mexico in 2018, (**A**) for the entire period (>50 d) for which transmitters and receivers were active and (**B**) for the first 100 h postrelease. Each cross along the curve indicates when data were censored because a fish emigrated away from acoustic receivers or shed its tag. The gray area indicates the 95% confidence interval for survival probability.

Table 4

Results from analysis with the Cox proportional hazards models fit to data for greater amberjack (*Seriola dumerili*) implanted with internal transmitters in the northern Gulf of Mexico in 2019 and 2020 (number of fish [*n*]=55). In the models, the following predictors (P) are considered: fork length (FL); use of a descender device or not (DC); bait type (BJ), live bait or jigging; fishing injury (FI), an injury attributed to fishing gear; tagging injury (TI), an injury associated with the tagging procedure; site depth (D); surface temperature (ST); and fish length (LG), with fish categorized as legal (≥864 mm FL) or sublegal size. Stepwise model selection based on Akaike information criterion (AIC) scores was used to evaluate the influence of these predictors. For each model, the AIC corrected for small sample sizes (AICc), the difference in AICc between the model and the best model (ΔAICc), and the likelihood ratio test statistic used to determine support of each model relative to a null model are provided. For each predictor in each model, the beta coefficient (β) and its standard error (SE) and the hazard ratio and its 95% confidence interval (95% CI) are provided. An asterisk (*) indicates that the predictor or model is significant (P<0.05).

AICc	ΔAICc	P	β	SE	Hazard ratio	Hazard ratio 95% CI	*P*	Likelihood ratio statistic	df	Overall *P*
Full model										
44.88	11.28							9.91	7	0.200
		FL	0.01	0.005	1.011	1.00–1.02	0.030*			
		DC	−0.81	1.175	0.447	0.05–4.47	0.493			
		D	0.07	0.107	1.070	0.87–1.32	0.524			
		BJ	−17.7	15,650	2.0×10^{-8}	~0 to ∞	0.999			
		FI	1.09	1.506	2.985	0.16–57.2	0.468			
		TI	−16.7	86,490	5.6×10^{-8}	~0 to ∞	1.000			
		ST	0.19	0.430	1.215	0.52–2.82	0.651			
Second-best model										
34.26	0.67							8.37	2	0.020*
		FL	0.01	0.004	1.011	1.00–1.02	0.011*			
		FI	1.80	1.351	6.021	0.43–85.1	0.184			
Best model										
33.59	0.00							6.88	1	0.009*
		FL	0.01	0.004	1.009	1.00–1.02	0.011*			
Null model										
38.40	4.81									
Model with categorical predictor: fish length (sublegal or legal)										
30.75								9.73	1	0.002*
		LG	3.01	1.120	20.22	2.25–181	0.007*			

the first minute after release to the end of the acoustic monitoring period (Fig. 5). Bottom temperature, examined for internally tagged fish for which data were available (n=35), was not a significant factor in PRM (Suppl. Table 7) (online only). Handling and fight times, examined for fish for which data were available (n=49), also were not significant factors in PRM (Suppl. Table 8) (online only).

Discussion

In this study, we found relatively high survivorship from recreational fishing methods (85%) for greater amberjack in the northern Gulf of Mexico. After accounting for all estimated sources of discard mortality, the probability of survival from PRM (89%) was lower than the probability of survival after AVM and CHM (95%). Notably, the recapture rate was relatively high (12%), underscoring the high fishing pressure in the area and likely increasing the chance of fish having repeated exposure to potential risks associated with discard mortality. In this study, fish size was the best predictor of PRM, and abiotic variables and factors associated with barotrauma (site depth) and mitigation of barotrauma (descender device use) were not associated with PRM.

Results from Cox proportional hazards modeling with data for internally tagged fish (from 2019 and 2020) indicate a substantially (20 times) increased mortality risk for legal-size fish. The survivorship curve for legal-size and sublegal-size fish indicates that, from 7.6 h to 40 d postrelease, mortality probabilities were 2% for legal-size and 44% for sublegal-size fish. Therefore, when predicting postrelease outcome, it is important to consider that fish discarded by anglers during closed seasons may include large fish (≥864 mm FL), with a higher PRM risk than smaller fish, but during the open recreational fishing periods anglers are more likely to discard sublegal-size fish when targeting legal-size fish for take.

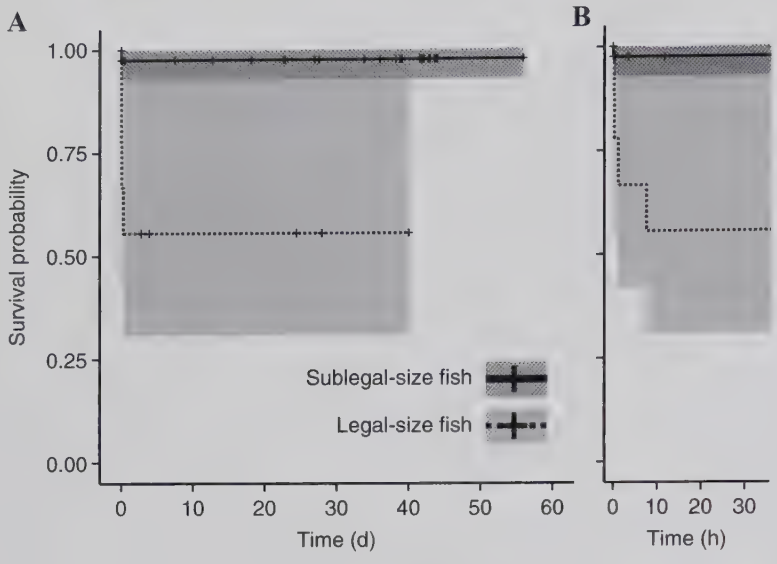

Figure 5

The Kaplan–Meier survivorship curve for greater amberjack (*Seriola dumerili*) of legal size (≥864 mm in fork length [FL]) and sublegal size (<864 mm FL) with internal acoustic tags, (**A**) for the entire period (>50 d) for which transmitters and receivers were active and (**B**) for the first 38 h postrelease. Each cross along the curve indicates when data were censored because a fish emigrated away from acoustic receivers. The gray area represents the 95% confidence interval for survival probability. Fish were caught and tagged on charter boats in the northern Gulf of Mexico in 2019 and 2020.

Having a body size smaller than legal size may reduce PRM. Results of exploratory Spearman rank correlation tests of predictor variables indicate a correlation of fight time with body size (Suppl. Table 1) (online only). This relationship is predicted because bigger fish are expected to fight harder. Although fight time was not explicitly predictive in Cox models, such a relationship may be confounded by body size. Long fight times are expected to increase stress, elevate oxygen demand, and cause exhaustion, all of which could increase discard mortality risk (including risk of PRM). Fight and handling times have been reported to have physiological effects that reduce postrelease survival in blacktip sharks (*Carcharhinus limbatus*) (Mohan et al., 2020). In our study, as expected, fish size also correlated negatively with handling time. These factors did not influence mortality in our Cox models but may be confounded by size. Effects of handling time may be less pronounced for fish discarded during normal recreational fishing compared to those in this study that involved tagging. Sublegal-size fish were more likely to be caught by jigging and to have observable fishing injuries, yet these factors did not appear to be correlated with PRM. Lastly, surface dissolved oxygen was a potential confounding variable in our study that weakly and negatively correlated with fish size in our data set, perhaps because more large fish were caught in summer in 2018 when most cases of low surface dissolved oxygen were observed in our study.

Seasonally warm temperatures in autumn (~18°C) have been considered a likely factor of PRM in a cold-temperate species, the haddock (*Melanogrammus aeglefinus*), in the Gulf of Maine (Capizzano et al., 2019). Cooler temperatures (e.g., at the surface, ~24°C in winter and spring versus 31°C in summer) have also been associated with increased postrelease survival of red snapper in the Gulf of Mexico (Curtis et al., 2015). We did not find direct support for temperature as a contributor to PRM of greater amberjack in the Gulf of Mexico. Note, however, that bottom temperature data were limited in our study for fish sampled in spring in 2019, and the sample size of observed mortalities is small (n=7). Therefore, the differential between surface and bottom temperatures and thermocline depth should be considered as potential factors in future studies.

One goal of our study was to assess the effects of 2 factors, site depth and descender device use, on PRM. We initially aimed to attach acoustic telemetry transmitters to external dart tags (Floy FH-69 tags). However, after a high rate of transmitters being shed in 2018 (56% of fish shed their tags, confirmed by the reported recapture of 17% of tagged fish), we modified our approach to monitor PRM for a longer duration after fish release. Although tag shedding was frequent in 2018, data for detections of tags that were later shed indicate survival over the first several days after release: for the 9 fish inferred to have shed tags, tags appeared to remain attached between 2.8 and 33.2 d (median: 7.2 d), and 4 recaptured fish lived beyond the study period. Only 2 fish with external acoustic transmitters died after release, and these deaths occurred between 2 h and 2.8 d postrelease. Both of these fish were from relatively shallow sites (with depths of 33 and 37 m), with one released at the surface and one released with a descender device. Therefore, there was no evidence of barotrauma-induced PRM in 2018. In 2019 and 2020, we placed transmitters in the posterior end of the coelomic cavity and did not attempt to vent the swim bladder. Although no ruptured swim bladders were observed during tag implantation, it is possible that some swim bladder gas was inadvertently released. For fish tagged in 2019 and 2020, there was no evidence that site depth increased mortality. Use of descender devices did not appear to mitigate PRM risk, but they did not add mortality risk, which might have been expected from predation of tethered fish on descent or from increased handling time when the descender device was used.

Susceptibility to barotrauma varies among species and capture depths (Jarvis and Lowe, 2008). Species that ascend rapidly and undergo diel depth migrations are

predicted to resist depth-related trauma. In a recent study in which discard mortality in 2 species, the red snapper and gray triggerfish (*Balistes capriscus*), was examined, descender device use was found to be associated with a decrease in PRM for red snapper but not for gray triggerfish (Bohaboy et al., 2020). In addition, barotrauma risk increases with capture depth. In a recent study on PRM of greater amberjack at 2 sites that varied in depth, site depth was found not to predict survivorship (Jackson et al., 2018). In the Jackson et al. (2018) study, fish were vented prior to release, given that previous observations (Murie and Parkyn[2]) indicate turgidity in swim bladders of fish caught at depths greater than 45 m. Therefore, the potential for capture depth as a factor in postrelease survivorship could still exist without mitigation of venting. Murie and Parkyn[2] noted that anatomy of greater amberjack in the region of the pectoral girdle lacerates near the medial supracleithrum upon depth-related swim bladder expansion and allows bubble release. This "self-venting mechanism" (Murie and Parkyn[2]), however, could still pose injury risk to released fish.

In a mark-recapture study of greater amberjack that were collected at depths of 15–95 m off the Atlantic coast of the southeastern United States and were vented prior to release, no trends in recapture rates related to site depth were observed (i.e., no increased mortality occurred at sites where barotrauma would be predicted) (McGovern et al., 2005). In our study (in which fish were captured at depths <65 m), it was not known if fish mitigated barotrauma by self-venting or if barotrauma simply was not a factor. It was also not known if greater amberjack faced higher PRM risk at capture sites with depths greater than 64 m. Greater amberjack occuppied a wide depth range throughout the day. Even at deep reef sites (>64 m), fish may be hooked at shallower depths and require less compensation for luminal gas expansion of the swim bladder than would be expected if they were hooked near the seafloor.

Fish that succumbed to PRM in this study tended to die quickly (median: 1.2 h postrelease; range: 0.02–68.00 h postrelease). Sixteen acoustically tagged fish (20.5%) were not detected for more than 68 h (median: 0.2 h; range: 0.00–3.50 h). The fate of these fish remains a question, although no evidence of predation existed. Emigration immediately following release is often reported from studies in which passive acoustic telemetry was used, and as a result, the fates of many fish remain unknown, leaving the potential for higher PRM (Topping and Szedlmayer, 2011; Curtis et al., 2015). Two fish in our study were detected only once at the reef where they were tagged and released, and they were subsequently detected at a reef 4.5 km away. Therefore, initial emigration is clearly not always associated with mortality. In our study, 16% of acoustically tagged fish that were detected alive ≥68 h postrelease moved between study sites with acoustic receivers, highlighting that movement of greater amberjack among reefs is relatively common. Additional emigration in this study appeared associated with cyclonic storms. Six fish in 2020 were not detected until 7–12 d after release. In addition, 11 fish moved to different reefs that happened to have acoustic receivers, and 3 of those fish did not return to the reef where they were tagged and released. Therefore, having acoustic receivers in multiple locations helped prevent underestimation of postrelease survival and should be a consideration in studies of discard mortality in mobile reef fishes.

Total discard mortality in our study, although comparable, was notably higher than the estimate for recreational fisheries (13.5% versus 10%, respectively) in the recent stock assessment of greater amberjack in the Gulf of Mexico (SEDAR, 2020). For greater amberjack in our study, PRM was the greatest component of discard mortality (AVM, CHM, and PRM). Discard mortality is an important component of total fishing mortality, and robust estimates of this rate are essential for effective stock management.

Conclusions

Results of this study, in which a broad range of abiotic factors, such as site depth, use of a descender device, and fish length were examined, indicate that fish size presents the greatest risk for PRM of greater amberjack at sites with depths ≤64 m. Our study followed up previous work by Jackson et al. (2018) that examined discard mortality over a narrower depth range for fish that were vented prior to release. In our study, with fish released at depths of 29–64 m, use of a descender device did not appear to influence PRM. In contrast to what occurred in the Jackson et al. (2018) study, we found that PRM risk increases with fish size. These findings point to important management considerations, given that the release of small individuals (<864 mm FL), required by restrictions on the size of fish that can be kept, appears to carry less PRM risk than the discard of legal-size fish. With our Cox proportional hazards model with fish size analyzed as a non-discrete variable, we estimated that mortality increases by 0.9% (hazard ratio: 1.009) per 1 mm increase in FL, a finding that should be considered when proposing changes to size regulations for greater amberjack in the northern Gulf of Mexico.

Resumen

El manejo de la pesca recreativa del medregal (*Seriola dumerili*) en el golfo de México incluye regulaciones de talla y temporadas de veda. La temperatura del agua, la salinidad, los tiempos de forcejeo y manipulación, así como el barotrauma pueden influir en la supervivencia de los peces liberados. Examinamos la mortalidad y el comportamiento

[2] Murie, D. J., and D. C. Parkyn. 2013. Preliminary release mortality of Gulf of Mexico greater amberjack from commercial and recreational hand-line fisheries: integration of fishing practices, environmental parameters, and fish physiological attributes. Southeast Data, Assessment, and Review SEDAR33-DW29, 13 p. [Available from website.]

posterior a la liberación utilizando telemetría acústica de los movimientos de 78 peces, monitoreados hasta 58 días a través de 3 esfuerzos de muestreo en 2018, 2019 y 2020 en un gradiente de profundidad de 29–64 m. Para evaluar los dispositivos de descenso como herramienta de mitigación, asignamos peces a 2 tratamientos: liberación en superficie sin ventilación de la vejiga natatoria y liberación con un dispositivo de descenso. Se utilizaron modelos de riesgos proporcionales de Cox para evaluar los efectos de la profundidad del lugar, el tratamiento de liberación, el tipo de carnada (señuelo o carnada viva), las lesiones por pesca, las lesiones por marcado, los tiempos de forcejeo y manipulación, las temperaturas de la superficie y del fondo, y la longitud de los peces. No se encontró una asociación positiva entre el riesgo de mortalidad y la profundidad del sitio de liberación, como se esperaría del barotrauma, ni una mayor supervivencia de los peces liberados con un dispositivo de descenso. El modelo mejor sustentado consideró únicamente la longitud de los peces como factor de mortalidad tras la liberación; los peces de tamaño legal (≥864 mm de longitud furcal) tuvieron un riesgo de mortalidad 20 veces mayor que los peces más pequeños. Nuestros resultados indican que, debido a las restricciones de tamaño, los peces de talla inferior a la legal liberados se enfrentan a un riesgo de mortalidad mucho menor que los peces de talla legal.

Acknowledgments

We would like to thank K. Anderson, G. Badlowski, J. Carver, R. Couterie, C. Dominique, L. Hijikota, A. Foulk, E. Greenheck, T. Guoba, D. Jones, D. Kiene, E. Kim, M. Lovell, J. McDonald, M. McCall, J. O'Brien, E. Shallow, T. Spearman, C. Walker, J. Wittinger, and J. Wittman for field assistance. We thank D. Shrestha for data management and the crews of the FV *Lady Ann* and FV *Escape* for fish collection and field support. This research was supported by a grant from the Marine Fisheries Initiative of the National Marine Fisheries Service (grant no. NA17NMF4330316) to S. Powers.

Literature cited

Bohaboy, E. C., T. L. Guttridge, N. Hammerschlag, M. P. M. Van Zinnicq Bergmann, and W. F. Patterson III.
2020. Application of three-dimensional acoustic telemetry to assess the effects of rapid recompression on reef fish discard mortality. ICES J. Mar. Sci. 77:83–96.

Burnham, K. P., and D. R. Anderson.
2002. Model selection and multimodel inference: a practical information-theoretic approach, 2nd ed., 488 p. Springer-Verlag, New York.

Capizzano, C. W., D. R. Zemeckis, W. S. Hoffman, H. P. Benoît, E. Jones, M. J. Dean, N. Ribblett, J. A. Sulikowski, and J. W. Mandelman.
2019. Fishery-scale discard mortality rate estimate for haddock in the Gulf of Maine recreational fishery. North Am. J. Fish. Manag. 39:964–979.

Cox, D. R.
1972. Regression models and life-tables. J. R. Stat. Soc. 34:187–220.

Curtis, J. M., M. W. Johnson, S. L. Diamond, and G. W. Stunz.
2015. Quantifying delayed mortality from barotrauma impairment in discarded red snapper using acoustic telemetry. Mar. Coast. Fish. 7:434–449.

Jackson, L. S., J. M. Drymon, T. R. Nelson, and S. P. Powers.
2018. Biotelemetry based estimates of greater amberjack (*Seriola dumerili*) post-release mortality in the northern Gulf of Mexico. Fish. Res. 208:239–246.

Jarvis, E. T., and C. G. Lowe.
2008. The effects of barotrauma on the catch-and-release survival of southern California nearshore and shelf rockfish (Scorpaenidae, *Sebastes* spp.). Can. J. Fish. Aquat. Sci. 65:1286–1296.

Kassambra, A., M. Kosinski, P. Biecek, and S. Fabian.
2021. survminer: drawing survival cures using 'ggplot2.' R package, vers. 0.4.9. [Available from website, accessed January 2022.]

Kneebone, J., H. P. Benoît, D. Bernal, and W. Golet.
2021. Application of a parametric survival model to understand capture-related mortality and predation of yellowfin tuna (*Thunnus albacares*) released in a recreational fishery. Can. J. Fish. Aquat. Sci. 78:386–399.

Lagler, K. F., J. E. Bardach, and R. R. Miller.
1962. Ichthyology, 545 p. Wiley, New York.

McGovern, J. C., G. R. Sedberry, H. S. Meister, T. M. Westendorff, D. M. Wyanski, and P. J. Harris.
2005. A tag and recapture study of gag, *Mycteroperca microlepis*, off the southeastern U.S. Bull. Mar. Sci. 76:47–59.

Mohan, J. A., E. R. Jones, J. M. Hendon, B. Falterman, K. M. Boswell, E. R. Hoffmayer, and R. J. D. Wells.
2020. Capture stress and post-release mortality of blacktip sharks in recreational charter fisheries of the Gulf of Mexico. Conserv. Physiol. 8:coaa041.

Patterson, W. F., III, J. C. Watterson, R. L. Shipp, and J. H. Cowan Jr.
2001. Movement of tagged red snapper in the northern Gulf of Mexico. Trans. Am. Fish. Soc. 130:533–545.

Pollock, K. H., and W. E. Pine III.
2007. The design and analysis of field studies to estimate catch-and-release mortality. Fish. Manag. Ecol. 14:123–130.

R Core Team.
2021. R: a language and environment for statistical computing. R Foundation for Statistical Computing, Vienna, Austria. [Available from website, accessed August 2021]

Runde, B. J., and J. A. Buckel.
2018. Descender devices are promising tools for increasing survival in deepwater groupers. Mar. Coast. Fish. 10:100–117.

SEDAR (Southeast Data, Assessment, and Review).
2014. SEDAR 33—Gulf of Mexico greater amberjack stock assessment report, 490 p. SEDAR, North Charleston, SC. [Available from website.]
2020. SEDAR 70 stock assessment report: Gulf of Mexico greater amberjack, 186 p. SEDAR, North Charleston, SC. [Available from website.]

Smith-Vaniz, W. F.
2002. Carangidae: jacks and scads (bumpers, pompanos, leatherjacks, amberjacks, pilotfishes, rudderfishes). *In* The living marine resources of the Western Central Atlantic. Volume 3: bony fishes part 2 (Opistognathidae to Molidae), sea turtles and marine mammals. FAO species identification guide for fishery purposes and Am. Soc. Ichthyol. Herpetol. Spec. Publ. 5 (K. E. Carpenter, ed.), p. 1426–1468. FAO, Rome.

Thernau, T. M.
2021. A package for survival analysis in R. R package, vers. 3.2-13. [Available from website, accessed January 2022.]
Topping, D. T., and S. T. Szedlmayer.
2011. Site fidelity, residence time and movements of red snapper *Lutjanus campechanus* estimated with long-term acoustic monitoring. Mar. Ecol. Prog. Ser. 437:183–200.
Venables, W. N., and B. D. Ripley.
2002. Modern applied statistics with S, 4th ed., 495 p. Springer, New York.
Whitney, N. M., C. F. White, A. C. Gleiss, G. D. Schwieterman, P. Anderson, R. E. Hueter, and G. B. Skomal.
2016. A novel method for determining post-release mortality, behavior, and recovery period using acceleration data loggers. Fish. Res. 183:210–221.
Woodland, W. N. F.
1913. Notes on the structure and mode of action of the "oval" in the pollack (*Gadus pollachius*) and mullet (*Mugil chelo*). J. Mar. Biol. Assoc. U.K. 9:561–565.

National Marine
Fisheries Service
NOAA

Fishery Bulletin
established in 1881

Spencer F. Baird
First U.S. Commissioner
of Fisheries and founder
of *Fishery Bulletin*

Life history differences between 2 anadromous populations of the northern form of the Dolly Varden (*Salvelinus malma malma*) in Bristol Bay in southwestern Alaska

Andrew T. Chin (contact author)[1]
Morgan H. Bond[2]
Thomas P. Quinn[1]

Email address for contact author: andrew.chin@noaa.gov

[1] School of Aquatic and Fishery Sciences
University of Washington
P.O. Box 355020
Seattle, Washington 98195

[2] Fish Ecology Division
Northwest Fisheries Science Center
National Marine Fisheries Service, NOAA
2725 Montlake Boulevard East
Seattle, Washington 98112

Abstract—The Dolly Varden (*Salvelinus malma*), an iteroparous, facultatively anadromous Pacific salmonid, displays diverse life history and migration patterns. Using otolith microchemistry, we inferred that individuals sampled in the Nushagak Commercial Salmon Fishery Management District, Alaska (sample size [*n*]=30; mean fork length=597 mm), had entered saltwater at ages 4–7 and were in their first (26%) or second (74%) summer at sea. Most (88%) of the fish that had spent 2 summers at sea migrated in consecutive years, but 2 of them skipped a migration to marine waters, remaining in fresh water for an additional year after migrating to sea in their first year. Only 15% of the individuals with 2 summers at sea had anadromous mothers. In contrast, conspecifics sampled on the other side of Bristol Bay in the Egegik Commercial Salmon Fishery Management District started migrating at an earlier age, migrated more often, and more often had anadromous mothers. Together, these results highlight the differences in life history among Dolly Varden and indicate that freshwater rather than marine conditions influence life history patterns, at least for fish within the Nushagak District.

Manuscript submitted 10 March 2022.
Manuscript accepted 11 August 2022.
Fish. Bull. 120:234–239 (2022).
Online publication date: 23 August 2022.
doi: 10.7755/FB.120.3-4.4

The views and opinions expressed or implied in this article are those of the author (or authors) and do not necessarily reflect the position of the National Marine Fisheries Service, NOAA.

Salmonids exhibit a wide variety of migratory patterns, among and within species (Klemetsen et al., 2003; Quinn, 2018). Some species reside in small streams, whereas others migrate between streams and larger rivers (Northcote, 1997), migrate between streams and lakes (Arostegui and Quinn, 2019), or are anadromous and spend weeks, months, or years at sea (Quinn and Myers, 2004). Anadromous salmonids that are iteroparous may vary in age of first marine migration (Swanson et al., 2010; Bond et al., 2015) and in the number or sequencing of those migrations (Spares et al., 2015). This variation is especially marked in the char species (*Salvelinus* spp.) (Dunham et al., 2008), with anadromy positively associated with key life history traits, such as growth rate, age at first spawning, fecundity, and longevity (Tallman et al., 1996), but also with high mortality (Brown et al., 2019).

The Dolly Varden (*S. malma*) is an iteroparous char species of the North Pacific Rim with 3 subspecies (Taylor and May-McNally, 2015), and there are fluvial (Denton et al., 2010; Ayer et al., 2018), adfluvial (Markevich et al., 2018), and anadromous or partially anadromous populations of this species (Bond and Quinn, 2013; Morrison et al., 2021). Anadromy is known for the 2 North American subspecies or forms in Alaska. The southern form of Dolly Varden, *S. m. lordii*, found south of the Alaska Peninsula, inhabits estuarine and nearshore habitats (Bond et al., 2014a) and may overwinter in marine waters (Bernard et al., 1995). In contrast, the northern form, *S. m. malma*, found north of the Alaska Peninsula, makes more extensive marine migrations (Morita et al., 2009; Courtney et al., 2018) and typically overwinters in fresh water after spawning and then migrates to sea annually; however, individuals of this subspecies may skip a year between migrations, remaining in freshwater habitats (Gallagher et al., 2018).

In Bristol Bay, in southwestern Alaska, populations of the northern form of Dolly Varden may be non-anadromous

(Denton et al., 2010) or partially anadromous, as has been inferred from catches at weirs (Lisac[1]) and from microchemical analysis of otoliths taken from fish sampled in marine waters at the mouth of the Egegik River (Hart et al., 2015) and taken in fresh water (Scanlon, 2000). Herein, we report life history data (size, total age, age at first migration, migration frequency, and maternal anadromy) on anadromous individuals of the northern subspecies of Dolly Varden sampled from the Nushagak Commercial Salmon Fishery Management District (hereafter, referred to as the *Nushagak District*), a commercial fishing zone within the Nushagak Bay estuary that opens into Bristol Bay. We compare them to data on conspecifics similarly sampled from the Egegik Commercial Salmon Fishery Management District (hereafter, referred to as the *Egegik District*) in the northeastern arm of Bristol Bay (Hart et al., 2015). The fish have access to common feeding areas, with the mouths of the rivers that drain into these bays only ~70 km apart (Fig. 1), allowing us to assess differences that might result from their respective freshwater ecosystems in the same region.

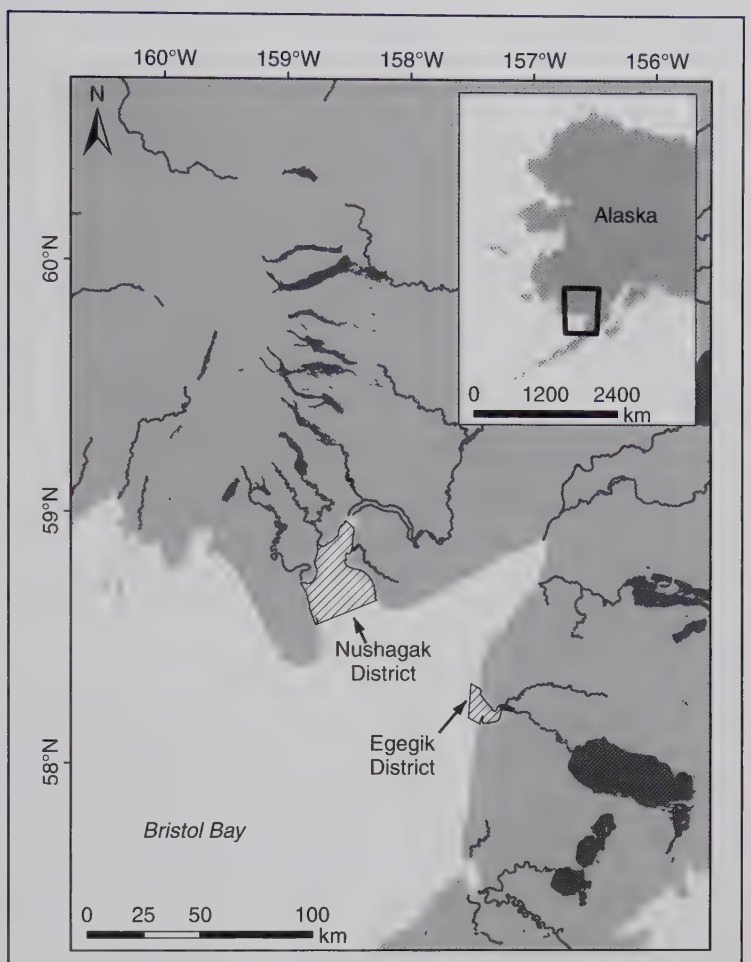

Figure 1

Map of the 2 locations in southwestern Alaska where individuals of the northern subspecies of Dolly Varden (*Salvelinus malma malma*) were taken as bycatch in the commercial gillnet fishery for sockeye salmon (*Oncorhynchus nerka*). Samples were collected from the Nushagak Commercial Salmon Fishery Management District on 25 June 2018 for this study, and comparable samples of the same subspecies of Dolly Varden were collected in the Egegik Commercial Salmon Fishery Management District by Hart et al. (2015) on 22 June and 2 July 2013.

Materials and methods

On 25 June 2018, 30 fish identified as the northern form of Dolly Varden (Taylor and May-McNally, 2015) by. E. Taylor[2], of the University of British Columbia, were taken as bycatch in the commercial gillnet fishery for sockeye salmon (*Oncorhynchus nerka*) in the Nushagak District (Salomone et al.[3]). The use of the samples examined in this study was permitted by the Alaska Department of Fish and Game. These fish could not be sold as food and would have been discarded if they had not been made available to us for study. The fish were frozen and later thawed, measured (fork length [FL]), and weighed. Paired *t*-tests were used to detect statistically significant differences between fish from the Nushagak and Egegik Districts.

Otoliths were removed for determination of life history characteristics by using visual and microchemical analyses. These analyses followed procedures used on conspecifics also taken as bycatch in the gillnet fishery between 22 June and 2 July 2013 in the Egegik District, on the opposite side of Bristol Bay from the Nushagak District (Hart et al., 2015). The similarities in gillnet mesh size (typically a mean diameter of 12.7 cm [standard deviation (SD) 0.3]) and in the times when these fisheries are open made it possible for us to compare life history patterns between these 2 collections. It is important to note, however, that neither collection fully represents the population in the district from which it was sampled owing to the limited collection dates and large basins from which these specimens may have originated, basins that include not only the basins of the Nushagak and Egegik Rivers but also other basins throughout Bristol Bay and southwestern Alaska.

Otoliths were extracted, sectioned, mounted, polished to expose the core and surrounding matrix, and aged visually by using reflected light. A subset of otoliths (sample size [*n*]=23) was selected for microchemical analysis on the

[1] Lisac, M. J. 2010. Abundance and run timing of Dolly Varden in the Middle Fork Goodnews River, 2008 and 2009. Alsk. Fish. Data Ser. Rep. 2010-13, 14 p. [Available from Togiak Natl. Wildl. Refug. Off., 6 Main St., Dillingham, AK 99576-0270.]

[2] Taylor, E. 2018. Personal commun. Dep. Zool., Univ. British Columbia, Beaty Biodivers. Cent., Rm. 310, Vancouver, Canada V6T 1Z4.

[3] Salomone, P., T. Elison, T. Sands, J. Head, and T. Lemons. 2019. 2018 Bristol Bay annual management report. Alsk. Dep. Fish Game, Fish. Manag. Rep. 19-12, 64 p. [Available from website.]

basis of the clarity of the preparation and ease of determination of the otolith's core from the surrounding area. Strontium (Sr) and barium (Ba) are incorporated into fish bony structures relative to their concentrations in the surrounding water. The concentration of these elements is typically correlated with salinity (Elsdon et al., 2008) and is highly conserved in fish otoliths (Kraus and Secor, 2004). Normalized to calcium (Ca) levels, Sr and Ba concentrations in otoliths have been used to indicate migratory patterns and life history in diadromous fish species (Walther, 2019) and especially in salmonids (Swanson et al., 2010; Bond et al., 2015; Austin et al., 2019).

Laser-ablation mass spectroscopy of otoliths was conducted with an iCap RQ ICP-MS[4] (Thermo Fisher Scientific, Waltham, MA). Element concentrations, adjusted to NIST-612 standards, were converted to molar mass ratios of ^{86}Sr:^{43}Ca and ^{138}Ba:^{43}Ca, presented as millimoles per mole and micromoles per mole, respectively. Winter annuli were visually identified by using dark growth rings and were measured from the core along the ablated transect. These measurements were then converted to a ratio of the total transect measured, and the corresponding ratio of lengths along the transect were overlaid onto a 9-point rolling mean of Sr:Ca and Ba:Ca ratios for individual otoliths to infer initial age of migration and annual migratory and overwintering patterns. Maternal anadromy was identified when core Sr:Ca ratios were elevated above the surrounding freshwater signals, reflecting the concentrations in the female during egg production (Kalish, 1990). Similarly, anadromy was inferred when the Sr:Ca ratio was >3 mmol/mol and the Ba:Ca ratio was <6 µmol/mol (Bond et al., 2015). In all cases, there was agreement between Sr:Ca and Ba:Ca ratios, indicating anadromy. The life history and microchemical data from our study can be accessed from GitHub.

Results and discussion

The Dolly Varden sampled from Nushagak District had an average length of 597.1 mm FL (SD 40.6), with a range of 522–690 mm FL, and an average mass of 2.16 kg (SD 0.42), with a range of 1.63–3.25 kg. Both of those means are greater than those of the fish caught in the Egegik District at essentially the same time of year, with a mean length of 509.0 mm FL (t=10.0, P<0.001) and a mean mass of 1.49 (t=4.1, P<0.001). However, the mean age of 6.1 years (range: 5–8 years) for fish from the Nushagak District did not differ from the mean age of 5.7 years (range: 4–9 years) for fish from the Egegik District (t=1.75, P=0.09) (Suppl. Table) (online only). These length and age values are comparable to those for conspecifics at similar latitudes (Maekawa and Nakano, 2002), although older individuals occur in Arctic populations (Stolarski and Sutton, 2013; Gallagher et al., 2016).

[4] Mention of trade names or commercial companies is for identification purposes only and does not imply endorsement by the National Marine Fisheries Service, NOAA.

Morrison et al. (2021) reported that rapid growth in fresh water was associated with early age at first migration in Dolly Varden and that growth rate in fresh water is typically inversely related to smolt age in salmonids (McCormick et al., 1998; Quinn, 2018). In contrast to the modest differences in size and age between the populations on opposite sides of Bristol Bay, a clear difference in age at migration was observed. The fish sampled from the Nushagak District first migrated to sea much later in life than the fish sampled from the Egegik District, with mean ages at migration of 5.2 years (range: 4–7) and 2.5 years (range: 2–3), respectively (t=15.33, P<0.001), indicating that the fish from the Nushagak District grew at a slower rate than the fish from the Egegik District. Similarly, a population of the southern subspecies of Dolly Varden along the southern Alaska Peninsula also migrated to sea at a younger age, although at a smaller body size at that age of migration (Bond et al., 2015). Dolly Varden at the northern end of their range also smolt at a younger age than the fish sampled from the Nushagak District (Morrison et al., 2021).

In addition to the difference between populations in age at first migration, 6 of the fish from the Nushagak District were in their first summer at sea, and the other 17 fish were in their second summer (mean age: 1.7 years) compared with the mean of 4.2 summers at sea (range: 3–8 summers) for the fish from the Egegik District.

Skipped migrations (i.e., remaining in fresh water for 2 winters rather than 1 winter between migrations) (Fig. 2A) were not common. Examining fish with multiple seasons at sea, we found that only 2 of 17 fish from the Nushagak District had skipped a migration to sea and that no fish from the Egegik District had skipped a marine migration. Skipped migrations were much more common (76% of the sample) in a study of fish sampled from an Arctic river that had a long (~800 km roundtrip) migration route (Gallagher et al., 2018). In comparison, the mouth of the Egegik River is only 45 km from Lake Becharof. Individuals from the Nushagak District migrate an unknown distance but likely less than the 450-km length of the Nushagak River because the Dolly Varden is common in the basin closer to Bristol Bay (May-McNally et al., 2015).

Finally, the incidence of maternal anadromy in our sampled individuals differed greatly (e.g., as evident in the data for 2 specimens shown in Figure 2, A and B): only 3 of 20 fish from the Nushagak District had mothers that migrated to sea in the season before spawning compared with 14 of 25 fish from the Egegik District having such mothers, yet all samples were collected in marine waters.

A skipped migration would create a freshwater chemical signal in a female that would not be distinguishable from a non-anadromous fish. In our sample, skipped migrations were rare; therefore, our results indicate that, in both populations, maternal migrations may not be common. However, a sample of juvenile Dolly Varden from tributaries of Lake Aleknagik, in the Wood River system of the Nushagak River basin, contained only individuals

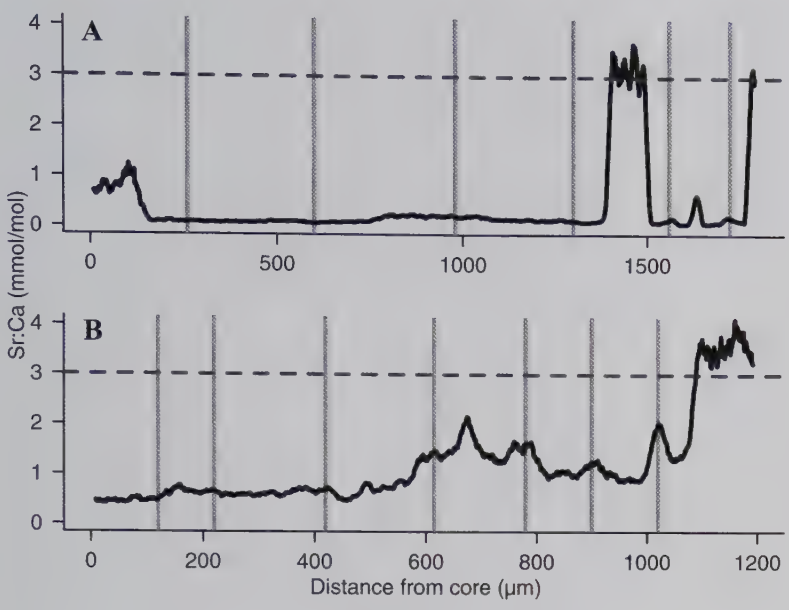

Figure 2

Profiles of the ratio of strontium to calcium (Sr:Ca) for otoliths from 2 Dolly Varden (*Salvelinus malma*) sampled on 25 June 2018 from the Nushagak Commercial Salmon Fishery Management District in southwestern Alaska, truncated to show the core at the origin. The vertical gray solid lines indicate the approximate positions of annuli. The horizontal dark gray dashed lines indicate the Sr:Ca threshold for interred marine residence (3 mmol/mol). (**A**) The top profile indicates maternal anadromy (elevated Sr:Ca at the core) and a year in freshwater between anadromous migrations (i.e., a skipped migration) at ages 4+ and 6+. (**B**) The bottom profile has no indication of maternal anadromy and indicates capture during the initial migration of the fish at age 7+. For clarity of the graphs, values of the ratio of barium and Ca are not shown.

whose mothers had been to sea in the summer prior to spawning (Dennert et al., 2016). The apparent differences among these results likely reflect the range of life history patterns of Dolly Varden in these large basins and the fact that our samples likely did not fully capture this variation. These variable life history patterns likely arise from differential survival and reproductive success, and therefore from differences in life history traits, across the heterogeneous freshwater landscape within the Nushagak River basin. These varied freshwater conditions may have more influence on the survival and reproductive success of fish migrating from the basin than the marine conditions to which all fish that migrate to sea are exposed. Regardless of the causes, however, the results indicate that the life history of the mother often differs from that of her offspring.

The fish used in this study were taken in gill nets that are size-selective (Todd and Larkin, 1971), affecting the range of phenotypes observed in a sample. Moreover, fishing mortality in general reduces age and longevity in populations (Sharpe and Hendry, 2009). Therefore, we cannot infer that fish smaller than the fish in our study do not enter marine waters, and repeat migrations might have been more common in the absence of fishing. We also acknowledge that interpreting age and microchemical data from otoliths is not without error (Stolarski and Sutton, 2013). For example, exposing otolith cores can be less reliable for adults than for juveniles, diluting or masking the core signature (Volk et al., 2000).

In addition, we made conclusions with the assumption that fish originated from the natal rivers within the district where they were caught. Dolly Varden have strong homing instincts, as indicated by results from tagging (Armstrong, 1974) and population genetics (Bond et al., 2014b) studies, but some individuals, especially those of the northern subspecies, can disperse widely (DeCicco, 1992; Morita et al., 2009). Still, the differences in life history observed in the samples from the Egegik and Nushagak Districts indicate that the examined samples did not represent a single mixed population but, rather, ones that were segregated to at least some extent. Despite issues with methods, common to the sampling of fish in both the Nushagak and Egegik Districts, and despite the access that these fish have to common, proximate foraging areas, the dramatic differences in life history of these populations indicate a dominant role of freshwater factors rather than marine factors on these traits. In this regard, the life history differences echo those found among populations of other salmonid species, including the sockeye salmon of Bristol Bay (Quinn et al., 2009).

Resumen

El salmón *Salvelinus malma*, es una especie iterópara del Pacífico, facultativamente anádroma que presenta ciclo vital y patrones de migración diversos. A partir de la microquímica de los otolitos, deducimos que los individuos muestreados en el Distrito de Administración de la pesquería comercial de salmón de Nushagak, Alaska (tamaño de muestra [*n*]=30; longitud furcal promedio=597 mm), habían entrado en el agua salada a los 4–7 años y estaban en su primer (26%) o segundo (74%) verano en el mar. La mayoría (88%) de los peces que habían pasado 2 veranos en el mar migraron en años consecutivos, pero 2 de ellos se saltaron una migración a aguas marinas, permaneciendo en agua dulce un año más después de haber migrado al mar en su primer año. Sólo el 15% de los individuos con 2 veranos en el mar tenían madres anádromas. Por el contrario, los congéneres muestreados al otro lado de la bahía de Bristol, en el Distrito de Administración de

la pesquería comercial de salmón de Egegik, empezaron a migrar a menor edad, con más frecuencia, y tuvieron más a menudo madres anádromas. En conjunto, todos estos resultados ponen de manifiesto las diferencias en el ciclo vital de este salmón e indican que son las condiciones de agua dulce y no las marinas las que influyen en los patrones del ciclo vital, al menos en el caso de los peces del distrito de Nushagak.

Acknowledgments

We thank W. Lew (Icicle Seafoods) for donating the fish, E. Taylor for confirming their identification, staff at the University of Washington IsoLab for sample processing, A. Gagnon and T. Ugrai for microchemistry data interpretation, and P. Chittaro and G. Williams for helpful comments on a draft of this paper.

Literature cited

Armstrong, R. H.
1974. Migration of anadromous Dolly Varden (*Salvelinus malma*) in southeastern Alaska. J. Fish. Res. Board Can. 31:435–444.

Arostegui, M. C., and T. P. Quinn.
2019. Reliance on lakes by salmon, trout and charr (*Oncorhynchus*, *Salmo* and *Salvelinus*): an evaluation of spawning habitats, rearing strategies, and trophic polymorphisms. Fish Fish. 20:775–794.

Austin, C. S., M. H. Bond, J. M. Smith, E. D. Lowery, and T. P. Quinn.
2019. Otolith microchemistry reveals partial migration and life history variation in a facultatively anadromous, iteroparous salmonid, bull trout (*Salvelinus confluentus*). Environ. Biol. Fishes 102:95–104.

Ayer, C. G., H. Katahira, S. Fukui, and I. Koizumi.
2018. Seasonal patterns of downstream movement in partially migratory stream-dwelling Dolly Varden. Ecol. Freshw. Fish 27:247–254.

Bernard, D. R., K. R. Helper, J. D. Jones, M. E. Whalen, and D. N. McBride.
1995. Some tests of the "migration hypothesis" for anadromous Dolly Varden (southern form). Trans. Am. Fish. Soc. 124:297–307.

Bond, M. H., and T. P. Quinn.
2013. Patterns and influences on Dolly Varden migratory timing in Chignik Lakes, Alaska, and comparison to populations throughout the northeastern Pacific and Arctic oceans. Can. J. Fish. Aquat. Sci. 70:655–665.

Bond, M. H., B. R. Beckman, L. Rohrbach, and T. P. Quinn.
2014a. Differential growth in estuarine and freshwater habitats indicated by plasma IGF1 concentrations and otolith chemistry in Dolly Varden *Salvelinus malma*. J. Fish Biol. 85:1429–1445.

Bond, M. H., P. A. Crane, W. A. Larson, and T. P. Quinn.
2014b. Is isolation by adaptation driving genetic divergence among proximate Dolly Varden char populations? Ecol. Evol. 4:2515–2532.

Bond, M. H., J. A. Miller, and T. P. Quinn.
2015. Beyond dichotomous life histories in partially migrating populations: cessation of anadromy in a long-lived fish. Ecology 96:1899–1910.

Brown, R. J., M. B. Courtney, and A. C. Seitz.
2019. New insights into the biology of anadromous Dolly Varden in the Canning River, Arctic National Wildlife Refuge, Alaska. Trans. Am. Fish. Soc. 148:73–87.

Courtney, M. B., B. Scanlon, R. J. Brown, A. H. Rikardsen, C. P. Gallagher, and A. C. Seitz.
2018. Offshore ocean dispersal of adult Dolly Varden *Salvelinus malma* in the Beaufort Sea. Polar Biol. 41:817–825.

DeCicco, A. L.
1992. Long-distance movements of anadromous Dolly Varden between Alaska and the U.S.S.R. Arctic 45:120–123.

Dennert, A. M., S. L. May-McNally, M. H. Bond, T. P. Quinn, and E. B. Taylor.
2016. Trophic biology and migratory patterns of sympatric Dolly Varden (*Salvelinus malma*) and Arctic char (*Salvelinus alpinus*). Can. J. Zool. 94:529–539.

Denton, K. P., H. B. Rich Jr., J. W. Moore, and T. P. Quinn.
2010. The utilization of a Pacific salmon *Oncorhynchus nerka* subsidy by three populations of charr *Salvelinus* spp. J. Fish Biol. 77:1006–1023.

Dunham, J., C. Baxter, K. Fausch, W. Fredenberg, S. Kitano, I. Koizumi, K. Morita, T. Nakamura, B. Rieman, K. Savvaitova, et al.
2008. Evolution, ecology, and conservation of Dolly Varden, white spotted char, and bull trout. Fisheries 33:537–550.

Elsdon, T. S., B. K. Wells, S. E. Campana, B. M. Gillanders, C. M. Jones, K. E. Limburg, D. H. Secor, S. R. Thorrold, and B. D. Walther.
2008. Otolith chemistry to describe movements and life-history parameters of fishes: hypotheses, assumptions, limitations and inferenes. Oceanogr. Mar. Biol., Annu. Rev. 46:297–330.

Gallagher, C. P., K. L. Howland, and R. J. Wastle.
2016. A comparison of different structures and methods for estimating age of northern-form Dolly Varden *Salvelinus malma malma* from the Canadian Arctic. Polar Biol. 39:1257–1265.

Gallagher, C. P., K. L. Howland, S. J. Sandstrom, and N. M. Halden.
2018. Migration tactics affect spawning frequency in an iteroparous salmonid (*Salvelinus malma*) from the Arctic. PLoS ONE 13(12):e0210202.

Hart, L. M., M. H. Bond, S. L. May-McNally, J. A. Miller, and T. P. Quinn.
2015. Use of otolith microchemistry and stable isotopes to investigate the ecology and anadromous migrations of Northern Dolly Varden from the Egegik River, Bristol Bay, Alaska. Environ. Biol. Fishes 98:1633–1643.

Kalish, J. M.
1990. Use of otolith microchemistry to distinguish the progeny of sympatric anadromous and non-anadromous salmonids. Fish. Bull. 88:657–666.

Klemetsen, A., P.-A. Amundsen, J. B. Dempson, B. Jonsson, N. Jonsson, M. F. O'Connell, and E. Mortensen.
2003. Atlantic salmon *Salmo salar* L., brown trout *Salmo trutta* L. and Arctic charr *Salvelinus alpinus* (L.): a review of aspects of their life histories. Ecol. Freshw. Fish 12:1–59.

Kraus, R. T., and D. H. Secor.
2004. Incorporation of strontium into otoliths of an estuarine fish. J. Exp. Mar. Biol. Ecol. 302:85–106.

Maekawa, K., and S. Nakano.
2002. Latitudinal trends in adult body size of Dolly Varden, with special reference to the food availability hypothesis. Popul. Ecol. 44:17–22.

Markevich, G., E. Esin, and L. Anisimova.
2018. Basic description and some notes on the evolution of seven sympatric morphs of Dolly Varden *Salvelinus malma* from the Lake Kronotskoe Basin. Ecol. Evol. 8:2554–2567.

May-McNally, S. L., T. P. Quinn, and E. B. Taylor.
2015. Low levels of hybridization between sympatric Arctic char (*Salvelinus alpinus*) and Dolly Varden char (*Salvelinus malma*) highlights their genetic distinctiveness and ecological segregation. Ecol. Evol. 5:3031–3045.

McCormick, S. D., L. P. Hansen, T. P. Quinn, and R. L. Saunders.
1998. Movement, migration, and smolting of Atlantic salmon (*Salmo salar*). Can. J. Fish. Aquat. Sci. 55(Suppl. 1):77–92.

Morita, K., S. H. Morita, M. Fukuwaka, and T. Nagasawa.
2009. Offshore Dolly Varden charr (*Salvelinus malma*) in the North Pacific. Environ. Biol. Fishes 86:451–456.

Morrison, C. M., C. P. Gallagher, K. B. Tierney, and K. L. Howland.
2021. Freshwater early life growth influences partial migration in populations of Dolly Varden (*Salvelinus malma malma*). Polar Biol. 44:1353–1364.

Northcote, T. G.
1997. Potamodromy in Salmonidae—living and moving in the fast lane. North Am. J. Fish. Manag. 17:1029–1045.

Quinn, T. P.
2018. The behavior and ecology of Pacific salmon and trout, 2nd ed., 520 p. Univ. Wash. Press, Seattle, WA.

Quinn, T. P., and K. W. Myers.
2004. Anadromy and the marine migrations of Pacific salmon and trout: Rounsefell revisited. Rev. Fish Biol. Fish. 14:421–442.

Quinn, T. P., K. Doctor, N. Kendall, and H. B. Rich Jr.
2009. Diadromy and the life history of sockeye salmon: nature, nurture, and the hand of man. Am. Fish. Soc. Symp. 69:23–42.

Scanlon, B. P.
2000. The ecology of the Arctic char and the Dolly Varden in the Becharof Lake drainage, Alaska. M.S. thesis, 73 p. Univ. Alaska Fairbanks, Fairbanks, AK. [Available from website.]

Sharpe, D. M. T., and A. P. Hendry.
2009. SYNTHESIS: life history change in commercially exploited fish stocks: an analysis of trends across studies. Evol. Appl. 2:260–275.

Spares, A. D., M. J. Dadswell, M. P. Dickinson, and M. J. W. Stokesbury.
2015. A critical review of marine adaptability within the anadromous Salmoninae. Rev. Fish Biol. Fish. 25:503–519.

Stolarski, J. T., and T. M. Sutton.
2013. Precision analysis of three aging structures for amphidromous Dolly Varden from Alaskan Arctic rivers. North Am. J. Fish. Manag. 33:732–740.

Swanson, H. K., K. A. Kidd, J. A. Babaluk, R. J. Wastle, P. P. Yang, N. M. Halden, and J. D. Reist.
2010. Anadromy in Arctic populations of lake trout *(Salvelinus namaycush)*: otolith microchemistry, stable isotopes, and comparisons with Arctic char (*Salvelinus alpinus*). Can. J. Fish. Aquat. Sci. 67:842–853.

Tallman, R. F., F. Saurette, and T. Thera.
1996. Migration and life history variation in Arctic charr, *Salvelinus alpinus*. Écoscience 3:33–41.

Taylor, E. B., and S. L. May-McNally.
2015. Genetic analysis of Dolly Varden (*Salvelinus malma*) across its North American range: evidence for a contact zone in southcentral Alaska. Can. J. Fish. Aquat. Sci. 72:1048–1057.

Todd, I. S. P., and P. A. Larkin.
1971. Gillnet selectivity on sockeye (*Oncorhynchus nerka*) and pink salmon (*O. gorbuscha*) of the Skeena River system, British Columbia. J. Fish. Res. Board Can. 28:821–842.

Volk, E. C., A. Blakley, S. L. Schroder, and S. M. Kuehner.
2000. Otolith chemistry reflects migratory characteristics of Pacific salmonids: using otolith core chemistry to distinguish maternal associations with sea and freshwaters. Fish. Res. 46:251–266.

Walther, B. D.
2019. The art of otolith chemistry: interpreting patterns by integrating perspectives. Mar. Freshw. Res. 70:1643–1658.

National Marine
Fisheries Service
NOAA

Fishery Bulletin
established in 1881

Spencer F. Baird
First U.S. Commissioner
of Fisheries and founder
of *Fishery Bulletin*

Climate-driven changes in growth and size at maturity of Gulf of Maine lobster stocks: implications for stock assessment models

Cameron T. Hodgdon (contact author)[1,2]
Noah S. Khalsa[2]
Mackenzie D. Mazur[3]
Yong Chen[2]

Email address for contact author: cameron.hodgdon@maine.edu

[1] School of Marine Sciences
University of Maine
5741 Libby Hall, Room 221
Orono, Maine 04469

[2] School of Marine and Atmospheric Sciences
Stony Brook University
Stony Brook, New York 11790

[3] Pacific Biological Station
Fisheries and Oceans Canada
3190 Hammond Bay Road
Nanaimo, British Columbia V9T6N7, Canada

Abstract—Crustacean species are socioeconomically and ecologically crucial across the world. For crustaceans, as ectotherms, anthropogenic climate change threatens to significantly alter key life history characteristics, such as size at maturity and growth rate. Because crustaceans are difficult to age, length data are used in assessments of crustacean stocks; however, climate-induced changes in maturation and growth can greatly influence the performance of size-structured stock assessment models. We coupled individual-based and size-structured models for American lobster (*Homarus americanus*) off northeastern North America in the Gulf of Maine—to conduct a novel sensitivity analysis of the effects of maturity and growth-related input parameters on model outputs. For this analysis, we used a bottom-up approach (with parameters shifted independently) and a top-down approach (with parameters shifted jointly as they were predicted to be influenced by climate change). We found that our American lobster stock assessment model is resilient to relatively extreme shifts in biological input parameters. For size-structured modeling in assessments of crustacean stocks, we recommend the expansion of sensitivity analyses to include evaluation of the influence of climate-driven changes on input parameters based on time-varying life history traits.

Manuscript submitted 21 February 2022.
Manuscript accepted 23 August 2022.
Fish. Bull. 120:240–251 (2022).
Online publication date: 21 September 2022.
doi: 10.7755/FB.120.3-4.5

The views and opinions expressed or implied in this article are those of the author (or authors) and do not necessarily reflect the position of the National Marine Fisheries Service, NOAA.

Anthropogenic climate change is transforming many marine ecosystems through warming waters, ocean acidification, freshening, and deoxygenation (Brander, 2010; Doney et al., 2012; Gattuso et al., 2018; Doney et al., 2020). Perturbations to the abiotic environment, in particular to temperature, are especially influential on marine ectotherms because they do not physiologically regulate their body temperature (Huey et al., 1993; Madeira et al., 2012); rather, their body temperature is driven by the environment. As a consequence, temperature directly influences individual and population-level biological processes of crustacean species, such as metabolism, recruitment, reproduction, growth, size at maturity, and natural mortality (Madeira et al., 2012), which have significant implications for assessment and management of crustacean fisheries (Audzijonyte et al., 2016). Typically, in data-rich crustacean stock assessments, size-structured models are used (Punt et al., 2013), and the outputs of such models can be influenced by environmentally driven variability in input parameters based on size-related life history characteristics, such as growth and size at maturity. Therefore, it is important to quantify how climate-driven shifts in key life history characteristics will influence crustacean stocks and will manifest in assessment models used for guiding future management decisions.

The American lobster (*Homarus americanus*) is an ecologically and socioeconomically vital crustacean species in the northwestern Atlantic Ocean (Le Bris et al., 2018), and the biology of this species is directly influenced by temperature. American lobster, like many crustaceans, grow through a series of molts, also known as ecdysis. During ecdysis, the old carapace is replaced with a new, larger one (Herrick, 1911). Molting typically occurs annually in adult American lobster, although it can happen more than once or be skipped entirely depending on the size, age, and maturity of the individual (Herrick, 1911; Aiken and Waddy, 1976; Aiken, 1977; Comeau and Savoie, 2001). Although the physiology of individual American lobster is known to influence growth processes, temperature is

a primary abiotic driver of growth changes in this species. Rising temperatures have been shown to increase molting frequency and decrease molting increment, the length a lobster grows in a given molting event (Aiken, 1977). Additionally, in several studies, rising temperatures were found to contribute to reduced sizes at maturities for American lobster (Little and Watson, 2003, 2005; Le Bris et al., 2017; Waller et al., 2021). Indeed, climate-driven changes in these life history characteristics can likely affect results from the size-structured stock assessment model currently used for management of American lobster (ASMFC, 2020).

Understanding the effect that climate-driven shifts in input parameters for life history characteristics have on stock assessment model outputs is critical for future model development and fisheries management. In a recent study, incorporating temperature-driven recruitment was found to improve the performance of a size-structured stock assessment model for American lobster (Tanaka et al., 2019). When simulating the effects of pooling multiple populations of red rock lobster (*Jasus edwardsii*) with varying growth rates, the performance of a size-structured stock assessment model was not reduced (Punt, 2003), indicating that accounting for different growth rates of assessed populations may not be consequential for estimating reference points. If pooling population data of red rock lobster had reduced model performance, it may have indicated a need to further consider the importance of variable growth in future assessments of the population. In contrast, other research results indicate that failing to account for the plasticity of growth in fisheries stock assessment models can lead to deviations of more than 30% in outputs, critically altering the calculation of reference points (Lorenzen, 2016). Indeed, depending on the species biology and stock assessment model design, changes in growth can have inconsistent effects on model outputs.

Typically, sensitivity analyses can evaluate whether uncertainties in model assumptions, input data sources, and biological parameters have an effect on reference points or other model outputs (Maunder and Punt, 2013; Maunder and Piner, 2015). However, in these analyses, adjustments to inputs usually are considered only on their own, rather than in combination (Lehuta et al., 2010; Saltelli et al., 2019), and these analyses seldom involve testing model sensitivity to inputs that are based on life history traits and developed outside of the assessment model, such as growth transition matrices. Given the potential for dissimilar consequences of changing life history characteristics for stock assessment model outputs and the yet unrealized but possible shifts in crustacean growth in the future, it is important to evaluate the sensitivity of size-structured stock assessment models on a case-by-case basis.

In our study, we conducted a novel sensitivity analysis of a length-structured stock assessment model for American lobster by using an individual-based simulation model to evaluate the sensitivity of the model to shifts in growth-related life history input parameters, specifically molting probability, molt increment probability, and size at maturity. In a series of sensitivity analyses, we used classical bottom-up methods in which each parameter was shifted independently, and we used a top-down approach in which parameters were jointly shifted under the driving mechanism of climate change. We used both approaches to ascertain at what point shifts in these input parameters could result in a significant change in the stock status time series estimated with the length-structured stock assessment model, relative to a historical baseline. Our overarching goal for this study was to determine the extent of the influence that climate change has on the reliability and robustness of outputs from the stock assessment model used for American lobster in the Gulf of Maine.

Materials and methods

Shifting growth and size at maturity

Seasonal growth matrices in this study were calculated by using an individual-based lobster simulator model (IBLS) first developed by Chen et al. (2005) and later expanded by Chang (2015) and Mazur et al. (2018). This model simulates individual lobster from recruitment to mortality by sending each lobster through random Bernoulli trials representative of life history and fishery parameters derived from prior field research and modeling (Chen et al., 2005; Chang, 2015; Mazur et al., 2018). This seasonal probabilistic model is used to simulate lobster fishery dynamics to capture complex fishery-dependent and fishery-independent processes (Chen et al., 2005; Zhang et al., 2011) and has historically been used to test the performance of the American lobster stock assessment model (Chen et al., 2005). The model creates individual lobster records over a given time series that include sex, size bin, carapace length (CL), maturity, and mortality, allowing calculation of population abundance, spawning stock biomass, and landings (Mazur et al., 2018). A full explanation of this model can be found in Mazur et al. (2018).

The IBLS can be used to create seasonal growth matrices by simulating lobster with total absence of fishery-dependent and fishery-independent mortality as well as recruitment. Effectively, the abundance of lobster remains constant over the simulated time series, but the biomass changes exclusively because of input of data on growth of the animals. At each step, a lobster is in 1 of 35 size bins (in increments of 5 mm, from 53 mm CL to ≥223 mm CL). The simulation was run long enough that every lobster ended up in the final size bin at the end of the time series. Every growth instance for every lobster for a given season over the entire time series is marked in a matrix with the size bin before the molting event on the x-axis and the size bin after the molting event on the y-axis, and the matrix is scaled so that the sum of each row is effectively 1. This simulation creates a probabilistic growth matrix in which each row is a function of size change for a given lobster of that size class. This process is done 4 times, once for each season: winter (January–March), spring (April–June), summer (July–September), and fall (October–December).

The growth inputs to the IBLS are 2 independent factors: molting probability and probability for different molt

increments. Molting probability is the probability of a lobster molting in a particular time step dependent on the CL, maturation status of the individual, and how many seasons it has gone without molting (Fig. 1). Molt increment probability is the probability of a lobster growing a certain size (1–20 mm CL in 1-mm-CL bins) because of a molting event and is dependent on the CL of the individual (Fig. 1). The input data for these parameters in the base case of the IBLS came from the stock assessment conducted in 2015 (ASMFC, 2015).

Because of climate change, American lobster are expected to molt more frequently but grow less per molt (ASMFC, 2015). To simulate these effects on overall growth, both molting probability (P_M) and molt increment probability (P_{MI}) were manipulated in the IBLS. Molting probability was increased by shifting left in relation to seasons since the prior molt (Fig. 1) and was described by the following equations:

$$P_M = \frac{yas + b_1}{k_{CL}}; \quad (1)$$

$$yas = \begin{cases} 1,\ldots,k_{CL} & \text{if immature} \\ 2,\ldots,k_{CL} & \text{if mature; and} \end{cases} \quad (2)$$

$$k_{CL} = 1 + e^{-8.08127 + 0.076535CL}, \quad (3)$$

where yas = time spent (in units of the time step of the model; in this case, the unit is seasons) at current size of an individual lobster;
k_{CL} = the longest time a lobster of a given CL (in millimeters) could feasibly go before molting (NEFSC, 1996; ASMFC[1]); and
b_1 = the shifting parameter.

Therefore, a b_1 of 1 would represent a shift of 1 season, increasing the overall probability of molting in comparison to the unshifted probability.

Average size increase per molt was lowered by shifting molt increment probability left in relation to the size increase per molt (Fig. 1), described by using the equations below:

$$P_{MI} = N(\overline{\Delta L_L} - b_2, \sigma^2), \quad (4)$$

$$\overline{\Delta L_L} = \begin{cases} 1.2236 + 0.1294L & \text{for males with } L < 95; \\ 1.2236 + (0.1294 \times 95) & \text{for males with } L \geq 95; \\ 1.2288 + 0.1285L & \text{for females with } L < 82; \text{ and} \\ 1.2288 + (0.1285 \times 82) & \text{for females with } L \geq 82, \end{cases} \quad (5)$$

where N = the normal distribution truncated by upper and lower boundary probabilities of 0.975 and 0.025, respectively, with standard deviation (σ) being equal to 2.1 (ASMFC[2]);
L = the current length (in millimeters);
$\overline{\Delta L_L}$ = the change in length (in millimeters), given L and sex; and
b_2 = the shifting parameter.

Therefore, a b_2 of 1 would represent a shift of 1 mm, decreasing the overall size increment change during a given molt.

To maintain some biological realism, shifts of molting probability and molt increment probability were paired, and the corresponding growth matrices reflect possible effects from climate change. Two paired shifts were used in this study. The first paired shift, hereafter referred to as *G1*, was a leftward shift of molting probability by 1 year and of molt increment probability by 1 size bin (b_1=b_2=1) (Fig. 1). The second paired shift, hereafter referred to as *G2*, was a leftward shift of molting probability by 2 seasons and of molt increment probability by 2 size bins (b_1=b_2=2) (Fig. 1).

Probabilistic size at maturity (P_{SAM}) in the IBLS is calculated with the below equation:

$$P_{SAM} = \frac{1}{1 + e^{-0.3 \times (CL - L_{50})}}, \quad (6)$$

where P_{SAM} = the probability of maturity of an individual lobster of a given CL (in millimeters); and
L_{50} = the predefined CL (in millimeters) at 50% maturity.

The parameter L_{50} was set to 90.81 mm CL for the IBLS base case (ASMFC, 2015). Given that size at maturity for American lobster is expected to decrease 2.8 mm CL per 1°C rise in bottom temperature (Le Bris et al., 2017) and that current projections of bottom temperature for the Gulf of Maine are for an increase up to 2°C by 2050 and up to 4°C by 2100 (IPCC, 2019; Brickman et al., 2021), the L_{50} values of 85.21 and 79.61 mm CL were additionally tested in this study. These lengths are not considered projected values of size at maturity, but rather they are the L_{50} values needed in calculations to provide reasonable levels of change from historical data for the sensitivity analyses.

The IBLS was used to generate a total of 7 sets of growth matrices in this study (with 4 matrices in each set corresponding to seasons) (Table 1). The first set (the IBLS base case) was calculated with the original (unshifted) molt probability and molt increment probability paired with the original L_{50} value of 90.81 mm. The next 4 sets of matrices were calculated under IBLS scenarios 2–5, with shifts of either growth (G1 or G2) or L_{50} (85.21 or 79.61 mm CL), and the last 2 sets were calculated under IBLS scenarios 6 and 7, with paired shifts of both growth and L_{50} (G1 and 85.21 mm CL or G2 and 79.21 mm CL). Scenarios 2–5 were

[1] ASMFC (Atlantic States Marine Fisheries Commission). 2000. American lobster stock assessment report for peer review. Atl. States Mar. Fish. Comm., Stock Assess. Rep. 00-01 (Suppl.), 334 p. ASMFC, Arlington, VA. [Available from website.]

[2] ASMFC (Atlantic States Marine Fisheries Commission). 2006. American lobster stock assessment report for peer review. Atl. States Mar. Fish. Comm., Stock Assess. Rep. 06-03 (Suppl.), 175 p. ASMFC, Boston, MA. [Available from website.]

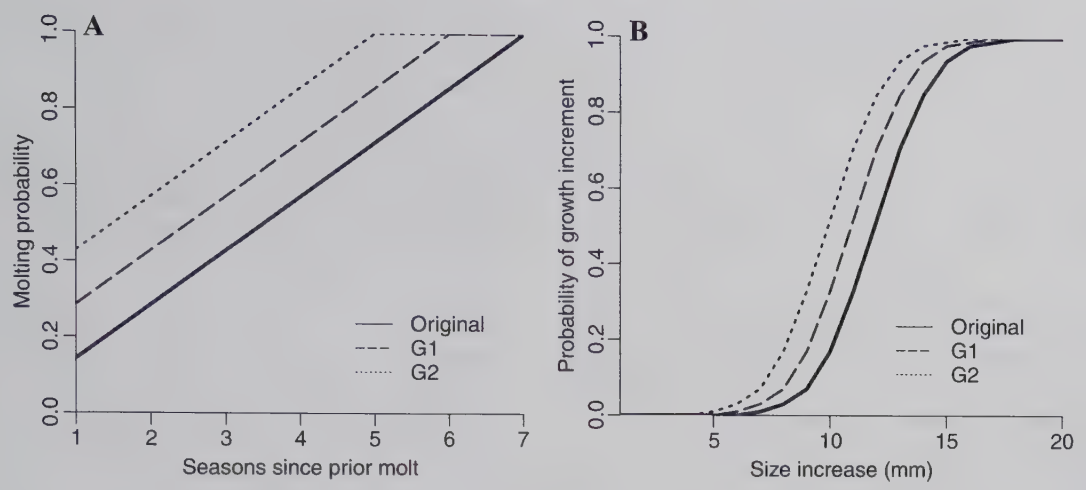

Figure 1

The relationships (**A**) of molting probability in the summer to number of previous seasons with no molting and (**B**) of cumulative molt increment probability to size increase for an American lobster (*Homarus americanus*) with a carapace length (CL) of 130 mm. The lines represent the probabilities in the individual-based lobster simulator model (IBLS) base case (or original scenario) and in each of the paired shifts from the IBLS base case used to simulate the effects of climate change on overall growth, a leftward shift of molting probability by 1 year and molt increment probability by 1 size bin of 1 cm CL (G1) and a leftward shift of molting probability by 2 seasons and molt increment probability by 2 size bins (G2).

Table 1

Individual-based lobster simulator (IBLS) scenarios for American lobster (*Homarus americanus*) in the Gulf of Maine. The parameters of the scenarios are a paired set of shifts in molting probability and molt increment probability for the growth dynamic and the predefined carapace length at 50% maturity (L_{50}) for each scenario. The IBLS base case or original scenario includes input data from the American lobster benchmark stock assessment conducted by the Atlantic States Marine Fisheries Commission in 2015. The paired shifts in growth factors are a leftward shift of molting probability by 1 year and molt increment probability by 1 size bin (G1) and a leftward shift of molting probability by 2 seasons and molt increment probability by 2 size bins (G2).

	IBLS scenario						
Parameter	1	2	3	4	5	6	7
Growth dynamic	Original	G1	G2	Original	Original	G1	G2
L_{50} (mm)	90.81	90.81	90.81	85.21	79.61	85.21	79.61

used to observe effects from specific parameters, whereas scenarios 6–7 were meant to provide outputs that are more biologically realistic and expected given the predicted relationships between climate change and the life history traits on which these parameters are based. Additionally, an analysis of time-varying growth and size-at-maturity parameters was conducted. Results of this analysis can be found in Supplementary Figure 1 (online only).

Stock assessment and sensitivity analyses

The University of Maine Lobster Stock Assessment Model (UMM) was initially developed by Chen et al. (2005) and expanded in ASMFC (2015) and Tanaka et al. (2019). It is a seasonal, sex-specific, length-structured assessment model for American lobster in the Gulf of Maine, Georges Bank, and Southern New England. It was designed with input from the Atlantic States Marine Fisheries Commission with the intent that it would be used for future lobster stock assessments. The population dynamics equation of the UMM is as follows:

$$N_{t,s} = \left(N_{t,s-1} \times G_s \times e^{-F_{t,s}+M_s}\right) + R_{t,s}, \quad (7)$$

where $N_{t,s}$ = a vector of the number of lobster in each size bin in year t and season s;

G = the seasonal growth transition matrix;
F = the seasonal fishing mortality;
M = the seasonal natural mortality; and
R = recruitment abundance for each size bin (Chen et al., 2005).

A list of all data used in the UMM consistently across scenarios can be found in Table 2. For more detailed descriptions of this model, see Chen et al. (2005) and Tanaka et al. (2019).

In the base case of the UMM, the original growth matrices and size at maturity of 90.81 mm CL from the IBLS base case were used as input data. Growth transition matrices and size-at-maturity data from the other 6 IBLS scenarios were individually input into the UMM, for a total of 7 scenarios including the UMM base case (all growth matrices used are provided in the Supplementary Material [online only]). For each scenario, biological reference points (BRPs) were calculated for output reference abundance (individuals larger than 53 mm CL) by using the methods outlined in ASMFC (2015): the target was calculated as the 75th percentile of reference abundance over the time series, and the threshold was calculated as the 25th percentile of reference abundance over the time series (ASMFC, 2015). It is important to note that the reference time series for these calculations used by the Atlantic States Marine Fisheries Commission was for the period of 1982–2003, but in this study, we used data from a reference period of 1984–2003 because of data input limitations. These BRPs allowed determination of historical fishery status over time, meaning simply the reference abundance of a given year in relation to the predefined BRPs (below the 25th percentile, between the 25th and 75th percentile, or above the 75th percentile). By using these reference points, terminal-year stock status was compared between all UMM runs in this study. However, for all sensitivity analyses in this study, historical fishery statuses over the entire time series were compared between each UMM scenario and the UMM base case.

Scenarios 6 and 7 in the IBLS were designed to represent small and large future climate effects, respectively. These effects on growth and size at maturity are plausible given climate projections (IPCC, 2019; Brickman et al., 2021), but it is unknown if these changes are large enough to affect stock status from what it would be under the UMM base case. To this end, a sensitivity analysis was conducted for scenarios 6 and 7 to examine whether stock status differed in consecutive years between the scenario and the UMM base case.

In the sensitivity analyses, IBLS scenarios representative of smaller and smaller incremental shifts in growth and size at maturity were added to determine the level of sensitivity (the breaking point), and those new growth matrices and sizes at maturity from these analyses were used in the UMM. For example, if historical fishery statuses from the UMM in which outputs from IBLS

Table 2

Settings and data that were consistent across scenarios used in the University of Maine Lobster Stock Assessment Model for American lobster (*Homarus americanus*) in the Gulf of Maine. IBLS=individual-based lobster simulator model; SSB/R=spawning stock biomass divided by the number of recruits to the stock; MEDMR=Maine Department of Marine Resources; MADMF=Massachusetts Division of Marine Fisheries; NHFGD=New Hampshire Fish and Game Department; NEFSC=NOAA Northeast Fisheries Science Center.

Setting or data category	Description
Period for time series	1984–2013
No. of seasons	4 (each a 3-month time block, same as IBLS)
No. of sexes	1 (data averaged across males and females)
Size range	53–223 mm carapace length
Size bin length	5 mm carapace length
Initial conditions	First-year size composition from survey data
Recruitment size	53–73 mm carapace length
SSB/R relationship	None
No. of commercial fleets	1
Commercial fleet selectivity at size	Double logistic
Survey data sources	MEDMR Ventless Trap Survey (2006–2012)
	Spring MEDMR/NHFGD inshore bottom-trawl survey (2001–2013)
	Fall MEDMR/NHFGD inshore bottom-trawl survey (2000–2013)
	Spring MADMF bottom-trawl survey (1984–2013)
	Fall MADMF bottomtrawl survey (1984–2013)
	Spring NEFSC bottomtrawl survey (1984–2013)
	Fall NEFSC bottom-trawl survey (1984–2013)
Survey selectivity at size	Double logistic
Fishing mortality rate	Instantaneous
Natural mortality rate	0.15 $year^{-1}$

scenario 6 were used did not differ from the status from the UMM base case but the statuses from the UMM in which IBLS scenario 7 outputs were used did differ from the status from the UMM base case, the breaking point of sensitivity would lie somewhere between the shifts represented in the 2 IBLS scenarios.

The next step was to produce growth matrices and estimate a size at maturity for a shift representative of halfway between these 2 shifts. For molting probability, the shift in this step was the average probability of both G1 and G2 for each season since the last molt. For molt increment probability, this shift was the average probability of both G1 and G2 for each size increase in millimeters. For size at maturity, it was simply the average of 85.21 and 79.61 mm CL. Historical fishery statuses and BRPs were then calculated for these new UMM scenarios. Retrospective patterns were also evaluated, and results from these tests can be found in Supplementary Figures 2–12 (online only). To further determine the breaking point of sensitivity, we used these new UMM scenarios in the methods described in the previous paragraph in place of either the UMM scenario in which IBLS scenario 6 was used or the UMM scenario in which IBLS scenario 7 was used (depending on whether the results of these new scenarios were significantly different from the UMM base case). This process of determining a breaking point of sensitivity was repeated and continued until a breaking point within one-sixteenth of a shift was found. The results of the sensitivity analyses described in this section can help determine the sensitivity of the UMM to growth and size at maturity and can help to focus future research efforts toward direct linkages of climate change to these life history parameters for use in stock assessment of American lobster.

Results

Target and threshold BRPs for the 7 UMM scenarios can be found in Table 3, and all accompanying reference abundance plots showcasing historical fishery statuses as compared to those of the UMM base case can be found in Figure 2. Terminal-year stock statuses did not change across any of the 7 UMM runs in this study (Table 4). Most alterations in historical reference abundance from the UMM base case appeared to be related to magnitude: consistent overestimations of abundance per year (except in the UMM scenario in which outputs from IBLS scenario 2 were used, where abundance was underestimated) but similar temporal trends, with slight alterations causing some discrepancies in historical fishery statuses. There was no clear pattern in how each instance of discrepancy across the runs either improved or worsened stock status estimates. Instances of consecutive years differing from the UMM base case are much more relevant because these instances are indicative of larger trend-based differences and not simply 1-year lags that seem to be the reason behind solitary instances of differing years. These instances of differences across consecutive years appeared in only one UMM scenario: scenario 7. In this scenario, a growth shift of G2 and a size at maturity of 79.61 mm CL were used (the large climate effect scenario).

Given that a change in size at maturity of over 10 mm CL did not appear to cause differences between consecutive years in reference abundance independent of a change in growth, a sensitivity analysis was not conducted for this variable. Likewise, changes in growth independent of size at maturity did not appear to cause consecutive-year differences. Therefore, a sensitivity analysis was not conducted for growth independent of size at maturity.

In the biologically realistic scenarios (UMM scenarios in which data from IBLS scenarios 6 and 7 were used), the combination of G1 and the size at maturity of 85.21 mm CL resulted in no consecutive-year differences in historical fishery status when compared to use of the UMM base case. However, the combination of G2 and the size at maturity of 79.61 mm CL resulted in consecutive-year differences compared to use of the UMM base case. Therefore, the breaking points of sensitivity existed somewhere between a small climate effect scenario (G1 and the size at maturity of 85.21 mm CL) and a large climate effect scenario (G2 and the size at maturity of 79.61 mm CL). Results from this sensitivity analysis for these biologically

Table 3

Target and threshold biological reference points (BRPs) for abundance (in millions of individuals) for all University of Maine Lobster Stock Assessment Model (UMM) scenarios for American lobster (*Homarus americanus*) in the Gulf of Maine. In each UMM scenario, the growth transition matrices and size at maturity produced with the corresponding scenario of the individual-based lobster simulator model were used (Table 1). The time series used in the UMM is from the period from 1984 through 2013.

	UMM scenario						
BRP	1	2	3	4	5	6	7
Target	976.0	823.1	1256.3	1078.1	1403.6	1067.0	2857.5
Threshold	707.8	579.6	919.6	801.2	1074.9	788.9	2170.5

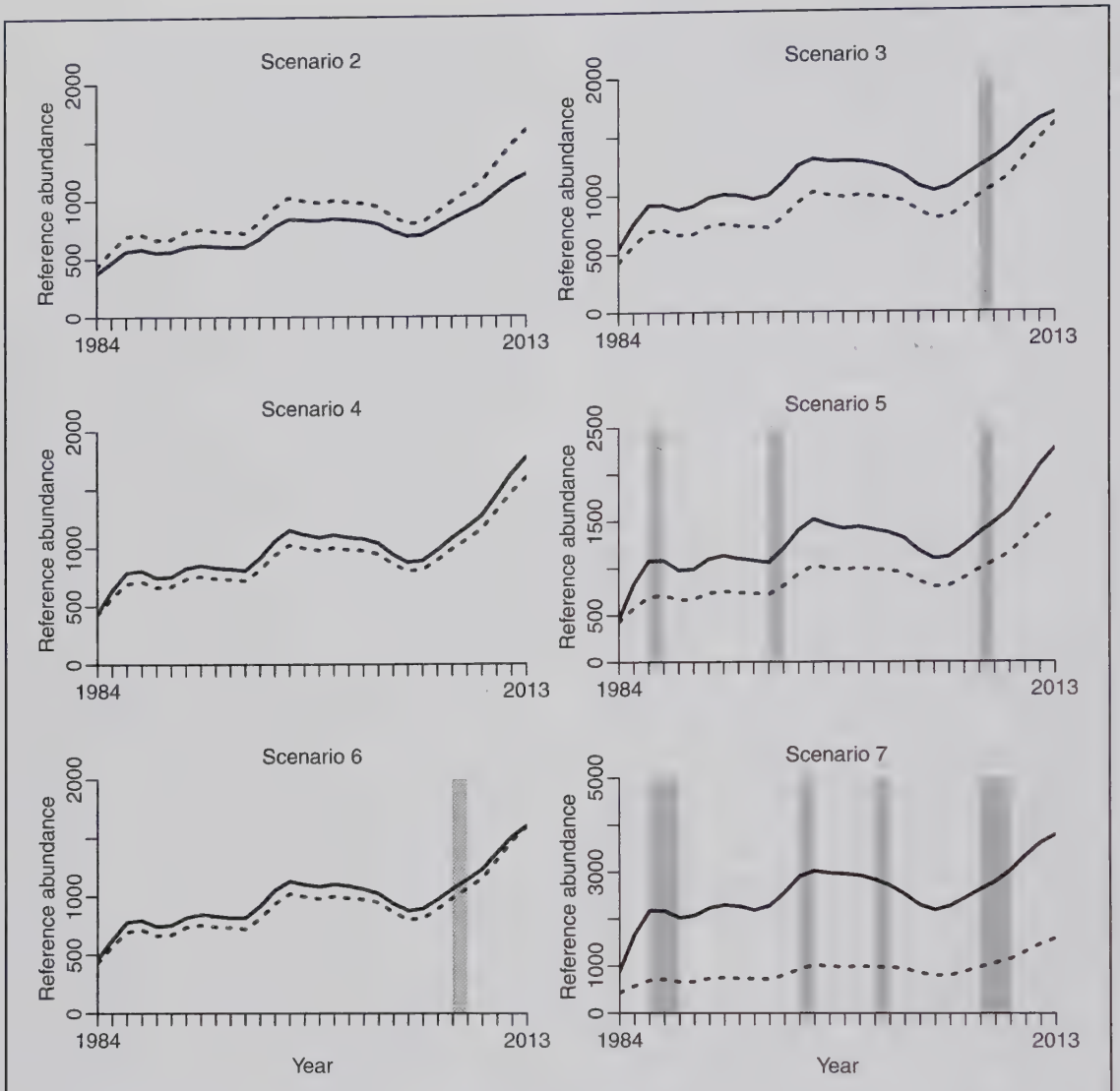

Figure 2

Estimated reference abundance (in millions of individuals) of American lobster (*Homarus americanus*) in the Gulf of Maine during 1984–2013 for 6 scenarios in the University of Maine Lobster Stock Assessment Model (UMM) corresponding to scenarios in Tables 1 and 3 (black lines). Estimated abundance under the first scenario or the UMM base case is provided for comparison (dotted lines). The gray bars indicate years for which the historical fishery status (as calculated from the biological reference points in Table 3) is different from that of the UMM base case for the same year. Note the differences between panels in the range of values on the *y*-axis.

realistic scenarios can be found in Figure 3. The final breaking point was between the growth shifts of 1.4375 and 1.5000 and the size at maturity values of 82.41 and 82.76 mm CL.

Discussion

Traditional sensitivity analyses are bottom-up: they are designed to determine how model output changes when specific parameters are altered (Booshehrian et al., 2012; Salciccioli et al., 2016). This practice is commonly used in stock assessment procedures to determine model stability and quantify uncertainty (Rosenberg and Restrepo, 1994; Hilborn, 2003; Salciccioli et al., 2016). The UMM scenarios in this study that involved IBLS scenarios 1–5 are an example of this classic type of analysis. The UMM scenarios in this study that involved IBLS scenarios 6–7, however, represent a top-down approach to sensitivity analysis. In this top-down approach, a large model-free mechanism controlled how multiple variables changed together and would affect model results. In this type of approach, the aim is to answer the question of how sensitive the model is to this large mechanism, which was climate change in this study.

Table 4

Terminal-year stock abundance (in millions of individuals) and stock status from each University of Maine Lobster Stock Assessment Model (UMM) scenario for American lobster (*Homarus americanus*) in the Gulf of Maine. Also presented are proportions of each estimate of terminal-year abundance in relation to the target reference point. Stock status is presented in comparison to the biological reference points in Table 3. In each UMM scenario, the growth transition matrices and size at maturity produced with the corresponding individual-based lobster simulator model were used (Table 1). The time series used in the UMM is from the period from 1984 through 2013.

Terminal-year parameter	UMM scenario						
	1	2	3	4	5	6	7
Abundance estimate	1594.5	1217.9	1687.7	1769.5	2265.5	1599.5	3792.7
Stock status	>target	>target	>target	>target	>target	>target	>target
Abundance proportion	1.63	1.48	1.34	1.64	1.61	1.50	1.33

Climate change affects molting probability, molt increment probability, and size at maturity of American lobster together. Therefore, this type of analysis is important to determine these cumulative effects on model outputs, succeeding where traditional sensitivity analyses fail. This type of analysis is sometimes referred to as a global sensitivity analysis and is very rarely used in fishery stock assessments (Lehuta et al., 2010; Saltelli et al., 2019; García, 2020). We agree with the notion of Saltelli et al. (2019) that a lack of the use of this method throughout the fields of environmental science and biology is concerning. We further postulate that both a bottom-up approach and a top-down approach may be beneficial and increasingly imperative in a changing world to ensure that a stock assessment model is stable under ensemble changes brought by large mechanisms.

The sensitivity of the UMM to growth and size at maturity is relatively and biologically low. Size-at-maturity values associated with breaking points in the biologically realistic scenarios are not expected to reach such low levels for at least 50 years (Le Bris et al., 2017; IPCC, 2019; Brickman et al., 2021). The relationship of growth of American lobster to temperature and climate change are well-known (Aiken, 1977; Le Bris et al., 2017), but strict predictions cannot be easily extrapolated and may be less appropriate (Punt et al., 2014). This information, coupled with the fact that most information on these parameters found in laboratory settings may not be directly applicable to scenarios designed to represent conditions in the wild (Jury and Watson, 2013), means that forecasting growth and size at maturity of American lobster is incredibly challenging. An advantage of our modeling framework is that strict relationships of tested parameters to the large mechanism (e.g., climate change or temperature change) are not necessary. The framework is not meant to be used to determine future changes to modeling efforts, but rather results from using it can highlight the limitations of a stock assessment under climate change.

It is important to consider that our study was focused on abundance as an output of interest because it is used to set management targets and thresholds. However, climate-driven changes to maturity and growth likely affect other aspects of a population and fishery dynamics, such as spawning stock biomass, recruitment, and fishing mortality. The aim of our study was not to analyze the effects of climate change on the full suite of outputs for population and fishery dynamics but rather was to understand whether determinations of fishery stock status would have been different under the climate effects we simulated.

Estimates of terminal-year stock status, most relevant to management of American lobster, did not change over all UMM scenarios in this study, indicating the robustness of the UMM to changes in life history parameters. However, results from using the combination of shifts in growth and size at maturity indicate differences in hindcasted fishery statuses. Consequently, scenarios tested in this study may not alter input data enough to produce different results for current management, but given that historical deviations were present, caution should be given to the assumptions of low sensitivity. Deviations of historical stock statuses were mostly related to magnitude, representing overestimations of abundance of American lobster throughout the time series but having very similar temporal trends. This result is due to the use of relative BRPs calculated for each scenario as opposed to the use of static values over all scenarios. Lobster management, like much of fisheries management in general, is more concerned with trends (ASMFC, 2015) than absolute values. Therefore, large shifts in growth and size at maturity can alter model results but would not have severely affected historical management decisions based on stock status.

As expected, these UMM scenarios all had worse model fits (higher objective function values) than the UMM base case (see Supplementary Table) (online only). These worse fits are most likely due to the approximation of biologically unrealistic, freely estimated parameters in an attempt to fit to the input data while also using the growth and size-at-maturity data provided (Slezak et al., 2010). These differences in fit are not relatively high, even for the largest shifts in this study, but in work

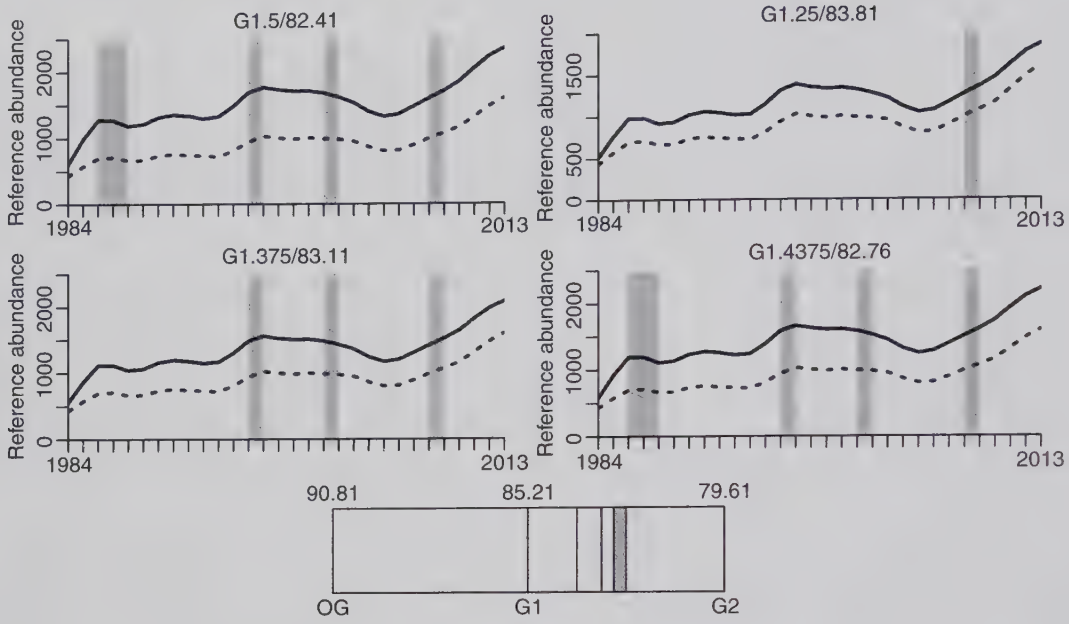

Figure 3

Estimated reference abundance (in millions of individuals) of American lobster (*Homarus americanus*) in the Gulf of Maine during 1984–2013 for the biologically realistic University of Maine Lobster Stock Assessment Model (UMM) scenarios used in the growth sensitivity analyses (black lines). The top-left panel represents a scenario between scenarios 6 and 7. Each of the other panels, the top-right panel, then the bottom panels from left to right, represents a consecutive scenario in the sensitivity analysis based on the scenario in the previous panel. In addition to the size at maturity (e.g., 82.41 cm carapace length [CL]), each panel title includes the shift from the individual-based lobster simulator model base case used to produce the abundance estimates shown, with the shift represented as a proportion between a full paired shift of molting probability by 1 year and molt increment probability by 1 size bin of 1 cm CL (G1) and a full paired shift of molting probability by 2 seasons and molt increment probability by 2 size bins (G2). Estimated abundance under the UMM base case (with original growth data [OG] and size at maturity) is provided for comparison in each panel (dotted lines). The gray bars indicate years for which the historical fishery status (as calculated from biological reference points in Table 3) is different from that of the UMM base case for the same year. The bottom panel shows the location of the breaking point of sensitivity within one-sixteenth of a shift (gray bar) in relation to the UMM base case data. In this bottom panel, the vertical lines represent the tests of partial shifts shown in the previous panels. Note the differences between panels in the range of values on the *y*-axis.

on other models, this phenomenon should be considered. Caution should be used when using this approach, and careful attention should be paid to the freely estimated parameters of the model.

It is important to note the combined effects of shifts in growth and size at maturity. The largest alteration in comparison to the UMM base case occurred when the largest effects from growth and size at maturity were combined. In contrast, results from use of shifts that were smaller than that alteration indicate that combined effects may not be strictly additive, and future work should be focused on the complex relationships of growth, size at maturity, and temperature, especially as they pertain to the American lobster stock assessment model. Quantifying the relationships between these parameters and thermal habitat is a research priority (ASMFC, 2015), but another priority is to develop modeling capacity to handle temporally dynamic life history parameters. If climate change affects key life history characteristics, traditional stock assessments in which static values for variables, such as growth, size at maturity, and others, are used may be inaccurate (Correa et al., 2021).

A problem, however, highlights a key limitation of the analysis used in the current stock assessment model: climate change affects many other aspects of the life history of American lobster besides growth and size at maturity. Key life history information, such as natural mortality (Mills et al., 2013) and recruitment (Goode et al., 2019; Tanaka et al., 2019), as well as important stock assessment model parameters, such as fishery-dependent and fishery-independent catchability or exploitation (Maunder et al., 2006; Conn, 2010; Shelton et al., 2014), are likely affected by changes in thermal habitat. Complex relationships with all of these factors exist, and a fully comprehensive top-down sensitivity analysis would see climate effects on all of them together.

The top-down approach used in the framework of our study can be used to examine a specific category of life history traits, but in future analyses, this work should be expanded to include effects from other life history and fishery components. Such a fully comprehensive analysis, however, would be possible only after individual studies, such as the one we describe herein or was done by Hodgdon et al. (2020), in which the UMM was tested in the presence of thermal effects on survey catchability, are completed. Temporally dynamic life histories in stock assessment may require quantification of relationships with environmental conditions, but use of them would ultimately increase accuracy in model results and precision of forecasts. Another avenue for future research would be the application of a management strategy evaluation within the current framework. In this work, the IBLS would be used as an operating model so that results from the UMM could have a "true" population to use in comparisons.

Ultimately, knowing the breaking points does not aid management if there is a lack of knowledge on the life history parameters tested a priori, specifically a lack of information concerning the relationship with each of them to thermal habitat and hypotheses as to the predicted scale of future change. Foremost, the need to quantify the relationship that parameters related to life history traits of American lobster have with a changing climate is critical and is a concern that management shares (ASMFC, 2015). Such work is considered essential because comparison of predicted changes to the stock assessment model's breaking points aids in determining research necessity. If the breaking points are higher than the predicted changes, changes under climate change may not significantly affect stock assessments if data for the life history parameters (e.g., growth and size at maturity) are not updated. If the breaking points are lower than the predicted changes, modeling efforts with parameter data that have not been updated may no longer yield accurate results, and the aim of future research should be to improve understanding of those parameters for which information is old.

Conclusions

In this study, we used a novel top-down sensitivity analysis for American lobster in the Gulf of Maine. This framework has great potential to better the management of the fishery for this species, but it should be expanded in future work. Lobster and, by extension, crustacean physiology and life history are directly linked to the environment and most often are consequences of thermal habitat (Madeira et al., 2012). As climate change alters the thermal habitats of crustaceans, the data used in stock assessment methods that rely on life history characteristics can become out of date. This issue can be mitigated with persistent monitoring efforts and scientific research. However, many crustacean fisheries, even in well-funded jurisdictions such as the United States, have limited resources for such cost-intensive research efforts. The framework proposed in this paper can be used to possibly lessen research loads by prioritizing the input parameters to which a specific stock assessment model is most sensitive under the top-down mechanism of climate change. A complete analysis of dependent and independent effects from all variables together under this framework has the potential to aid management practices, to advance crustacean stock assessment, and to steer future research projects.

Resumen

Las especies de crustáceos son socioeconómica y ecológicamente cruciales en todo el mundo. Para los crustáceos, como ectotermos, el cambio climático antropogénico amenaza con alterar significativamente las características clave de su historia de vida, como la talla de madurez y la tasa de crecimiento. Dado que es difícil determinar la edad de los crustáceos, los datos de longitud se utilizan en las evaluaciones de sus poblaciones; sin embargo, los cambios en la maduración y el crecimiento, por efecto del clima pueden influir en gran medida en el desempeño de los modelos estructurados por talla en la evaluación de las poblaciones. Acoplamos modelos individuales y estructurados por talla para la langosta americana (*Homarus americanus*) frente al noreste de Norteamérica, en el golfo de Maine, para realizar un novedoso análisis de sensibilidad del efecto de los parámetros de entrada de madurez y crecimiento en los resultados del modelo. Para este análisis, utilizamos un enfoque ascendente (con parámetros modificados de forma independiente) y un enfoque descendente (con parámetros modificados de forma conjunta a medida que se preveía su influencia por el cambio climático). Encontramos que nuestro modelo de evaluación de la población de langosta americana es resiliente a los cambios relativamente extremos de los parámetros biológicos de entrada. Para la evaluación de poblaciones de crustáceos con modelos estructurados por talla, recomendamos ampliar los análisis de sensibilidad para incluir la evaluación de la influencia de los cambios provocados por el clima sobre los parámetros de entrada basados en los rasgos del ciclo de vida que varían con el tiempo.

Acknowledgments

We thank all members of the Chen Lab at the University of Maine and Stony Brook University for their help and feedback throughout this process. We would also like to thank B. Shank of the NOAA Northeast Fisheries Science Center for providing much supportive feedback and to J. Kipp of the Atlantic States Marine Fisheries Commission for supplying the necessary trawl survey data. This study was financially supported by the National Marine Fisheries Service Sea Grant Joint Fellowship Program in Population and Ecosystem Dynamics and Marine Resource Economics (award no. NA20OAR4170464).

Literature cited

Aiken, D. E.
1977. Molting and growth in decapod crustaceans, with particular reference to the lobster *Homarus americanus*. *In* Workshop on lobster and rock lobster ecology and physiology. CSIRO Circ. 7 (B. F. Phillips and J. S. Cobb, eds.), p. 41–73. CSIRO, Melbourne, Australia.

Aiken, D. E., and S. L. Waddy.
1976. Controlling growth and reproduction in the American lobster. Proc. Annu. Meet. World Maric. Soc. 7:415–430.

ASMFC (Atlantic States Marine Fisheries Commission).
2015. American lobster benchmark stock assessment and peer review report, 417 p. ASMFC, Arlington, VA. [Available from website.]
2020. 2020 American lobster benchmark stock assessment and peer review report, 447 p. ASMFC, Arlington, VA. [Available from website.]

Audzijonyte, A., E. Fulton, M. Haddon, F. Helidoniotis, A. J. Hobday, A. Kuparinen, J. Morrongiello, A. D. M. Smith, J. Upston, and R. S. Waples.
2016. Trends and management implications of human-influenced life-history changes in marine ectotherms. Fish Fish. 17:1005–1028.

Booshehrian, M., T. Möller, R. M. Peterman, and T. Munzner.
2012. Vismon: facilitating analysis of trade-offs, uncertainty, and sensitivity in fisheries management decision making. Comput. Graph. Forum 31:1235–1244.

Brander, K.
2010. Impacts of climate change on fisheries. J. Mar. Syst. 79:389–402.

Brickman, D., M. A. Alexander, A. Pershing, J. D. Scott, and Z. Wang.
2021. Projections of physical conditions in the Gulf of Maine in 2050. Elem. Sci. Anthrop. 9(1):00055.

Chang, J.-H.
2015. Population dynamics of American lobster: environmental, ecological, and economic perspectives. Ph.D. diss., 160 p. Univ. Maine, Orono, ME. [Available from website.]

Chen, Y., M. Kanaiwa, and C. Wilson.
2005. Developing and evaluating a size-structured stock assessment model for the American lobster, *Homarus americanus*, fishery. N.Z. J. Mar. Freshw. Res. 39:645–660.

Comeau, M., and F. Savoie.
2001. Growth increment and molt frequency of the American lobster (*Homarus americanus*) in the southwestern Gulf of St. Lawrence. J. Crustac. Biol. 21:923–936.

Conn, P. B.
2010. Hierarchical analysis of multiple noisy abundance indices. Can. J. Fish. Aquat. Sci. 67:108–120.

Correa, G. M., C. R. McGilliard, L. Ciannelli, and C. Fuentes.
2021. Spatial and temporal variability in somatic growth in fisheries stock assessment models: evaluating the consequences of misspecification. ICES J. Mar. Sci. 78:1900–1908.

Doney, S. C., M. Ruckelshaus, J. E. Duffy, J. P. Barry, F. Chan, C. A. English, H. M. Galindo, J. M. Grebmeier, A. B. Hollowed, N. Knowlton, et al.
2012. Climate change impacts on marine ecosystems. Annu. Rev. Mar. Sci. 4:11–37.

Doney, S. C., D. S. Busch, S. R. Cooley, and K. J. Kroeker.
2020. The impacts of ocean acidification on marine ecosystems and reliant human communities. Annu. Rev. Environ. Resour. 45:83–112.

García, D.
2020. FLBEIA fisheries management simulation model. Definition of new criteria and guidelines for efficient validation of the model using global sensitivity analysis. Ph.D. diss., 229 p. Univ. Basque Ctry., Leioa, Spain. [Available from Univ. País Vasco, Barrio Sarriena s/n, 48940 Leioa, Spain.]

Gattuso, J.-P., A. K. Magnan, L. Bopp, W. W. L. Cheung, C. M. Duarte, J. Hinkel, E. Mcleod, F. Micheli, A. Oschlies, P. Williamson, et al.
2018. Ocean solutions to address climate change and its effects on marine ecosystems. Front. Mar. Sci. 5:337.

Goode, A. G., D. C. Brady, R. S. Steneck, and R. A. Wahle.
2019. The brighter side of climate change: how local oceanography amplified a lobster boom in the Gulf of Maine. Glob. Chang. Biol. 25:3906–3917.

Herrick, F. H.
1911. Natural history of the American lobster. Fish. Bull. 29:149–408.

Hilborn, R.
2003. The state of the art in stock assessment: where we are and where we are going. Sci. Mar. 67(suppl. 1):15–20.

Hodgdon, C. T., K. R. Tanaka, J. Runnebaum, J. Cao, and Y. Chen.
2020. A framework to incorporate environmental effects into stock assessments informed by fishery-independent surveys: a case study with American lobster (*Homarus americanus*). Can. J. Fish. Aquat. Sci. 77:1700–1710.

Huey, R. B., and J. G. Kingsolver.
1993. Evolution of resistance to high temperature in ectotherms. Am. Nat. 142:S21–S46.

IPCC (Intergovernmental Panel on Climate Change).
2019. Technical summary *In* IPCC special report on the ocean and cryosphere in a changing climate (H.-O. Pörtner, D. C. Roberts, V. Masson-Delmotte, P. Zhai, M. Tignor, E. Poloczanska, K. Mintenbeck, A. Alegría, M. Nicolai, A. Okem, et al., eds.), p. 39–69. Camb. Univ. Press, Cambridge, UK. [Available from website.]

Jury, S. H., and W. H. Watson III.
2013. Seasonal and sexual differences in the thermal preferences and movements of American lobsters. Can. J. Fish. Aquat. Sci. 70:1650–1657.

Le Bris, A., A. J. Pershing, J. Gaudette, T. L. Pugh, and K. M. Reardon.
2017. Multi-scale quantification of the effects of temperature on size at maturity in the American lobster (*Homarus americanus*). Fish. Res. 186:397–406.

Le Bris, A., K. E. Mills, R. A. Wahle, Y. Chen, M. A. Alexander, A. J. Allyn, J. G. Schuetz, J. D. Scott, and A. J. Pershing.
2018. Climate vulnerability and resilience in the most valuable North American fishery. Proc. Natl. Acad. Sci. 115:1831–1836.

Lehuta, S., S. Mahévas, P. Petitgas, and D. Pelletier.
2010. Combining sensitivity and uncertainty analysis to evaluate the impact of management measures with ISIS-fish: marine protected areas for the Bay of Biscay anchovy (*Engraulis encrasicolus*) fishery. ICES J. Mar. Sci. 67:1063–1075.

Little, S. A., and W. H. Watson III.
2003. Size at maturity of female American lobsters from an estuarine and coastal population. J. Shellfish Res. 22:857–863.
2005. Differences in the size at maturity of female American lobsters, *Homarus americanus*, captured throughout the range of the offshore fishery. J. Crustac. Biol. 25:585–592.

Lorenzen, K.
2016. Toward a new paradigm for growth modeling in fisheries stock assessments: embracing plasticity and its consequences. Fish. Res. 180:4–22.

Madeira, D., L. Narciso, H. N. Cabral, and C. Vinagre.
2012. Thermal tolerance and potential impacts of climate change on coastal and estuarine organisms. J. Sea Res. 70:32–41.

Maunder, M. N., and A. E. Punt.
2013. A review of integrated analysis in fisheries stock assessment. Fish. Res. 142:61–74.
Maunder, M. N., and K. R. Piner.
2015. Contemporary fisheries stock assessment: many issues still remain. ICES J. Mar. Sci. 72:7–18.
Maunder, M. N., J. R. Sibert, A. Fonteneau, J. Hampton, P. Kleiber, and S. J. Harley.
2006. Interpreting catch per unit effort data to assess the status of individual stocks and communities. ICES J. Mar. Sci. 63:1373–1385.
Mazur, M., B. Li, J.-H. Chang, and Y. Chen.
2018. Using an individual-based model to simulate the Gulf of Maine American lobster (*Homarus americanus*) fishery and evaluate the robustness of current management regulations. Can. J. Fish. Aquat. Sci. 76:1709–1718.
Mills, K. E., A. J. Pershing, C. J. Brown, Y. Chen, F.-S. Chiang, D. S. Holland, S. Lehuta, J. A. Nye, J. C. Sun, A. C. Thomas, et al.
2013. Fisheries management in a changing climate: lessons from the 2012 ocean heat wave in the Northwest Atlantic. Oceanography 26(2):191–195.
NEFSC (Northeast Fisheries Science Center).
1996. Report of the 22nd northeast regional stock assessment workshop (22nd SAW): stock assessment review committee (SARC) consensus summary of assessments. Northeast Fish. Sci. Cent. Ref. Doc. 96-13, 242 p. [Available from website.]
Punt, A. E.
2003. The performance of a size-structured stock assessment method in the face of spatial heterogeneity in growth. Fish. Res. 65:391–409.
Punt, A. E., T. Huang, and M. N. Maunder.
2013. Review of integrated size-structured models for stock assessment of hard-to-age crustacean and mollusc species. ICES J. Mar. Sci. 70:16–33.
Punt, A. E., T. A'mar, N. A. Bond, D. S. Butterworth, C. L. de Moor, J. A. A. De Oliveira, M. A. Haltuch, A. B. Hollowed, and C. Szuwalski.
2014. Fisheries management under climate and environmental uncertainty: control rules and performance simulation. ICES J. Mar. Sci. 71:2208–2220.
Rosenberg, A. A., and V. R. Restrepo.
1994. Uncertainty and risk evaluation in stock assessment advice for U.S. marine fisheries. Can. J. Fish. Aquat. Sci. 51:2715–2720.
Salciccioli, J. D., Y. Crutain, M. Komorowski, and D. C. Marshall.
2016. Sensitivity analysis and model validation. *In* Secondary analysis of electronic health records, p. 263–271. Springer, Cham, Switzerland.
Saltelli, A., K. Aleksankina, W. Becker, P. Fennell, F. Ferretti, N. Holst, S. Li, and Q. Wu.
2019. Why so many published sensitivity analyses are false: a systematic review of sensitivity analysis practices. Environ. Model. Softw. 114:29–39.
Shelton, A. O., J. T. Thorson, E. J. Ward, and B. Feist.
2014. Spatial semiparametric models improve estimates of species abundance and distribution. Can. J. Fish. Aquat. Sci. 71:1655–1666.
Slezak, D. F., C. Suárez, G. A. Cecchi, G. Marshall, and G. Stolovitzky.
2010. When the optimal is not the best: parameter estimation in complex biological models. PLoS ONE 5(10):e13283.
Tanaka, K. R., J. Cao, B. V. Shank, S. B. Truesdell, M. D. Mazur, L. Xu, and Y. Chen.
2019. A model-based approach to incorporate environmental variability into assessment of a commercial fishery: a case study with the American lobster fishery in the Gulf of Maine and Georges Bank. ICES J. Mar. Sci. 76:884–896.
Waller, J. D., K. M. Reardon, S. E. Caron, B. P. Jenner, E. L. Summers, and C. J. Wilson.
2021. A comparison of the size at maturity of female American lobsters (*Homarus americanus*) over three decades and across coastal areas of the Gulf of Maine using ovarian staging. ICES J. Mar. Sci. 78:1267–1277.
Zhang, Y., Y. Chen, and Y.-J. Chang.
2011. Estimating biological reference points using individual-based per-recruit models for the Gulf of Maine American lobster, *Homarus americanus*, fishery. Fish. Res. 108:385–392.

National Marine
Fisheries Service
NOAA

Fishery Bulletin
established in 1881

Spencer F. Baird
First U.S. Commissioner
of Fisheries and founder
of *Fishery Bulletin*

Effects of incomplete sampling and standardization on indices of abundance from a fishery-independent trawl survey off the Atlantic coast of the southeastern United States

Amy Zimney
Tracey Smart (contact author)

Email address for contact author: smartt@dnr.sc.gov

Marine Resources Research Institute
South Carolina Department of Natural Resources
217 Fort Johnson Road
Charleston, South Carolina 29412

Abstract—Abundance indices from fishery-independent surveys are preferred in stock assessments for their robust scientific designs that minimize uncertainty and bias. When sampling does not adhere to the design, researchers employ techniques such as imputation or standardization to improve accuracy and reduce bias. We examined 2 methods for adjusting for incomplete sampling within the Coastal Trawl Survey (CTS) of the Southeast Area Monitoring and Assessment Program—South Atlantic for 3 species commonly encountered in survey sampling, the Atlantic croaker (*Micropogonias undulatus*), bluefish (*Pomatomus saltatrix*), and white shrimp (*Litopenaeus setiferus*): design-based imputation of missing data and standardization through the delta-generalized-linear-model approach. Additionally, we determined the effect of modifying the seasonal component of the survey design through retrospective simulation. For all 3 species, standardization improved precision in annual abundance estimates relative to values estimated with the design-based method. When a stratum missed in sampling overlapped with an area or time of high variability for a species (e.g., 2019), standardization did not improve precision over the design-based method. Results from examination of the effects of dropping entire seasons, because of funding or logistical challenges, indicate that rotating which season is dropped was the best approach to balancing characteristics of each species. Overall, we recommend the standardization approach for accounting for missing data within the CTS time series.

Manuscript submitted 12 April 2022.
Manuscript accepted 2 September 2022.
Fish. Bull. 120:252–267 (2022).
Online publication date: 28 September 2022.
doi: 10.7755/FB.120.3-4.6

The views and opinions expressed or implied in this article are those of the author (or authors) and do not necessarily reflect the position of the National Marine Fisheries Service, NOAA.

Generally, the purpose of fishery-independent surveys is to provide population data to stock assessments to reduce uncertainty in stock statuses and management measures informed by the stock assessments (Walters and Pearse, 1996). Reduction in uncertainty relies on fishery-independent surveys having robust scientific designs that are not influenced by management or fishing practices (Cochran, 1977; Williams and Carmichael[1]). To reduce assessment uncertainty, considerable effort has been applied to developing best practices for minimizing error in abundance indices derived from survey data (Walters, 2003; Maunder and Punt, 2004; Shelton et al., 2014). Additionally, much work has been done to address bias in index calculation due to spatial variability in sampling or fishing and to ensure that effort is defined appropriately (Campbell, 2004, 2015). Precision can be gained in fishery-independent surveys either by increasing sampling effort or by using a stratified-random sampling design to optimize effort allocation (Xu et al., 2015). However, the realities of funding, weather, and vessel reliability and availability more often than not result in decreased or incomplete sampling effort decreasing precision of a survey. In particular, changing environmental conditions and funding concerns that affect completion of surveys are highly pervasive issues among surveys, and many survey programs are facing hard decisions regarding reducing effort while still providing comparable time series. In the absence of increased precision from a priori design, researchers may turn to analytical tools.

Stock assessment models often rely on the inclusion of catch rate time series (either fishery-independent or fishery-dependent) that are proportional to population abundance (generally referred to as indices of abundance) (Francis, 2011). Often it is assumed that these time series are proportional to stock size (Hilborn and Walters, 1992; Arreguín-Sánchez, 1996; Quinn and Deriso, 1999), on the basis of the sampling design, stability of catchability, and consistency in trends among

[1] Williams, E. H., and J. Carmichael (eds.). 2009. South Atlantic fishery independent monitoring program workshop final report, 85 p. South Atl. Fish. Manag. Counc. and Natl. Mar. Fish. Serv., Southeast Fish. Sci. Cent., Beaufort, NC. [Available from Southeast Fish. Sci. Cent., Natl. Mar. Fish. Serv., 101 Pivers Island Rd., Beaufort, NC 28516.]

indices of abundance (Quinn and Deriso, 1999). For an index of abundance to reflect stock size trends, the data must be collected according to a robust scientific design consistently through time. When deviations from the design occur, those deviations should be accounted for in some way. Standardizing catch data increases the accuracy of estimates (Walters, 2003; Maunder and Punt, 2004) and allows accounting for incomplete sampling during the time series. Typical statistical standardization techniques (e.g., generalized linear models or generalized additive models) provide the opportunity to quantify the effects of either sampling or environmental characteristics on estimates of abundance and to essentially correct those estimates for deviations in sampling or environmental conditions (Wilberg et al., 2009).

Off the Atlantic coast of the southeastern United States, fish, elasmobranch, and invertebrate species in nearshore, coastal waters are surveyed through fishery-independent sampling of the Southeast Area Monitoring and Assessment Program—South Atlantic's Coastal Trawl Survey (SEAMAP-SA CTS). Sampling of trawlable habitats through the CTS began in this region (Fig. 1) in

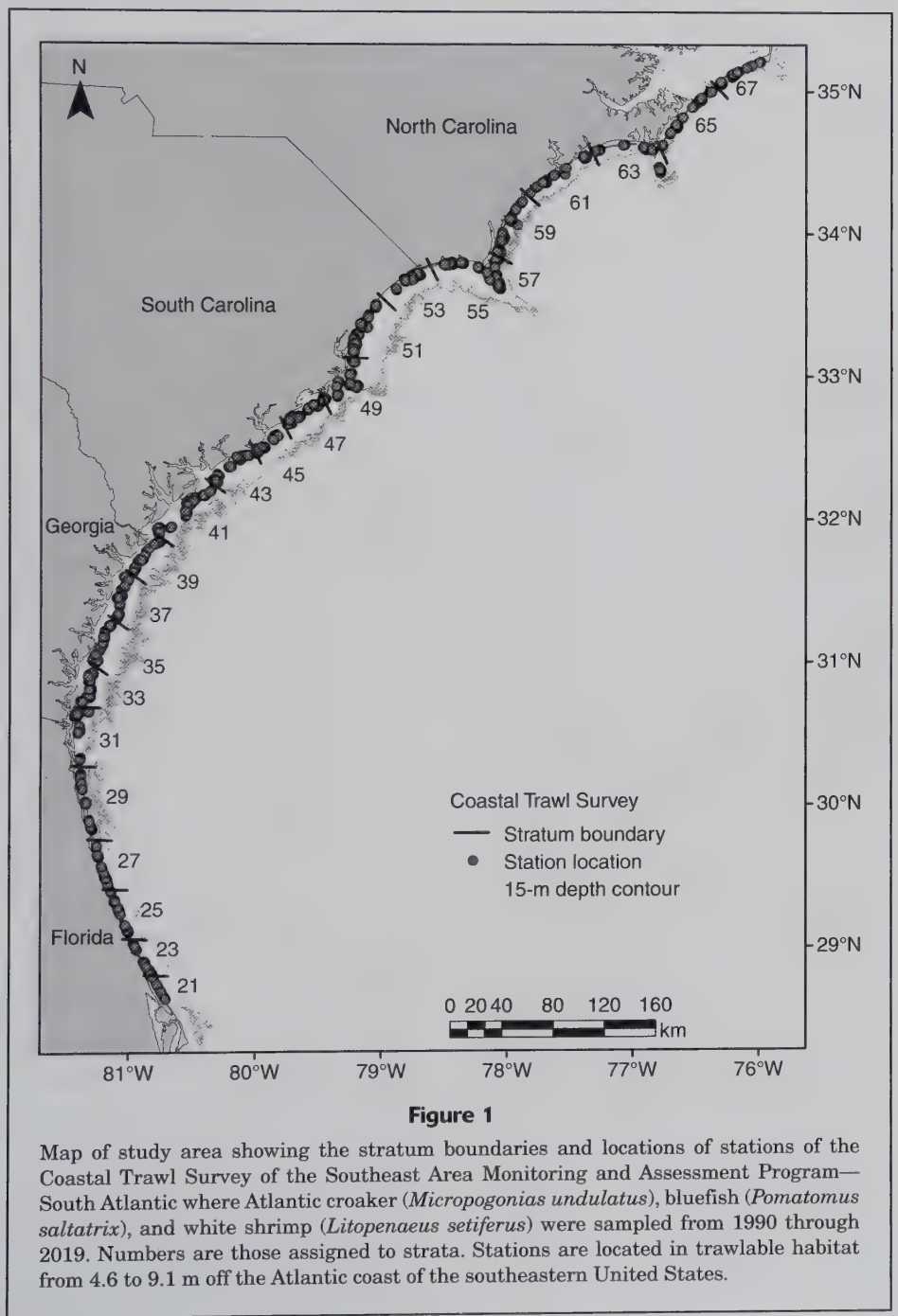

Figure 1

Map of study area showing the stratum boundaries and locations of stations of the Coastal Trawl Survey of the Southeast Area Monitoring and Assessment Program—South Atlantic where Atlantic croaker (*Micropogonias undulatus*), bluefish (*Pomatomus saltatrix*), and white shrimp (*Litopenaeus setiferus*) were sampled from 1990 through 2019. Numbers are those assigned to strata. Stations are located in trawlable habitat from 4.6 to 9.1 m off the Atlantic coast of the southeastern United States.

1986, and since 1990 the CTS has monitored abundance trends in shallow depths (<9.1 m) using a standardized stratified-random sampling design. Each year, the number of stations allocated for sampling is determined by available funding, but the spatial and temporal portions of the survey design have remained consistent over time. This consistency makes it possible for estimates based on catch rate time series from this survey to serve as indices of abundance for stock assessments.

Historically, the rates at which stations were missed were low, and the missed stations were generally spread out among strata instead of entire strata being missed. More recently, however, the CTS has experienced challenges to sampling all of the stations allocated for sampling as a result of the increased frequency of weather conditions unsuitable for sampling (including prolonged periods of winds and sea states above sampling cut-offs and major hurricanes), damaged gear (caused by debris from river run-off following hurricanes and major rain events), logistical challenges (including low tidal amplitude preventing departures), and mechanical failures making the aging vessel unavailable for sampling. In some seasons during 2018 and 2019, these challenges meant that entire strata were not sampled. Given these challenges, it has become more likely that annual abundance estimates based on survey data from years with completely unsampled strata or high numbers of unsampled stations will not be proportional to true abundance or will not index the same portion of the population as estimates based on data from other years with more complete sampling of strata.

Herein, we present catch and effort time series for 3 species of management interest commonly encountered in CTS sampling: the Atlantic croaker (*Micropogonias undulatus*), bluefish (*Pomatomus saltatrix*), and white shrimp (*Litopenaeus setiferus*). These species have a variety of distributions (spatially and temporally) (senior author, unpubl. data), and incomplete sampling may affect abundance estimates in different ways. In light of recent difficulties completing CTS sampling, we present annual abundance for these species in 2 ways, a nominal, design-based estimate and a standardized estimate, to assess if these time series need correcting through standardization because of incomplete sampling. In addition, we provide results of our examination of the effects of sampling and environmental covariates on the standardized estimate of abundance to identify potential drivers of abundance and the need for correction for each species. Because the challenges for completing survey sampling as designed are expected to continue, changes to the survey design, such as dropping a sampling season, are under consideration. To determine the effects of these potential design modifications on abundance estimates, we also conducted retrospective simulations on the standardized indices of abundance for all 3 species. On the basis of these analyses, we provide a recommendation on which estimate is most appropriate for use as an index of abundance and on whether there is a preferred design modification strategy.

Materials and methods

Study design and gear

Sampling for the CTS, a fishery-independent research program, was conducted by the South Carolina Department of Natural Resources (SCDNR) in coastal Atlantic waters off the southeastern United States between Cape Hatteras, North Carolina, and Cape Canaveral, Florida (Fig. 1). Consistent sampling methods were in place from 1990 through 2019 and were used to target the full spatial range in each of 3 seasons: spring (April and May), summer (July and August), and fall (September and November). Trawl surveys were conducted at randomly selected stations from a pool of stations within 24 strata based on latitude and depth (Fig. 1) between the inshore 4.6-m depth contour and the offshore 9.1-m depth contour. To reduce variability of the data, the method of allocating stations was changed in 2001 from proportional allocation (based on the total surface area of each stratum) to optimal allocation (Thompson, 1992), with higher effort allocated to strata with historically higher variability and with the number of stations allocated within each stratum determined anew each year. The total number of allocated stations per season has ranged between 78 and 112, depending on funding and other survey priorities, but the spatial footprint of the survey has remained consistent.

Sampling was conducted during daylight hours (between 1 h after sunrise to 1 h before sunset) on board the R/V *Lady Lisa*, a 22.9-m wooden-hulled, double-rigged St. Augustine shrimp trawler owned and operated by the SCDNR Marine Resources Division, by using a pair of 22.9-m mongoose-type Falcon trawl nets (Beaufort Marine Supply Inc.[2], Beaufort, SC) without turtle excluder devices (Willis et al., 2015; Zimney[3]). The body of the trawl net was constructed of #15 net twine with 47-mm stretch mesh, and the codend was constructed of #30 net twine with 41-mm stretch mesh. At each station, the pair of nets were towed for 20 min, excluding wire-out and haul-back times, with a target speed of 1.3 m/s, relative to the bottom.

The catch from each net was processed independently and assigned a unique collection number. The contents of each net were sorted to species (with limited exceptions sorted to genus or family only), and the total biomass and number of individuals were recorded. When trawl nets contained high volume catches, selected species were removed (e.g., endangered species and species that posed a risk to staff during handling), the remaining net contents were placed into shrimp baskets and weighed, and a randomly selected basket was sorted and processed as described above. Abundance and biomass data for each

[2] Mention of trade names or commercial companies is for identification purposes only and does not imply endorsement by the National Marine Fisheries Service, NOAA.

[3] Zimney, A. 2021. SEAMAP-SA Coastal Trawl Survey data and sample collection methods. Southeast Data, Assessment, and Review SEDAR78-WP01, 4 p. [Available from website.]

species were then used to estimate the total abundance and biomass of each species in the full catch by using the ratio of the weight of subsampled catch placed in baskets to the total weight of the full catch. When large numbers of an individual species occurred in the processed catch, all individuals of that species were weighed, and then a haphazardly selected subsample was counted (subsamples were approximately 30–60 individuals). The total number of individuals of a species in the catch was then estimated by using the ratio of the weight of the processed species subsample to the total species weight.

Hydrographic data, measurements of surface and bottom temperature and salinity, were logged at each station, with a Van Dorn water sampler (Eijkelkamp North America Inc., Wilmington, NC) in 1990–1992, an SBE 19 SeaCAT Profiler CTD in 1993–2005 and 2017 (Sea-Bird Scientific, Bellevue, WA), or an SBE 19plus SeaCAT Profiler CTD in 2006–2019 (V1 or V2, Sea-Bird Scientific). From these CTD casts, we extracted the deepest measurement of temperature and salinity, as long as it was within 1 m of the bottom, to use in analyses (hereafter, these measurements are referred to as *bottom temperature* and *bottom salinity*).

Data and nominal abundance estimation

The data available for use in abundance estimation included a unique collection number, date of deployment, season, tow duration (in minutes), stratum, station, latitude, longitude, depth, bottom temperature, bottom salinity, and the number of individuals and aggregate weight of each species captured. Data from the paired nets were pooled for analysis to form a standard unit of effort at each station sampled (a trawl tow). Estimates of abundance were expressed as the number of individuals per hectare. Estimated area swept by a net was calculated by multiplying the expected average width of the net opening (13.5 m), based on Stender and Barans (1994), by the distance in meters trawled and dividing the product by 10,000 m^2/ha. Then, the estimated area swept for each of the paired nets was combined. If area swept could not be accurately estimated (e.g., if a U-turn was executed to avoid entanglement with a gill net), data for that tow were omitted from analyses.

From 1990 through 2019, sampling was conducted at 8403 of the 8568 allocated stations, and 24 strata were fully missed (Table 1, Fig. 1): 1 stratum (21) in fall 1990, 2 strata (65 and 67) in spring 2013, 4 strata (37, 39, 65, and 67) in spring 2018, 7 strata (29, 57, 59, 61, 63, 65, and 67) in fall 2018, 3 strata (63, 65, and 67) in spring 2019, and 7 strata (21, 23, 25, 27, 63, 65, and 67) in fall 2019. Where entire strata were missed, the average long-term nominal abundance was calculated for each species in each stratum and season and imputed for the missing value as the nominal abundance. In total, 58 trawl tows were excluded from analyses (Table 1). Nine tows were excluded because the area swept could not be accurately estimated, and 14 tows were eliminated because the tow duration was not equal to 20 min, indicating deviation from normal operations. Additionally, 35 tows were excluded from standardization because covariate information was missing.

Annual nominal abundance (A) was calculated by determining the sum of the number of individuals (*individuals*) caught per hectare (*area swept*) and dividing it by the total number of tows (t) for a given combination of stratum (st), season (se), and year (y):

$$A_y = \sum_{t=1}^{t} \frac{individuals_{t,st,se,y}}{area\,swept_{t,st,se,y}} \Big/ t_{st,se,y}. \quad (1)$$

The nominal index of abundance was then normalized by dividing the annual nominal abundance by the overall mean abundance for the full time series, producing a value of relative abundance for each year. These values provide reference points for individual years in relation to the time series, with a value of 1 being the long-term mean.

In recent years (2015–2019), sampling for the CTS has not been completed at all of the allocated stations for the reasons described in the "Introduction." Consequently, entire strata have been missed in some seasons primarily in the outer ranges of the study area where longer windows of suitable weather conditions are needed for travel and sampling (Table 1). Where an entire stratum was missed during a season, the long-term average nominal abundance was calculated for each stratum and season and imputed as a proxy for the nominal abundance of the missed stratum for use in Equation 1 (Little and Rubin, 1987; Walters, 2003). The long-term average was used rather than the average for the most recent years because using only data from recent years could have introduced bias if a stratum was sampled unusually early or late in a season (timing can vary by up to 6 weeks) or was missed in several of the recent years, as occurred for strata 65 and 67, for example.

Standardization with delta-generalized linear models

Because of incomplete seasonal and regional sampling coverage, annual abundance was standardized among years through the "delta-GLM" method (Lo et al., 1992; Dick, 2004; Ballenger et al.[4]), in which the standardized abundance is produced by using the product of predicted values from 2 generalized linear models (GLMs). In the first GLM, species presence and absence is the response variable, sampling or environmental covariates are included, and the binomial error distribution is used. In the second GLM, only data from the tows for which the species of interest were present are used, and the number per hectare is the response variable. Sampling and environmental covariates are also included in this second model, and this positive GLM is fitted with either the gamma or lognormal error distribution. Both gamma and lognormal error distributions were considered for the positive GLM because preliminary analyses found that both error distributions

[4] Ballenger, J., T. Smart, K. Kolmos, and M. Reichert. 2013. Trends in relative abundance of gray triggerfish in waters off the SE US based on fishery-independent surveys. Southeast Data, Assessment, and Review SEDAR32-DW04, 77 p. [Available from website.]

Table 1

The number of stations allocated for sampling each year, the number of stations at which survey tows were completed, the survey strata with missed stations, and the number of stations with available data that were included in analysis for standardization of indices of abundance for Atlantic croaker (*Micropogonias undulatus*), bluefish (*Pomatomus saltatrix*), and white shrimp (*Litopenaeus setiferus*) sampled during the Coastal Trawl Survey of the Southeast Area Monitoring and Assessment Program—South Atlantic off the Atlantic coast of the southeastern United States from 1990 through 2019. Percent positive rates, the percentage of tows with species present, are given for each species in each year. An asterisk (*) indicates that a stratum was missed in at least one season in the given year.

Year	No. of stations allocated	No. of stations with complete sampling	Strata with missed stations	No. of stations with data used	Percent positive rate (%)		
					Atlantic croaker	Bluefish	White shrimp
1990	234	231	21*, 61	227	65.2	43.2	50.2
1991	234	233	61	231	64.5	36.8	47.6
1992	234	234	–	232	56.0	40.1	37.5
1993	234	234	–	233	50.2	30.0	39.9
1994	234	234	–	233	53.2	32.6	43.8
1995	234	234	–	232	59.1	47.8	51.7
1996	234	234	–	229	58.5	45.3	48.3
1997	234	234	–	232	43.8	30.5	47.2
1998	234	234	–	232	64.4	33.5	57.9
1999	234	234	–	233	44.6	35.6	55.8
2000	234	234	–	234	44.9	37.2	54.7
2001	306	306	–	295	63.0	46.9	44.6
2002	306	306	–	301	45.9	23.9	49.2
2003	306	306	–	304	63.1	46.1	43.5
2004	306	306	–	304	54.9	36.9	46.7
2005	306	306	–	301	58.5	28.8	39.5
2006	306	306	–	303	54.8	20.7	45.6
2007	306	306	–	305	54.2	27.8	55.6
2008	306	306	–	304	53.3	36.3	62.1
2009	336	336	–	335	60.9	40.9	51.6
2010	336	336	–	335	50.1	40.0	40.3
2011	336	336	–	336	59.8	38.1	44.9
2012	336	336	–	336	69.9	33.3	64.0
2013	306	295	63, 65*, 67*	294	83.1	39.7	62.4
2014	306	306	–	306	70.9	38.9	43.8
2015	336	329	35, 63, 65	329	71.4	35.0	50.2
2016	336	331	29, 33, 35, 39	330	70.0	31.5	64.2
2017	306	294	21, 31, 35, 59, 61, 63, 67	293	71.8	22.1	65.6
2018	306	228	21, 23, 25, 27, 29*, 31, 33, 35, 37*, 39*, 41, 51, 53, 55, 57*, 59*, 61*, 63*, 65*, 67*	228	78.9	23.2	60.5
2019	306	258	21*, 23*, 25*, 27*, 29, 31, 61, 63*, 65*, 67*	258	84.9	24.0	69.0
Total	8568	8403		8345	61.1	34.8	51.3

fit data from the CTS for several species relatively well. Additionally, although other zero-inflated models have been used for standardization, the design of the CTS works well with the delta-GLM framework, and other models do not provide large improvements in variability for common species such as those examined here (Smart and Zimney[5]).

[5] Smart, T., and A. Zimney. 2021. Spanish mackerel indices of abundance in U.S. South Atlantic waters based on the SEAMAP-SA fishery-independent Coastal Trawl Survey. Southeast Data, Assessment, and Review SEDAR78-WP02, 22 p. [Available from website.]

Both error distributions were compared with the Akaike information criterion (AIC) in identical base models, and the one with the lowest AIC value was chosen as the model to use for analysis (Akaike, 1973).

Year, *season*, *stratum*, *bottom temperature*, and *bottom salinity* were included as model covariates. *Season* was defined as spring, summer, and fall as described earlier. *Stratum* was previously defined in the first paragraph of the "Materials and methods" section and in Figure 1 and served as a proxy for location (latitude and longitude). Observed values of bottom temperature and bottom salinity were binned by using quantiles, with 5 bins for bottom

temperature (<20.2°C, 20.2–23.0°C, 23.1–26.5°C, and ≥26.6°C) and 2 bins for bottom salinity (<34.9 and ≥34.9). The data for these covariates were binned rather than left continuous for consistency with accepted index formulations for the CTS in recent stock assessments (Smart and Boylan[6]). The addition of these covariates also is consistent with recent standardization techniques used in many recent assessments in the region. The delta-GLM for all species started with the same base model:

$$A_y = Pr(y, se, st, temp, sal) \times A_p(y, se, st, temp, sal), \quad (2)$$

where Pr = the likelihood of a species being present in year y, season se, stratum st, bottom temperature $temp$, and bottom salinity sal; and

A_p = the abundance of a species when it is present in year y, season se, stratum st, bottom temperature $temp$, and bottom salinity sal.

No interaction terms were included in the delta-GLM formula for consistency with recent accepted index formulations (Smart and Boylan[6]; Smart and Zimney[5]). Results of preliminary data analysis indicate no obvious interactive trends for any individual species examined in this study, and no multicollinearity was found for covariates included in the equation.

The covariates included in the final delta-GLM models (both the binomial GLM and positive GLM) were chosen by using AIC with backward selection, with the exception that *year* was always included in each model to allow an annual abundance value to be produced. The effect of covariates on standardized abundance estimates for each species was determined by using separate analyses of variance (ANOVA) for both the presence of a given species and the abundance of that same species estimated with model covariates as fixed factors. The final delta-GLM standardized abundance index for each species is the product of the mean responses from the linear predictors of *year* and any selected covariates from the 2 GLMs. Jackknifing was used to determine coefficients of variation, standard error, and standard deviations for each delta-GLM analysis. Residual and quantile-quantile (Q-Q) plots were used as diagnostic tools to determine the fit of the models. All analyses were performed in R, vers. 4.1.1 (R Core Team, 2021).

The delta-GLM used in this study was based primarily on code adapted from Dick (2004). As with the nominal index, the delta-GLM standardized index was normalized by dividing the annual standardized abundance by the overall mean standardized abundance for the time series, with a value of 1 being the mean for the time series. Nominal abundance calculations and delta-GLM analysis were performed for 3 species of management interest: the Atlantic croaker, bluefish, and white shrimp. Because these species also have generally been commonly caught in tows over the full length (1990–2019) of the CTS time series, their distributions and abundances lend themselves to the analyses outlined herein. Over the period of the CTS time series, the Atlantic croaker was often the most abundant species caught during CTS sampling annually, having widespread spatial and temporal distributions. Bluefish primarily were caught in northern strata in spring and fall. Given the recent sampling challenges during these seasons, estimates of the abundance of bluefish have the potential to be heavily affected by incomplete sampling. The white shrimp was another widely distributed species, largely occurring from northern Florida to central North Carolina.

In addition to comparison of design-based and standardized indices, the effects of several potential survey design modifications were investigated for each species. Design modifications under consideration are primarily focused on dropping a season from sampling in any given year. Potential scenarios for this design change are permanently dropping a season (3 scenarios: spring, summer, or fall), rotating the season that is dropped each year, or randomly selecting a season to drop each year. We retrospectively applied these 5 scenarios to the raw data for the 3 species during the period 2014–2019 to investigate the effect of the design for years when sampling coverage was severely incomplete (i.e., in 2018 and 2019) or was complete or mostly complete (i.e., in 2014–2017). Once these scenarios were applied to the raw data, we ran the delta-GLM analysis again for the full time series and examined the standardized abundance estimates and variability for all 5 scenarios and for the current survey design that includes all seasons.

Results

All covariates (*year*, *season*, *stratum*, *bottom temperature*, and *bottom salinity*) were selected for inclusion by using the AIC for both the binomial and positive delta-GLMs for the Atlantic croaker, bluefish, and white shrimp. For all 3 species the lognormal error structure had the lowest AIC value, indicating that it was the most appropriate error distribution to be used for the positive model.

Atlantic croaker

The Atlantic croaker was the most abundant species caught in CTS sampling, of the 3 species examined in this study. It was also the most common, occurring in 61% of all tows between 1990 and 2019 (Table 1). Atlantic croaker were distributed relatively evenly, both spatially and temporally, throughout the study area with specimens caught in all seasons and strata (Fig. 2, A and B). Atlantic croaker generally were more abundant in summer than in spring and least abundant in fall. Although this species occurred in all strata, abundance of Atlantic croaker increased from the southern portion of the study area to the northern portion. Atlantic croaker were abundant in a range of bottom temperatures but were more

[6] Smart, T. I., and J. Boylan. 2013. King mackerel index of abundance in coastal US South Atlantic waters based on a fishery-independent trawl survey. Southeast Data, Assessment, and Review SEDAR38-DW-11, 39 p. [Available from website.]

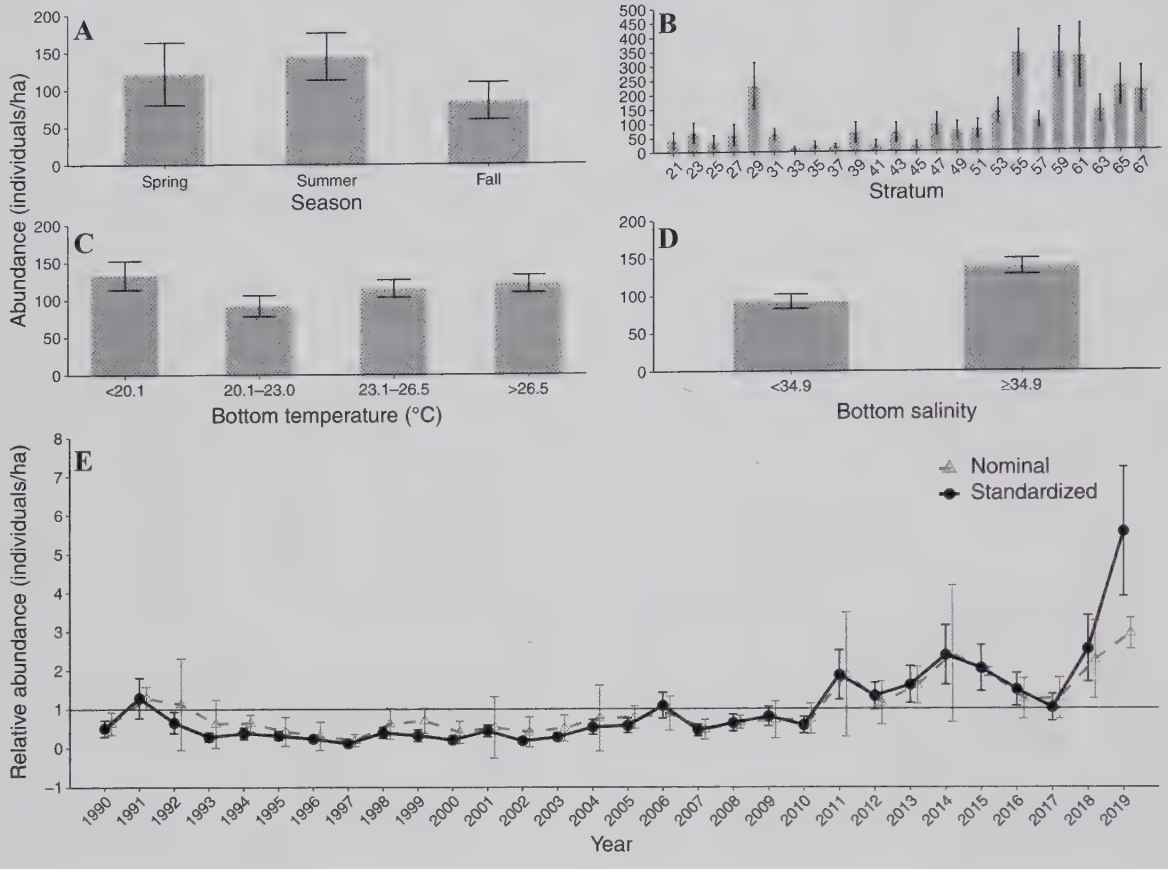

Figure 2

Nominal abundance of Atlantic croaker (*Micropogonias undulatus*), by (**A**) season, (**B**) stratum, (**C**) bottom temperature, and (**D**) bottom salinity, based on data from sampling off the Atlantic coast of the southeastern United States from 1990 through 2019, with design-based imputation of missing values. (**E**) Nominal and standardized relative abundances of Atlantic croaker estimated by using the design-based method and delta-generalized linear models, respectively, are provided by year. Error bars indicate the standard errors of the means. The horizontal gray line indicates the long-term mean of 1 for relative abundance over the full period of the time series.

abundant in waters with bottom salinities greater than 34.9 than in waters with other salinities (Fig. 2, C and D).

From 1990 through 2010, nominal abundance of Atlantic croaker remained relatively low compared with the mean nominal abundance for the time series, with the normalized nominal abundance below the time series mean for most years (Fig. 2E). After 2010, nominal abundance was more variable and had a general trend of values increasing to levels above the time series mean (Fig. 2E).

The trend in delta-GLM standardized abundance of Atlantic croaker was similar to that in nominal abundance, although the trend in standardized estimates was less variable (Fig. 2E, Suppl. Table [online only]). The exception to this similarity is that, for 2019, the predicted abundance of Atlantic croaker in the standardized index was almost twice the abundance predicted in the nominal index. This large difference between the nominal and standardized abundance values in 2019 coincides with the only occasion when the variability in the standardized estimate was higher than that of the nominal estimate for this species, indicating that variability drove the disagreement between the estimates produced with the 2 methods. In 2018 and 2019, limited sampling occurred in the northernmost strata where Atlantic croaker were generally more abundant than in other strata. The raw average nominal abundance in 2019 (excluding the imputed values for missed strata) was the highest in the history of the CTS (359.8 individuals/ha) (senior author, unpubl. data), possibly contributing to the standardized estimate being higher than the nominal estimate. In contrast, the data imputed for missed strata for nominal abundance were from years with lower abundance. All covariates were significant in the binomial and positive delta-GLMs for predicting the presence and abundance of Atlantic croaker (Table 2). Results from the use of diagnostics, such as residual and Q-Q plots, indicate reasonable fits for both models (Suppl. Fig. 1) (online only).

Table 2

Results from analysis of variance for presence and abundance of Atlantic croaker (*Micropogonias undulatus*), bluefish (*Pomatomus saltatrix*), and white shrimp (*Litopenaeus setiferus*) from standardization with binomial and positive delta-generalized linear models. Data used in models are from sampling of the Coastal Trawl Survey of the Southeast Area Monitoring and Assessment Program—South Atlantic conducted during 1990–2019 off the Atlantic coast of the southeastern United States. The significance level is 0.05.

Covariate	df	Deviance	Residual df	Residual deviance	*F*	*P*
Atlantic croaker						
Binomial model						
Null			8344	11,159.10		
Year	29	413.00	8315	10,746.10		<0.01
Season	2	498.71	8313	10,247.40		<0.01
Stratum	23	1188.01	8290	9059.40		<0.01
Temperature	3	11.06	8287	9048.30		0.01
Salinity	1	63.89	8286	8984.40		<0.01
Positive model						
Null			5092	31,609.00		
Year	29	2590.40	5063	29,019.00	19.61	<0.01
Season	2	1293.70	5061	27,725.00	142.02	<0.01
Stratum	23	4554.10	5038	23,171.00	43.47	<0.01
Temperature	3	140.80	5035	23,030.00	10.31	<0.01
Salinity	1	103.00	5034	22,927.00	22.62	<0.01
Bluefish						
Binomial model						
Null			8344	10,788.80		
Year	29	202.78	8315	10,586.00		<0.01
Season	2	242.50	8313	10,343.50		<0.01
Stratum	23	547.31	8290	9796.20		<0.01
Temperature	3	166.85	8287	9629.30		<0.01
Salinity	1	25.37	8286	9604.00		<0.01
Positive model						
Null			2906	6282.10		
Year	29	330.53	2877	5951.50	7.22	<0.01
Season	2	157.77	2875	5793.70	49.95	<0.01
Stratum	23	1093.65	2852	4700.10	30.11	<0.01
Temperature	3	197.89	2849	4502.20	41.77	<0.01
Salinity	1	4.43	2848	4497.80	2.80	0.09
White shrimp						
Binomial model						
Null			8344	11,562.80		
Year	29	251.60	8315	11,311.20		<0.01
Season	2	385.29	8313	10,925.90		<0.01
Stratum	23	1217.70	8290	9708.20		<0.01
Temperature	3	90.63	8287	9617.60		<0.01
Salinity	1	65.95	8286	9551.60		<0.01
Positive model						
Null			4282	17,992.00		
Year	29	1244.47	4253	16,748.00	13.29	<0.01
Season	2	1436.22	4251	15,312.00	222.40	<0.01
Stratum	23	1545.00	4228	13,767.00	20.80	<0.01
Temperature	3	46.54	4225	13,720.00	4.81	<0.01
Salinity	1	81.40	4224	13,639.00	25.21	<0.01

Bluefish

Bluefish were collected in 35% of all CTS tows from 1990 through 2019 (Table 1). Temporally, bluefish were more abundant in spring and fall (Fig. 3A). The spatial distribution of bluefish was primarily in the northern portion of the study area (strata ≥55), with the highest abundances occurring off North Carolina (Fig. 3B). Bluefish were more abundant in waters with bottom temperatures below 20.1°C and in waters with bottom salinities less than 34.9 (Fig. 3, C and D).

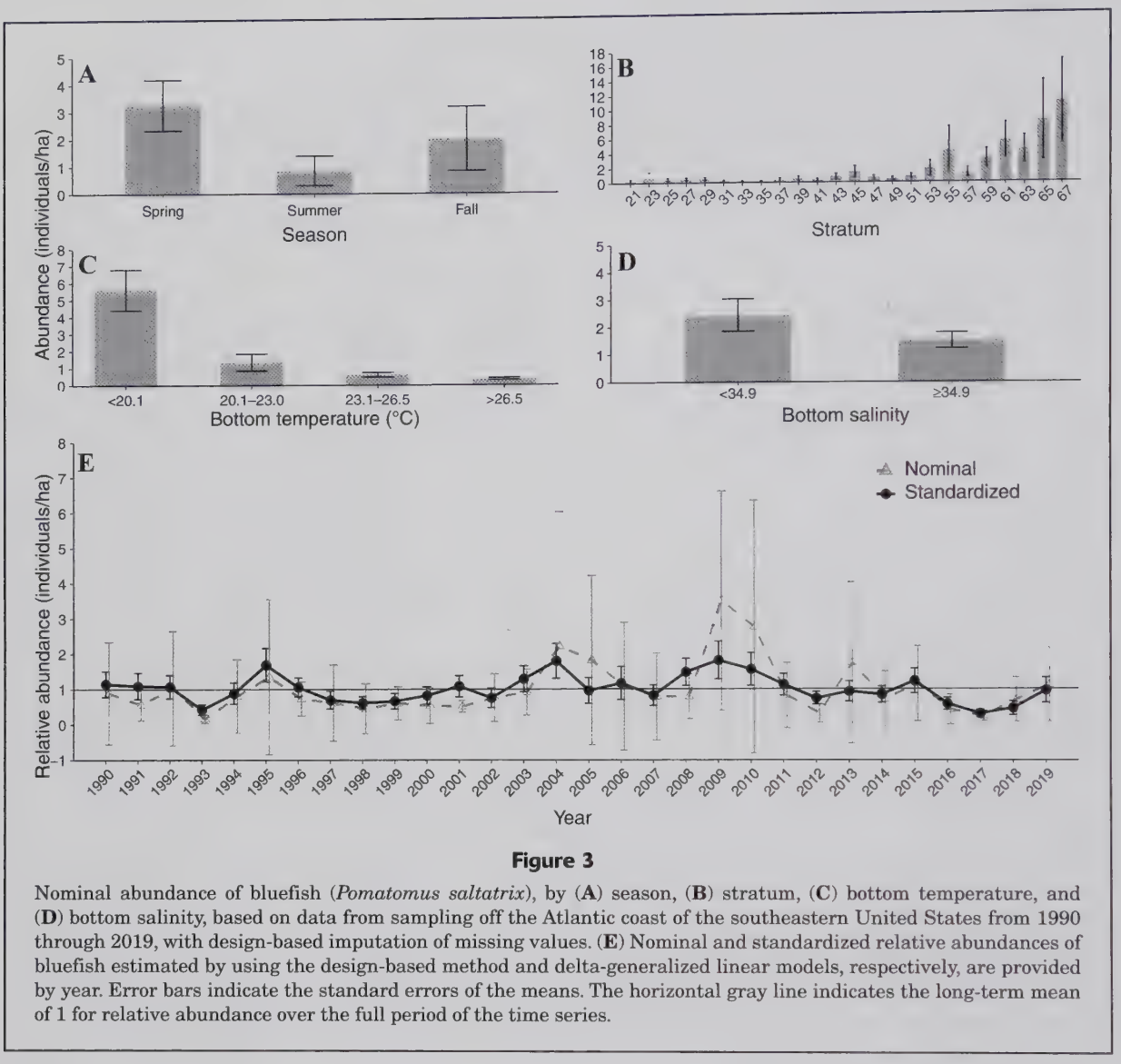

Figure 3

Nominal abundance of bluefish (*Pomatomus saltatrix*), by (**A**) season, (**B**) stratum, (**C**) bottom temperature, and (**D**) bottom salinity, based on data from sampling off the Atlantic coast of the southeastern United States from 1990 through 2019, with design-based imputation of missing values. (**E**) Nominal and standardized relative abundances of bluefish estimated by using the design-based method and delta-generalized linear models, respectively, are provided by year. Error bars indicate the standard errors of the means. The horizontal gray line indicates the long-term mean of 1 for relative abundance over the full period of the time series.

Nominal abundance of bluefish was generally stable near the time series mean without large positive or negative swings. Additionally, variability in nominal abundance of bluefish tended to be low when abundance was below the mean and high when abundance was above the mean (2004–2013) (Fig. 3E). Nominal abundance was similar to or below the time series mean from 2014 through 2019.

The trend in delta-GLM standardized abundance of bluefish was similar to that in nominal abundance, although with less variability, particularly when compared with trends for the years of peak nominal abundance: 1995, 2004, 2005, 2009, 2010, and 2013 (Fig. 3E, Suppl. Table [online only]). One exception is the estimate for 2001, which is almost twice as high with higher variability than that of the nominal estimate for that year. Although the error bars overlap, standardization also reduced the abundance estimates in 2009 and 2010 relative to the nominal estimates for those years. All covariates were significant in both the binomial and positive GLMs, except for bottom salinity, which was not significant in the positive model (Table 2). Examination of residual and Q-Q plots reveals reasonable fits for both the binomial and positive models (Suppl. Fig. 2) (online only).

White shrimp

White shrimp occurred in 51% of tows (Table 1) and were the most abundant penaeid shrimp species caught in CTS sampling. White shrimp were most abundant during the fall, relative to the other seasons (Fig. 4A). White shrimp were spatially distributed throughout the region but were most abundant in waters of northern Florida, with smaller peaks in abundance off South Carolina and New River, North Carolina (Fig. 4B). White shrimp were most abundant in bottom temperatures ranging between 20.1°C and 26.5°C (Fig. 4C) and in waters with bottom salinities less than 34.9 (Fig. 4D).

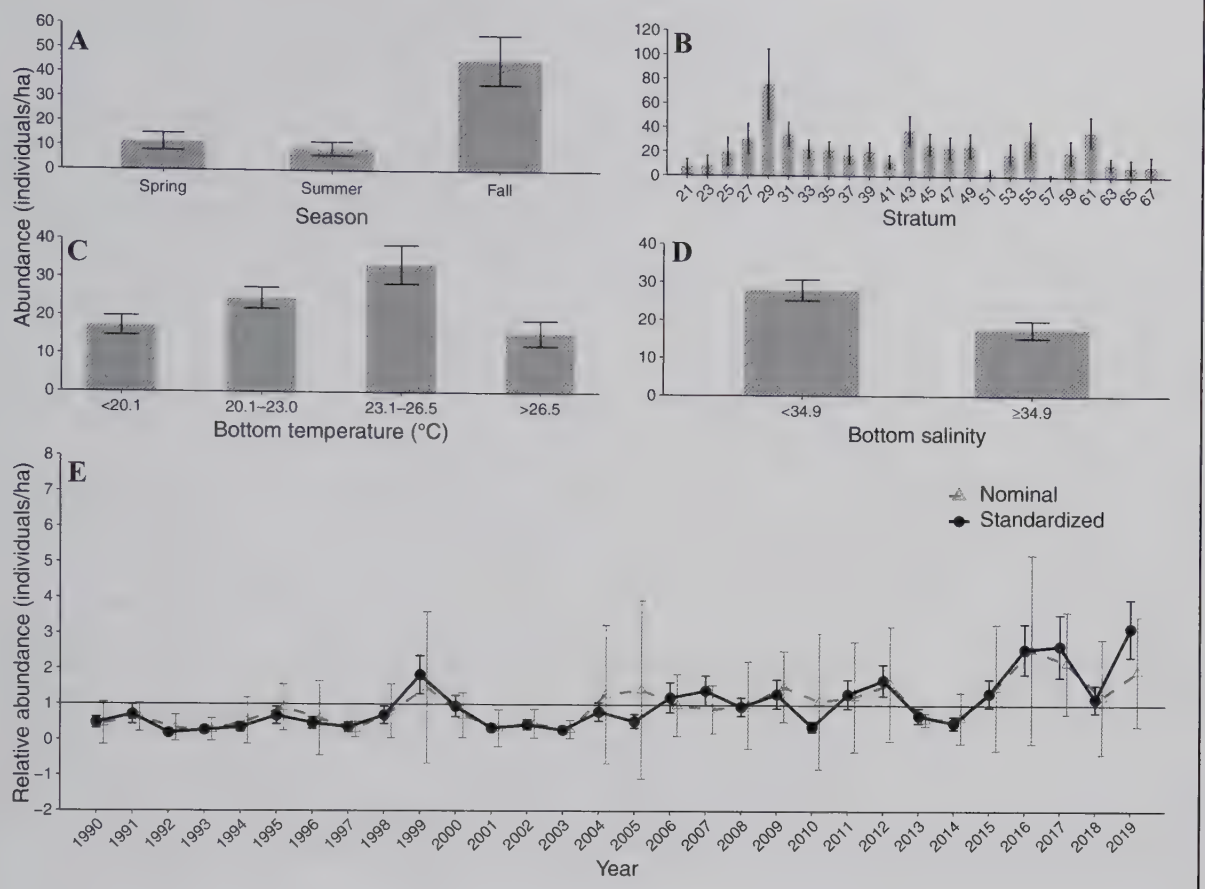

Figure 4

Nominal abundance of white shrimp (*Litopenaeus setiferus*), by (**A**) season, (**B**) stratum, (**C**) bottom temperature, and (**D**) bottom salinity, based on data from sampling off the Atlantic coast of the southeastern United States from 1990 through 2019, with design-based imputation of missing values. (**E**) Nominal and standardized relative abundances of white shrimp estimated by using the design-based method and delta-generalized linear models, respectively, are provided by year. Error bars indicate the standard errors of the means. The horizontal gray line indicates the long-term mean of 1 for relative abundance over the full period of the time series.

Nominal abundance of white shrimp was generally below, or relatively similar to, the mean for the time series from 1990 through 2003 (Fig. 4E). From 2004 through 2019, nominal abundance of white shrimp was variable but with a generally increasing trend compared with the trend of the time series mean. Variability in nominal abundance generally increased as abundance increased.

The trend in delta-GLM standardized abundance of white shrimp was similar to that in nominal abundance but with lower variability (Fig. 4E, Suppl. Table [online only]). Although the error bars overlap, the only notable difference between nominal and standardized estimates was in the abundance estimate for 2019, when the standardized abundance of white shrimp was higher than the nominal abundance. All covariates were statistically significant in predicting the presence (binomial model) and abundance (positive model) of white shrimp (Table 2). Examination of residual and Q-Q plots reveals reasonable fits for both delta-GLMs (Suppl. Fig. 3) (online only).

All species

For the 3 species examined in this study, the standardization of abundance through the use of delta-GLMs primarily affected the variability in annual estimates, reducing the average variability in nominal values for Atlantic croaker by 3%, for bluefish by 90%, and for white shrimp by 75% (Figs. 2E, 3E, and 4E). The magnitude of the variability of abundance estimates generally changed with the extent of spatial and temporal distribution and percent positive rate (i.e., the percentage calculated as the number of tows in which a given species was collected divided by the total number of tows conducted per year) among the 3 species examined. The Atlantic croaker had the widest distribution and highest occurrence of the 3 species, with the smallest annual nominal errors. The bluefish had the narrowest distribution and lowest occurrence of the 3 species and had an average normalized nominal standard error over 2 times higher than that for the Atlantic

croaker (0.60 for bluefish and 0.26 for Atlantic croaker) and just slightly higher than that for the white shrimp (0.55). Standardization had little effect on annual abundance estimates, with the exception of increasing abundance estimates in 2019 for Atlantic croaker and in 2001 for bluefish (based on error bars that do not overlap; Figs. 2E and 3E). The years with strata that were missed in sampling (1990, 2013, 2018, and 2019) did not have noticeable differences between nominal and standardized abundance estimates, with the exception of 2019 for Atlantic croaker and white shrimp (although the latter had overlapping error bars) (Table 1, Figs. 2E and 4E).

The effect of scenarios of potential survey modifications on standardized abundance was not consistent among the 3 species examined in this study (Fig. 5, A–C). The Atlantic croaker had the most variable change to index values of the 3 species, with the scenario in which the dropped season was systematically rotated generally tracking most closely with the abundance index from the delta-GLM analysis that used the current survey design, which includes all seasons (Fig. 5A). The effect of each of the 3 scenarios in which a particular season was consistently dropped on the abundance of Atlantic croaker depended on the year examined, likely because the annual abundance is informed by the mean response to the other seasons, which itself is inconsistent among years, seasons, and strata. The effect of randomly selecting a season to be dropped was also relatively variable for Atlantic croaker and resulted in noticeable deviations from the values in the abundance index produced in the model analysis that included all seasons.

All 5 scenarios had minimal effects on the standardized abundance index for both bluefish and white shrimp relative to the model for all seasons (Fig. 5, B and C), and this outcome is most likely related to the more restricted (and predictable) spatiotemporal distribution of abundance for these 2 species relative to that of the Atlantic croaker. The few examples of noticeable deviations from the full index occurred for bluefish and white shrimp under the scenarios in which a single season was consistently not sampled and for white shrimp under the scenario in which the dropped season was rotated. The variability in the scenarios for survey design modifications differed among species and years, but not in a consistent way (Table 3).

Discussion

As a long-term fishery-independent survey, the CTS provides abundance and life history data for a variety of species of management interest. A stratified-random sampling design is used to conduct the CTS, with survey stations allocated to minimize variability in catch abundance estimates. Historically, annual sampling at the vast majority of allocated stations was completed and sampling occurred in all strata. However, in recent years (i.e., 2018 and 2019), allocated stations and full strata were left unsampled because of the use of an aging vessel, mechanical failures, stagnant funding and increased costs, and prolonged periods of weather conditions above levels deemed safe for sampling. In particular, strata at the northernmost and southernmost portions of the survey area were those most likely to remain unsampled.

In this study, we investigated whether or not our inability to complete the full spatial scope of the survey in each season affected the accuracy of abundance estimates by comparing nominal (design-based) and standardized (delta-GLM) estimates of abundance for Atlantic croaker, bluefish, and white shrimp. Surprisingly, only one major difference between estimates produced with these 2 methods was observed: one for Atlantic croaker for a year with incomplete sampling. Other than this instance, there were almost no discernible differences in estimates of abundance for the years with incomplete sampling relative to estimates for years with complete sampling. One reason for the lack of differences in estimates may be the use of average long-term values for nominal abundances for years with incomplete sampling versus the use of the standardization technique in which average values are applied within each model cell to account for missing data. Although standardization may involve the use of an improved average estimate because of the inclusion of more covariates than the relatively simple imputation method used to produce the nominal estimate (Walters, 2003), any loss of precision in an index resulting from decreased or lost effort can be balanced if stratification is incorporated into the design of a given survey and because of the similarity of using averages as empirical information (Xu et al., 2015).

In the case of the CTS, the stratified-random sampling design has been consistent over time, allowing minimization of loss of information when sampling was incomplete. This assumption that the design will balance incomplete sampling, however, may not remain true if completion of sampling continues to be eroded. It is currently unknown what the effect of incomplete sampling may be for species that are less common or less ubiquitous than the 3 species examined in this study.

The relationships between environmental covariates included in the standardization models and species abundance varied among the species examined in this study. The association between abundance and bottom temperature varied among species. There was little difference in abundance among temperatures for Atlantic croaker (Fig. 2C), but bluefish were most associated with temperatures <20.1°C, likely related to their presence in the northern strata of the study area in the spring and fall (Fig. 3, B and C). Abundance of white shrimp was less influenced by temperature than estimates for bluefish, but abundances generally increased with increasing temperatures for white shrimp, most likely reflecting the warmer waters in southern strata where white shrimp were abundant (Fig. 4, B and C). Salinity was less influential on species-specific abundance: there was no significant difference in abundance of bluefish among salinity levels, Atlantic croaker were significantly more abundant in waters with higher salinities (≥34.9) than in those with lower salinities (<34.9), and abundance of white shrimp followed the opposite trend.

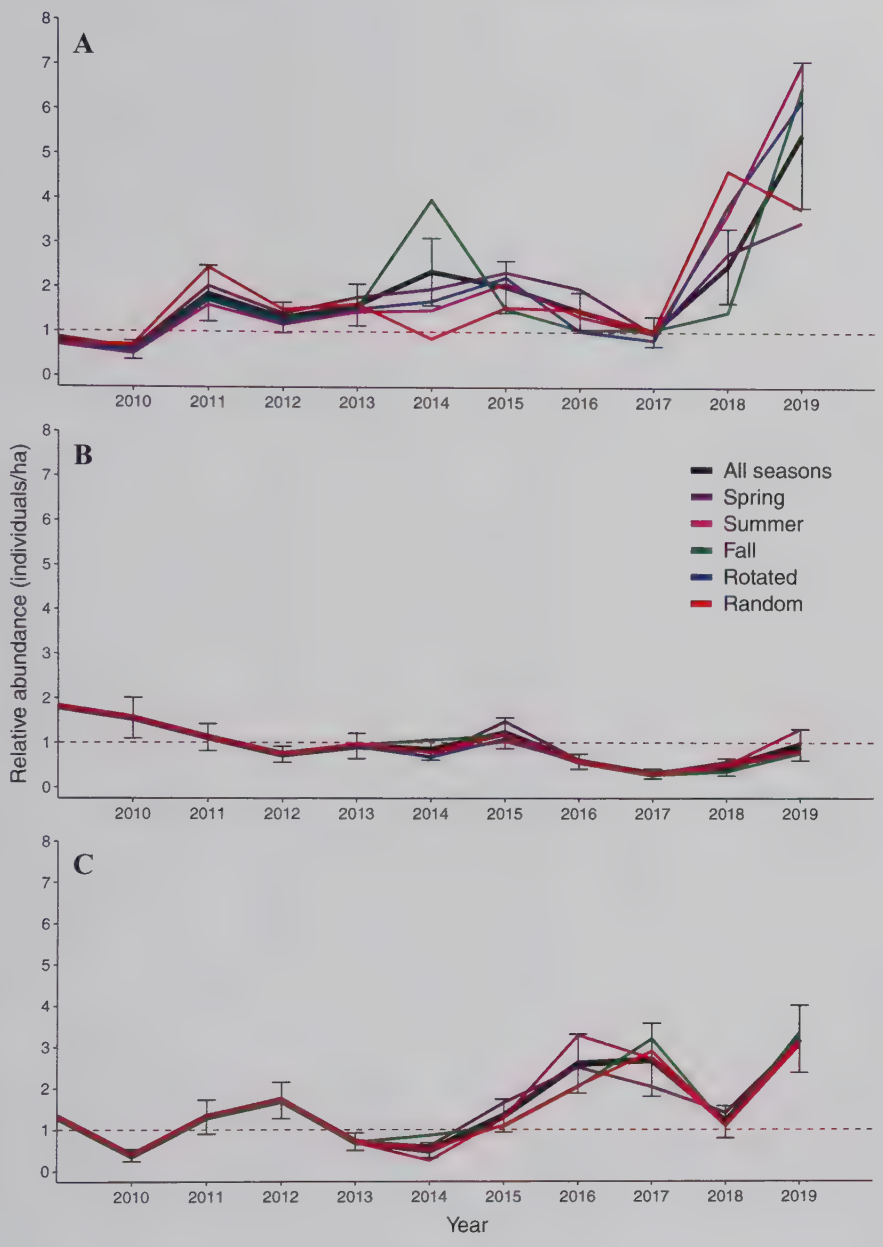

Figure 5

Abundance estimates for (**A**) Atlantic croaker (*Micropogonias undulatus*), (**B**) bluefish (*Pomatomus saltatrix*), and (**C**) white shrimp (*Litopenaeus setiferus*) standardized with generalized linear models for the 5 scenarios of potential design modifications of the Coastal Trawl Survey of the Southeast Area Monitoring and Assessment Program—South Atlantic: dropping spring (April and May), summer (July and August), or fall (September through November), rotating which season is dropped, or randomly dropping a season. The full time series was used in models with the survey design modifications applied to sampling conducted between 2014 and 2019 off the Atlantic coast of the southeastern United States. The black line in each panel indicates the standardized estimates of relative abundance produced under the current survey design, in which no season is dropped, with error bars for standard errors of the annual means. The dashed orange line in each panel indicates the long-term mean of 1 for relative abundance over the full period of the time series (1990–2019).

Table 3

Standard errors of standardized abundance estimates for (**A**) Atlantic croaker (*Micropogonias undulatus*), (**B**) bluefish (*Pomatomus saltatrix*), and (**C**) white shrimp (*Litopenaeus setiferus*) off the Atlantic coast of the southeastern United States between 2014 and 2019 for the 5 scenarios of potential design modifications of the Coastal Trawl Survey of the Southeast Area Monitoring and Assessment Program—South Atlantic: dropping spring (April and May), summer (July and August), or fall (September–November), randomly dropping a season, and rotating which season is dropped. For comparison, standard errors of abundance estimates produced under the current survey design, with no season dropped, are provided.

Year	All seasons	Spring	Summer	Fall	Random	Rotated
Atlantic croaker						
2014	57.08	47.03	58.54	109.40	27.66	47.23
2015	44.14	50.90	63.67	46.00	39.89	62.46
2016	31.67	43.37	40.72	29.07	34.23	27.66
2017	25.50	23.93	34.36	34.77	27.46	23.49
2018	63.52	68.38	127.71	50.56	129.87	125.47
2019	124.35	82.39	242.09	176.95	82.46	168.03
Bluefish						
2014	0.09	0.09	0.11	0.14	0.11	0.09
2015	0.14	0.18	0.15	0.18	0.19	0.14
2016	0.07	0.09	0.09	0.08	0.08	0.08
2017	0.04	0.06	0.05	0.05	0.04	0.06
2018	0.08	0.09	0.12	0.07	0.12	0.11
2019	0.14	0.17	0.22	0.14	0.18	0.14
White shrimp						
2014	1.73	2.61	1.11	2.98	1.78	2.66
2015	3.81	5.19	4.54	4.00	4.23	4.56
2016	6.83	7.54	10.74	6.80	7.08	7.16
2017	8.48	8.06	11.58	10.82	11.42	8.38
2018	3.71	5.11	4.95	3.62	4.76	4.69
2019	7.81	9.11	10.19	9.30	9.10	9.66

Population levels for Atlantic croaker are driven by the combination of temperature and salinity, with winter temperatures being primarily influential on survivorship and salinities above 10 potentially mitigating the effects of extremely low temperatures on survivorship (Lankford and Targett, 2001; Hare and Able, 2007). Bluefish are known to overwinter between North Carolina and Florida, and they generally migrate northward in the spring as water temperatures increase and then migrate southward in the fall as water temperatures decrease (Wilk[7]; Fahay et al., 1999). In previous studies, the low temperature tolerance of juvenile bluefish was found to be 13–15°C (Hare and Cowen, 1996), and their growth slowed at water temperatures greater than 24°C (Hartman and Brandt, 1995). It is possible that the binary binning of bottom salinity meant the relationship could not be resolved for bluefish or that bluefish were present at times with more variable salinities (e.g., variable run-off in fall due to seasonal rains and tropical systems). The reduced abundance of white shrimp above a salinity of 34.9 likely reflects their high abundances around large estuarine systems with relatively high freshwater or estuarine outflow. Results from previous studies support the notions that abundance of adult white shrimp is positively correlated with water temperature and negatively correlated with salinity and that mortality occurs at temperatures below 10°C (Joyce, 1965; SAFMC, 1981; Diop et al., 2007; Fowler et al., 2018).

In general, standardization decreased variability relative to design-based estimation of abundance in 18 of 30 survey years (60%) for Atlantic croaker, in 12 survey years (40%) for bluefish, and in 16 survey years (53%) for white shrimp (Figs. 2E, 3E, and 4E). For all 3 species examined in this study, the primary variables of *season* and *stratum* in the design-based GLMs accounted for more of the deviance explained by GLMs than either *bottom temperature* or *salinity* and often explained levels of deviance similar to those explained by *year* (Table 2). Both the spatial and temporal elements of the survey design enabled us to find that those species with more restricted distributions have greater variability in estimates of abundance. This pattern of small distribution and larger variability may be partially accounted

[7] Wilk, S. J. 1977. Biological and fisheries data on bluefish, *Pomatomus saltatrix* (Linnaeus). Natl. Mar. Fish. Serv., Northeast Fish. Sci. Cent., Sandy Hook Lab. Tech. Ser. Rep. 11, 44 p. [Available from website.]

for through the nominal estimation used in this study but is likely more adequately addressed by using the standardization method that can incorporate other drivers such as environmental conditions (Figs. 2E, 3E, and 4E).

The bluefish had the most uneven spatial distribution of the 3 species examined and had some of the highest annual standard error estimates, but the white shrimp was the species most unevenly distributed among seasons and had moderate standard error estimates (Figs. 3B, 3E, 4B, and 4E). Carruthers et al. (2011) suggested that the choice to impute missing data rather than to standardize by using conventional GLM techniques should be dependent on the spatial dynamics of a population and the spatial grain of the missing data. This choice between methods is especially important if there are area and time interactions and the unobserved areas do not adhere to the mean abundance trend. Use of imputation tends to lead to greater bias than use of a GLM, unless the spatial scale of imputation is relatively fine and the imputed data are representative of the overall population.

In our study, we chose to impute a mean based on the full time series, although imputing a mean based on data from only recent years may have been more representative of more recent trends for each species. However, for bluefish, using *stratum* in the imputation method is more appropriate than using larger latitudinal bins because *stratum* has the finest spatial scale consistent with the survey design (*station* cannot be used as a variable because not every station is sampled each year). Because of the uneven spatial distribution of bluefish, future work should determine if the use of *station* for imputation is more appropriate than the use of *stratum*. One caveat to using *station* is that, because not every station is selected for sampling each year, the use of *station* may result in a decrease in sample sizes that inform calculations.

There were only 2 observed differences in abundance estimates between the nominal and standardization methods as revealed by error bars not overlapping for Atlantic croaker in 2019 and for bluefish in 2001. The year 2019 was the only year of incomplete sampling during which the 3 northernmost strata were not sampled in both spring and fall. In general, these strata are also the ones that typically have moderate to high abundances of Atlantic croaker (Fig. 2B). Not surprisingly, for 2019, the nominal abundance estimate was markedly lower than the standardized value. The difference between the nominal and standardized abundance estimates is likely a result of the standardization method better accounting for the effects of covariates on abundance, for the general increasing trend in 2019, and for the typically higher catches in these strata than the design-based approach, even with the average nominal abundance imputed as a proxy for the missing data. By comparison, there was no change in the estimates for either bluefish or white shrimp in 2019. Catches of white shrimp in survey tows in the northernmost strata were generally low (Fig. 4B); therefore, missing data for these strata likely did not have a great effect on the annual abundance estimate from either calculation. Generally, the highest abundances observed for bluefish occurred in the 3 northernmost strata and in spring and fall (Fig. 2, A and B). This consistent positive relationship between *stratum* (latitude) and abundance likely allowed those consistently high catches to be captured in the calculations of both the nominal and standardized methods, resulting in very similar estimates for 2019. In contrast to survey effort in 2019, all allocated stations were sampled in 2001.

Two of the few exceptions to improvement in accuracy (i.e., reduced error) of the standardized abundance estimates were for Atlantic croaker in 2019 and for bluefish in 2001. For Atlantic croaker in 2019, the estimate of abundance increased significantly following standardization, and the error rate increased almost 3-fold. Strata were missed in sampling or not sampled completely in both spring and fall in 2019, the most variable and least abundant seasons in the full time series for Atlantic croaker, respectively. Abundance of Atlantic croaker in fall 2019 was higher than in any other previous fall but also was more variable, likely a result of not sampling in the northernmost strata where this species is abundant but the abundance is variable and of not sampling in the southernmost strata where this species is least abundant, reducing the number of strata in which there were zero or near zero encounters. In addition, the use of imputation in the design-based calculation did not account for uncertainty in the imputed estimates for multiple seasons and strata and, therefore, reduced variability for 2019 by default (Carruthers et al., 2010). In contrast, errors for all seasons and strata in 2019 continued to be incorporated when the standardization technique was used, potentially leading to the higher variability in estimates for that year. Further comparisons should examine variability of estimates based on imputed data.

Regarding bluefish in 2001, there is no record of unusual circumstances in CTS historic data for that year; therefore, there may have been unusual conditions that were not accounted for in the current analyses. If so, these conditions were likely specific to bluefish because the estimates for the other 2 species in 2001 were similar and had decreased standardized variability as expected.

Results of the exercise of retrospectively dropping seasons for the years 2014–2019 indicate that the likely effects of major modifications to the survey would be species-specific (i.e., not all species abundance estimates remained consistent among all modification scenarios). Removing whole seasons did not change the pattern of increased abundance of Atlantic croaker in 2019 for most scenarios: dropping fall, dropping summer, and systematically rotating which season was dropped from analysis (Fig. 5A). By comparison, removing spring or randomly dropping seasons between 2014 and 2019, decreased the standardized abundance estimate for Atlantic croaker in 2019 compared with the standardized estimate produced with data for all seasons. Interestingly, dropping seasons did not change the pattern of abundance for bluefish or white shrimp (Fig. 5, B and C). Both species had lower abundance estimates and more variability compared with estimates for Atlantic croaker, but with standardization we were able to successfully predict abundances for these

species even with the loss of full seasons. Therefore, there may be an interaction between annual abundance of each species, species distributions or predictability, strata or seasons that are sampled, and effects of standardization on variability and estimates of abundance that need to be considered before making changes to the survey design.

Fishery-independent indices of abundance generally are essential for most stock assessment models currently in use, are preferred over fishery-dependent indices, and are often upweighted relative to other indices because of their adherence to standardized designs and resistance to temporal changes in catchability or sampling systems (Wilberg et al., 2009). For the CTS, delta-GLM indices of abundance indicate that standardization decreased variability in annual abundance estimates for all species examined and potentially "corrected" data from the year in which sampling was most incomplete for one of the species most commonly encountered in the survey, the Atlantic croaker. On the basis of the improvements in variability alone, we recommend moving forward with standardization for species for which long-term time series are available. Because of the advanced age of the vessel used for surveys and the trend of more extreme weather events, standardization may become even more important in future years (and for more species) as completion of CTS sampling is likely to continue to be challenging.

Given that the survey design needs to be modified to account for these potential constraints on sampling completion, that the effect on variability among modification scenarios was not informative, and that the best performing model varied among species and years (Table 3), we also recommend rotating the season that is not sampled, rather than any of the other modification scenarios examined in this study, if modifications become necessary. The effect of a given season on the abundance index is species specific, and results of this study indicate that rotation of the dropped season is the best approach for a multispecies survey if sampling effort needs to be reduced.

Conclusions

In this study, as expected, a common standardization technique (the delta-GLM method) improved estimation of variability in abundance time series from a fishery-independent survey over that of the simpler approach of imputation of average abundance values for Atlantic croaker, bluefish, and white shrimp. These improvements in uncertainty become increasingly important as costs of conducting surveys increase and funding for long-term surveys stagnates, as has been experienced for the CTS. The results of this study indicate that survey programs that cannot complete sampling as designed in a given year could deal with that incompletion through techniques that involve a delta-GLM. We also found that, when funding is severely limited, rotating the season that is not sampled may be the most appropriate approach for multispecies surveys. For surveys without a seasonal structure, incorporating a time element, such as month, a posteriori and rotating which months are prioritized may be a way to cope with limited funding and sampling effort as well, although it would need to be examined on a case-by-case basis.

In addition, for the CTS, over 24 species currently are of management interest and are sampled sufficiently to produce indices of abundance. For this high variety of species, more work needs to be done to examine the effects of survey design modifications because the results of this study were not consistent among species. The delta-GLM method is just one of many standardization techniques that can be employed. Other types of models, such as those that use continuous covariates or other error structures, may be more appropriate or better at improving variability estimation than the analyses for which results are presented herein.

Resumen

Los índices de abundancia procedentes de estudios independientes de la pesca son los preferidos en las evaluaciones de poblaciones debido a sus sólidos diseños científicos que minimizan la incertidumbre y el sesgo. Cuando el muestreo no se ajusta al diseño, los investigadores emplean técnicas como la imputación o la estandarización para mejorar la precisión y reducir el sesgo. Examinamos 2 métodos para ajustar el muestreo incompleto en la Prospección de Arrastre Costero (CTS) del Programa de Monitoreo y Evaluación del Área sureste del Atlántico Sur para 3 especies comúnmente encontradas en el muestreo de la prospección, la corvina del Atlántico (*Micropogonias undulatus*), la anjova (*Pomatomus saltatrix*) y el camarón blanco (*Litopenaeus setiferus*): la imputación de datos faltantes con base en el diseño y la estandarización a través del enfoque del modelo lineal generalizado delta. Además, determinamos el efecto de modificar el componente estacional del diseño de la prospección mediante una simulación retrospectiva. Para las 3 especies, la estandarización mejoró la precisión de las estimaciones de abundancia anual con relación a los valores estimados con el método basado en el diseño. Cuando un estrato omitido en el muestreo coincidía con un área o época de alta variabilidad para una especie (p. ej., 2019), la estandarización no mejoró la precisión con respecto al método basado en el diseño. Los resultados del análisis de los efectos de la exclusión de temporadas enteras, debido a problemas de financiación o logísticos, indican que la rotación de la temporada a excluirse fue el mejor enfoque para equilibrar las características de cada especie. En general, recomendamos el enfoque de estandarización para contabilizar los datos faltantes en las series temporales de la CTS.

Acknowledgments

We would like to thank the numerous field biologists involved with the SEAMAP-SA CTS and the vessel crews for their collection of the data included in our study. In addition, we appreciate the suggestions and feedback from 3 anonymous reviewers that greatly improved the

manuscript. This paper is contribution no. 852 for the SCDNR Marine Resources Research Institute. Funding was provided by NOAA through the SEAMAP-SA grant (NA21NMF4350372) to SCDNR.

Literature cited

Akaike, H.
1973. Information theory and an extension of the maximum likelihood principle. *In* Second international symposium on information theory; Tsaghkadzor, 2–8 September 1971 (B. N. Petran and F. Csaki, eds.), p. 267–281. Akadémiai Kiadó, Budapest, Hungary.

Arreguín-Sánchez, F.
1996. Catchability: a key parameter for fish stock assessment. Rev. Fish Biol. Fish. 6:221–242.

Campbell, R. A.
2004. CPUE standardisation and the construction of indices of stock abundance in a spatially varying fishery using general linear models. Fish. Res. 70:209–227.
2015. Constructing stock abundance indices from catch and effort data: some nuts and bolts. Fish. Res. 161:109–130.

Carruthers, T. R., M. K. McAllister, and R. N. M. Ahrens.
2010. Simulating spatial dynamics to evaluate methods of deriving abundance indices for tropical tunas. Can. J. Fish. Aquat. Sci. 67:1409–1427.

Carruthers, T. R., R. N. M. Ahrens, M. K. McAllister, and C. J. Walters.
2011. Integrating imputation and standardization of catch rate data in the calculation of relative abundance indices. Fish. Res. 109:157–167.

Cochran, W. G.
1977. Sampling techniques, 3rd ed., 448 p. John Wiley and Sons, New York.

Dick, E. J.
2004. Beyond 'lognormal versus gamma': discrimination among error distributions for generalized linear models. Fish. Res. 70:351–366.

Diop, H., W. R. Keithly Jr., R. F. Kazmierczak Jr., and R. F. Shaw.
2007. Predicting the abundance of white shrimp (*Litopenaeus setiferus*) from environmental parameters and previous life stages. Fish. Res. 86:31–41.

Fahay, M. P., P. L. Berrien, D. L. Johnson, and W. W. Morse.
1999. Essential fish habitat source document: bluefish, *Pomatomus saltatrix*, life history and habitat characteristics. NOAA Tech. Memo NMFS-NE-144, 64 p.

Francis, R. I. C. C.
2011. Data weighting in statistical fisheries stock assessment models. Can. J. Fish. Aquat. Sci. 68:1124–1138.

Fowler, A. E., J. W. Leffler, S. P. Johnson, L. B. DeLancey, and D. M. Sanger.
2018. Relationships between meteorological and water quality variables and fisheries-independent white shrimp (*Litopenaeus setiferus*) catch in the ACE Basin NERR, South Carolina. Estuar. Coasts 41:79–88.

Hare, J. A., and R. K. Cowen.
1996. Transport mechanisms of larval and pelagic juvenile bluefish (*Pomatomus saltatrix*) from South Atlantic Bight spawning grounds to Middle Atlantic Bight nursery habitats. Limnol. Oceanogr. 41:1264–1280.

Hare, J. A., and K. W. Able.
2007. Mechanistic links between climate and fisheries along the east coast of the United States: explaining population outbursts of Atlantic croaker (*Micropogonias undulatus*). Fish. Oceanogr. 16:31–45.

Hartman, K. J., and S. B. Brandt.
1995. Comparative energetics and the development of bioenergetics models for sympatric estuarine piscivores. Can. J. Fish. Aquat. Sci. 52:1647–1666.

Hilborn, R., and C. J. Walters.
1992. Quantitative fisheries stock assessment: choice, dynamics and uncertainty, 570 p. Chapman and Hall, London.

Joyce, E. A., Jr.
1965. The commercial shrimps of the northeast coast of Florida. Fla. Board Conserv. Mar. Lab., Prof. Pap. Ser. 6, 224 p.

Lankford, T. E., Jr., and T. E. Targett.
2001. Low-temperature tolerance of age-0 Atlantic croakers: recruitment implications for U.S. Mid-Atlantic estuaries. Trans. Am. Fish. Soc. 130:236–249.

Little, R. J. A., and D. B. Rubin.
1987. Statistical analysis with missing data, 304 p. John Wiley and Sons, New York.

Lo, N. C.-h., L. D. Jacobson, and J. L. Squire.
1992. Indices of relative abundance from fish spotter data based on delta-lognormal models. Can. J. Fish. Aquat. Sci. 49:2515–2526.

Maunder, M. N., and A. E. Punt.
2004. Standardizing catch and effort data: a review of recent approaches. Fish. Res. 70:141–159.

Quinn, T. J., II, and R. B. Deriso.
1999. Quantitative fish dynamics, 542 p. Oxford Univ. Press, New York.

R Core Team.
2021. R: a language and environment for statistical computing. R Foundation for Statistical Computing, Vienna, Austria. [Available from website, accessed September 2021.]

SAFMC (South Atlantic Fishery Management Council).
1981. Profile of the penaeid shrimp fishery in the South Atlantic, 286 p. SAFMC, Charleston, SC. [Available from website.]

Shelton, A. O., J. T. Thorson, E. J. Ward, and B. E. Feist.
2014. Spatial semiparametric models improve estimates of species abundance and distribution. Can. J. Fish. Aquat. Sci. 71:1655–1666.

Stender, B. W., and C. A. Barans.
1994. Comparison of the catch from tongue and two-seam shrimp nets off South Carolina. North Am. J. Fish. Manag. 14:178–195.

Thompson, S. K.
1992. Sampling, 343 p. John Wiley and Sons, New York.

Walters, C.
2003. Folly and fantasy in the analysis of spatial catch rate data. Can. J. Fish. Aquat. Sci. 60:1433–1436.

Walters, C., and P. H. Pearse.
1996. Stock information requirements for quota management systems in commercial fisheries. Rev. Fish Biol. Fish. 6:21–42.

Wilberg, M. J., J. T. Thorson, B. C. Linton, and J. Berkson.
2009. Incorporating time-varying catchability into population dynamic stock assessment models. Rev. Fish. Sci. 18:7–24.

Willis, C. M., J. Richardson, T. Smart, J. Cowan, and P. Biondo.
2015. Diet composition, feeding strategy, and diet overlap of 3 sciaenids along the southeastern United States. Fish. Bull. 113:290–301.

Xu, B., Y. Ren, Y. Chen, Y. Xue, C. Zhang, and R. Wan.
2015. Optimization of stratification scheme for a fishery-independent survey with multiple objectives. Acta Oceanol. Sin. 34:154–169.

National Marine
Fisheries Service
NOAA

Fishery Bulletin
established in 1881

Spencer F. Baird
First U.S. Commissioner
of Fisheries and founder
of *Fishery Bulletin*

Effects of salinity and turbidity on development of bamboo sole (*Heteromycteris japonicus*)

Tu T. C. Phan (contact author)[1,2]
Albert V. Manuel[2]
Naoaki Tsutsui[2]
Takao Yoshimatsu[2]

Email address for contact author: ptctu@ctu.edu.vn

[1] College of Aquaculture and Fisheries
Can Tho University
Campus II, 3/2 Street
Xuan Khanh Ward, Ninh Kieu District, Can Tho City 94000, Vietnam

[2] Graduate School of Bioresources
Mie University
1577 Kurimamachi Yacho
Tsu, Mie 514-8507, Japan

Abstract—Heavy rain can decrease salinity and increase turbidity of the water in coastal areas, negatively affecting the development of organisms, particularly during their early life stages. In this study, the effects of salinity and turbidity on embryos of the bamboo sole (*Heteromycteris japonicus*) were evaluated to improve understanding of its tolerance to global climate change. Three experiments were carried out over a 7-d period. In the first experiment, embryos of bamboo sole were exposed for 3 h to 1 of 6 salinity levels (14–34). Low salinity levels (14 and 18) resulted in significantly shorter total lengths of newly hatched larvae in comparison with larval sizes in treatments with higher salinities, but no significant differences were observed in hatching rate and larval survival rate among treatments. In the second experiment, embryos were exposed to turbidities of 0, 100, 300, 500, and 700 nephelometric turbidity units for 3 h. Turbidity significantly decreased hatching rate, survival rate, and total length and increased onset hatching time and percentage of abnormality. In the third experiment, embryos were exposed to different combinations of salinity and turbidity. The interaction effect of salinity and turbidity on total length of newly hatched larvae was significant. These findings indicate that embryo development of bamboo sole was more affected by changes in turbidity than by changes in salinity.

Manuscript submitted 29 March 2022.
Manuscript accepted 19 September 2022.
Fish. Bull. 120:268–276 (2022).
Online publication date: 11 October 2022.
doi: 10.7755/FB.120.3-4.7

The views and opinions expressed or implied in this article are those of the author (or authors) and do not necessarily reflect the position of the National Marine Fisheries Service, NOAA.

Flatfish species are found globally in marine habitats and are important food fish to humans (Gibson et al., 2015). However, the global catch of flatfish in fisheries has decreased gradually since the 1970s, from about 3 million metric tons (t) to below 2 million t in the 2000s, and is predicted to decline by 20% by the year 2100 (Cheung and Oyinlola, 2018).

Although overfishing has resulted in decreases in flatfish populations, there is another related reason for these reductions: climate change (Cheung and Oyinlola, 2018). In fact, in many studies, fluctuations in fish populations have been found to be closely associated with climate change (Lehodey et al., 2006; Brander, 2010; Holsman et al., 2012; Barange et al., 2014). Baudron et al. (2014) also reported that negative changes in environmental conditions of habitats due to climate change can directly affect fish population dynamics through physiological effects.

One of the effects of climate change in coastal areas is the increased intensity and frequency of heavy rainfall, and those changes in rainfall reduce salinity and increase turbidity as a result of runoff from the land and rivers (Thrush et al., 2004; Poloczanska et al., 2009). According to Allen and Pechenik (2010), salinity in the upper water column may fluctuate from 30 to 15 in short periods during heavy rainfall events, leading to pelagic fish eggs likely being exposed to low salinity during development. In a recent study, Fukuda et al. (2021) found that, after heavy rains, the salinity level was less than 28 in Hakata Bay, which is located in the city of Fukuoka on the northern end of Kyushu in Japan. In the natural environment, turbidity is usually less than 50 nephelometric turbidity units (NTU) (Boyd, 2015); however, heavy rainfall events cause high runoff to flow more directly into coastal areas, resulting in turbidity values that can be greater than 50 NTU. During heavy rains, the turbidity of outflow can exceed 130 NTU (Zhou et al., 2015) and even reach levels as high as 467 NTU (Zheng et al., 2016), but it rarely exceeds 1000 NTU (Boyd, 2015).

Seawater salinity and turbidity are 2 important ecological variables that

have individual or interactive effects on development, growth, and survival of fish at any life history stage (Bœuf and Payan, 2001; Hasenbein et al., 2013; Phan et al., 2019). In particular, drastic changes in coastal salinity and turbidity, such as those due to extreme weather events, can profoundly affect egg fertilization and incubation, yolk sac absorption, early embryogenesis, and larval survival (Berlinsky et al., 2004; Bilotta and Brazier, 2008). For example, the short-term effect of low salinity (<3) was to lower embryonic survival and egg hatching in a study of Pacific herring (*Clupea pallasii*) (Mikhailenko, 2000). Gray et al. (2012) found that short-term experimental elevation of turbidity had a significant effect on the hatching success rate of embryos of the spotted gar (*Lepisosteus oculatus*), a species that was then considered threatened and is now considered endangered in Canada (COSEWIC, 2015). Phan et al. (2019) reported that increased larval abnormality was recorded in bastard halibut (*Paralichthys olivaceus*) when embryos were exposed to high turbidity (>100 NTU) or low salinity (<30). Although prior to the study we describe herein the short-term effects of salinity and turbidity on the embryonic stage of bamboo sole were unknown, these findings indicate how the bamboo sole (*Heteromycteris japonicus*) might respond to climate change.

The bamboo sole is a small soleid flatfish distributed along southern Japan, in the Yellow Sea, and in the East China Sea (Nakabo, 2002). It is a common species found on sandy seabeds in the Seto Inland Sea of Japan (Yamamoto and Katayama, 2013). Although the bamboo sole is a noncommercial species, it plays an important ecological role in coastal areas. As reported by Jawad (2021), the early life stages of many noncommercial species are essential components of the diets of important commercial species. The spawning season for bamboo sole is from May through June, and their pelagic eggs are often caught in estuaries or bays (Yamamoto and Katayama, 2013), where salinity and turbidity fluctuate because of heavy rainfall events. Therefore, the objective of this study was to evaluate the effects of salinity and turbidity changes on various characteristics of the early stage of bamboo sole. Specifically, we examined the hatching time and hatching rate of embryos, the percentage of abnormality, size, and yolk sac volume of newly hatched larvae, and the survival rate of larvae.

Materials and methods

Collection and preparation of fertilized eggs

Embryos of bamboo sole were obtained in July 2019 from the National Research Institute of Aquaculture, which is part of the Fisheries Research Agency of Japan and located in the Mie Prefecture. The fertilized eggs were collected and transferred to the Shallow Sea Aquaculture laboratory, Mie University, in oxygen-filled plastic bags. Then, eggs were placed in a 5-L glass tank at a salinity of 34 and a temperature of 23°C, with gentle aeration. Only viable (buoyant) embryos were used for our experiments. The fertilization rate of eggs was 80.2%, and the mean diameter of eggs was 1.02 mm (standard error of the mean [SE] 0.04). For experiments, we created seawater at different levels of salinity by diluting artificial seawater powder (LIVESea Salt[1], Delphis Co. Ltd., Itami City, Japan) with distilled water and checking the salinity with a handheld refractometer (Master-S/Mill Alpha, Atago Co. Ltd, Tokyo, Japan). To achieve the desired turbidity, kaolin clay (with the chemical composition $Al_2Si_2O_5(OH)_4$ and a particle diameter of approximately 0.4 µm) was dissolved in water with a salinity of 34. Turbidity was measured by using a HACH DR/850 portable colorimeter (Hach Co., Loveland, CO).

Experimental design

The experimental conditions were set up to mimic, for a short period, the stressful conditions that organisms typically are exposed to in bays, estuaries, and coastal areas during heavy rains, and then conditions were returned to normal (Phan et al., 2020). Salinity and turbidity are the 2 major variables for water quality in coastal areas of the ocean during and shortly after heavy rainfall events (Phan et al., 2020). In this study, 3 experiments were conducted to examine the following: 1) effect of low salinity levels (6 treatments with salinities of 34 [control], 30, 26, 22, 18, and 14) on embryos of bamboo sole, 2) effect of high turbidity levels (5 treatments with turbidities of 0 [control], 100, 300, 500, and 700 NTU) on embryos of bamboo sole, and 3) combined effect of salinity and turbidity (8 treatments with combinations of salinities of 14 and 18 and turbidities of 100, 300, 500, and 700 NTU) on embryos of bamboo sole.

All experiments were conducted in 6-well plastic microplates, so that each treatment had 6 replicates. When embryos developed to the gastrula stage, 13 normal embryos were removed from the 5-L tank and randomly allocated into each of the 6 wells of a plastic microplate, with each well containing 5 mL of artificial seawater (with a salinity of 34). The embryos were exposed to single and combined salinity and turbidity levels for 3 h. Then embryos were transferred to 100-mL glass beakers with seawater at a temperature within 1°C of the target temperature of 23°C, a salinity of 34, and a turbidity of 0 NTU under a natural photoperiod (embryos were exposed to 12 h of daylight per day) in an electric incubator. Embryos remained in the beakers in the incubator until the end of the experiment. Gradual changes in salinity or in combined conditions of salinity and turbidity were achieved by using an automatic pipette and a water exchange rate of 1 mL until the desired environmental condition was reached. During the incubation period, 50% of the seawater in all treatments was exchanged daily, and dead embryos and larvae were removed by using a wide-mouthed pipette. Embryos

[1] Mention of trade names or commercial companies is for identification purposes only and does not imply endorsement by the National Marine Fisheries Service, NOAA.

were determined to be dead if morphology had collapsed (embryos appeared white or opaque) or the heartbeat had stopped. Seawater in the beakers had dissolved oxygen of 5.2–5.7 mg/L and pH of 8.0–8.5. Larvae at 3 d post-hatch were fed with live rotifers, specifically with *Brachionus plicatilis* (4 rotifers/mL). All experiments were carried out for a period of 7 d.

Measurements and calculations

Onset hatching time, hatching rate, percentage of abnormality, survival rate, total length, and yolk sac volume of embryos and larvae were recorded. Onset hatching time was determined as the total number of hours from fertilization to the time of hatch. Hatching rate was calculated on the basis of the number of hatching embryos compared to the number of stocked fertilized eggs. The larval survival rate was determined as the total number of live larvae at 5 d post-hatch. The percentage of abnormality at 24 h post-hatch was calculated by using the numbers of normal and abnormal larvae. Individuals were considered abnormal if the notochord was bent or the tail tip was deformed. Only a few abnormal larvae appeared across all treatments in the first experiment; however, all abnormal larvae died by 24 post-hatch. Therefore, the percentage of abnormality was not recorded. Shortly after hatching, 18 larvae from each treatment were randomly collected and preserved in 4% formalin solution, and total length and yolk sac volume of newly hatched larvae were measured under an inverted microscope (CKX53, Olympus Corp., Tokyo, Japan) with an ocular micrometer that had a precision of 10 µm. Yolk sac volume (in cubic millimeters) of newly hatched larvae was calculated by using this formula:

$$Yolk\ sac\ volume = \frac{\pi}{6} \times LH^2,$$

where L = the length of the yolk sac (in millimeters); and
H = the height of the yolk sac (in millimeters).

Statistical analysis

The software SPSS Statistics (vers. 22.0, IBM, Armonk, NY) was used for statistical analyses. All data are expressed as means with their SEs. Results were analyzed by using 1-way (first and second experiments) and 2-way (third experiment) analysis of variance (ANOVA). Before analysis, percentages in data were arcsine transformed. Significant treatment effects were detected by using the Tukey's honestly significant difference test, a post hoc multiple-range test. The significance level was 0.05.

Results

Effect of low salinity levels on embryos

In the first experiment, 468 embryos of bamboo sole were exposed to a control level of salinity or to 1 of 5 different salinities (78 individuals for each of 6 treatments). Embryos had great tolerance to a gradual decrease in salinity. In fact, salinity had no effect on onset hatching time (range: 39.3–39.7 h) (1-way ANOVA: $F[5, 30]=46.39$, $P>0.05$) or on hatching rate (range: 91.0–97.4%) (1-way ANOVA: $F[5, 30]=0.649$, $P>0.05$). Larval total length was positively related to salinity, ranging from 1.69 mm at a salinity of 34 to 1.61 mm at a salinity of 14. The total lengths of newly hatched larvae in the treatments with salinities of 14 and 18 were significantly smaller than those of larvae in the control treatment with a salinity of 34, but no significant differences in the total lengths of larvae were recorded between the treatments with salinities of 14 and 18 or among treatments with salinities of 22, 26, 30, and 34. Yolk sac volume ranged from 0.100 to 0.110 mm^3 across all treatments, but no significant differences were observed among treatments.

On day 5 after hatching, there were no significant differences in survival rates among all salinity treatments ($F[5, 30]=1.626$, $P>0.05$) (Table 1).

Table 1

Mean measurements of characteristics of the early stage development of bamboo sole (*Heteromycteris japonicus*) in laboratory experiments conducted at Mie University in Japan in July 2019 to examine the effect of salinity on development. Embryos were exposed to 1 of 6 levels of salinity for 3 h. After treatment, embryos were transferred to a controlled environment and monitored for 7 d. The survival rate of larvae was measured 5 d post-hatch. The different letters after values indicate that the means are significantly different ($P<0.05$) among treatments. Standard errors of the means are provided in parentheses.

Salinity treatment	Onset hatching time (h)	Hatching rate (%)	Survival rate (%)	Total length (mm)	Yolk sac volume (mm^3)
34 (control)	39.3 (0.09)[a]	97.4 (1.6)[a]	80.0 (2.6)[a]	1.69 (0.01)[a]	0.110 (0.004)[a]
30	39.3 (0.07)[a]	93.6 (3.1)[a]	78.3 (4.0)[a]	1.68 (0.01)[a]	0.100 (0.003)[a]
26	39.5 (0.08)[a]	92.3 (4.0)[a]	75.0 (2.2)[a]	1.67 (0.01)[a]	0.101 (0.004)[a]
22	39.5 (0.10)[a]	93.6 (2.4)[a]	71.7 (3.1)[a]	1.67 (0.01)[a]	0.103 (0.004)[a]
18	39.7 (0.18)[a]	91.0 (2.4)[a]	73.3 (3.3)[a]	1.62 (0.01)[b]	0.105 (0.004)[a]
14	39.5 (0.11)[a]	91.0 (3.7)[a]	70.0 (2.6)[a]	1.61 (0.01)[b]	0.103 (0.003)[a]

Effect of high turbidity levels on embryos

In the second experiment, 390 embryos of bamboo sole were exposed to a control level of turbidity or to 1 of 4 different turbidities (78 individuals for each of 5 treatments). Turbidity had a significantly positive effect on the onset hatching time of bamboo sole eggs (range: 39.3–41.8 h) (1-way ANOVA: $F[4, 25]=84.932$, $P<0.05$) (Table 2). The times to onset hatching in turbidities of 300 and 500 NTU were significantly longer than the time in the control treatment with a turbidity of 0 NTU and in the treatment with a turbidity of 100 NTU and were significantly shorter than the time in the treatment with a turbidity of 700 NTU ($P<0.05$). Hatching rate was also affected by turbidity (range: 85.9–96.2%) (1-way ANOVA: $F[4, 25]=4.667$, $P<0.05$). The lowest hatching rate was observed in the treatment with the turbidity of 700 NTU and was significantly lower than the rate recorded in the control treatment and the treatment with a turbidity of 100 NTU. However, no significant differences in hatching rate were found among treatments with the control, 100-, 300-, and 500-NTU turbidities. As for abnormality rates, the results of statistical analysis indicate that there were significant differences between the control treatment and the other treatments (with turbidities of 100, 300, 500, and 700 NTU), but there were no significant differences among those other treatments.

The total length of newly hatched larvae significantly decreased with increasing turbidity levels. The size of larvae in the treatment with a turbidity of 700 NTU was significantly lower than the size of larvae in the other treatments. No significant differences were recorded among the treatments with turbidities of 100, 300, and 500 NTU ($P>0.05$). Yolk sac volume in the treatment with 700-NTU turbidity was significantly smaller than that in the control treatment ($P>0.05$), but significant effects were not found among the control treatment and the treatments with turbidities of 100, 300, 500 NTU. At the end of the experiment, the survival rate of larvae in the treatment with a turbidity of 700 NTU was significantly different from the rate in the control treatment, but no significant differences were found in the larval survival rate between the treatments with turbidities of 500 and 700 NTU or among the control treatment and the treatments with turbidities of 100, 300, and 500 NTU.

Combined effect of salinity and turbidity on embryos

In the third experiment, 624 embryos of bamboo sole were exposed to 1 of 2 levels of salinity and to 1 of 4 levels of turbidity (78 individuals for each of 8 treatments). Although both salinity and turbidity affect the hatching of embryos of bamboo sole, turbidity had a greater effect on embryo development and larval survival rate than salinity (Tables 3 and 4). The results of 2-way ANOVA analysis indicate that turbidity had an effect on onset hatching time ($F[3, 40]=20.933$, $P<0.05$) but that the effects of salinity ($F[3, 40]=1.458$, $P>0.05$) and of interactions of salinity and turbidity ($F[3, 40]=0.972$, $P>0.05$) were not statistically significant. The same pattern was observed for hatching rates, percentages of abnormality, and survival rates. Neither salinity nor the interaction between salinity and turbidity affected hatching rate (2-way ANOVA: $F[3, 40]=0.047$, $P>0.05$), percentage of abnormality (2-way ANOVA: $F[3, 40]=0.218$, $P>0.05$), or survival rate (2-way ANOVA: $F[3, 40]=0.278$, $P>0.05$) of bamboo sole eggs and larvae. However, turbidity had a significant effect on each of these characteristics (Table 4). A similar pattern was observed for yolk sac volume of newly hatched larvae. Turbidity alone affected volume ($F[3, 136]=2.768$, $P>0.05$), but there were no significant differences in volume among treatments with different salinities ($F[3, 136]=0.062$, $P>0.05$) or among treatments with interactions of different levels of turbidity and salinity ($F[3, 136]=0.049$, $P>0.05$). Total length of newly hatched larvae in all treatments ranged from 1.53 to 1.65 mm. The results of 2-way ANOVA indicate

Table 2

Mean measurements of characteristics of the early stage development of bamboo sole (*Heteromycteris japonicus*) in laboratory experiments conducted at Mie University in Japan in July 2019 to examine the effect of turbidity on development. Embryos were exposed to 1 of 5 levels of turbidity for 3 h. After treatment, embryos were transferred to a controlled environment and monitored for 7 d. The survival rate of larvae was measured 5 d post-hatch. The different letters after values indicate that the means are significantly different ($P<0.05$) among treatments. Standard errors of the means are provided in parentheses. NTU=nephelometric turbidity units.

Turbidity treatment (NTU)	Onset hatching time (h)	Hatching rate (%)	Percentage of abnormality (%)	Survival rate (%)	Total length (mm)	Yolk sac volume (mm^3)
0 (control)	39.3 (0.10)^{a}	96.2 (1.7)^{a}	2.6 (1.6)^{a}	81.7 (1.7)^{a}	1.69 (0.01)^{a}	0.110 (0.004)^{a}
100	39.6 (0.06)^{a}	94.9 (1.6)^{a}	18.8 (3.2)^{b}	75.0 (2.2)^{ab}	1.64 (0.01)^{b}	0.094 (0.004)^{ab}
300	40.9 (0.07)^{b}	91.0 (2.4)^{ab}	19.9 (2.0)^{b}	70.0 (3.7)^{ab}	1.63 (0.01)^{bc}	0.090 (0.006)^{ab}
500	40.8 (0.16)^{b}	88.5 (1.7)^{ab}	24.6 (2.5)^{b}	65.0 (3.4)^{bc}	1.60 (0.01)^{bc}	0.090 (0.006)^{ab}
700	41.8 (0.12)^{c}	85.9 (2.4)^{b}	27.0 (3.3)^{b}	56.7 (4.2)^{c}	1.59 (0.01)^{c}	0.089 (0.004)^{b}

Table 3

Mean measurements of characteristics of the early stage development of bamboo sole (*Heteromycteris japonicus*) in laboratory experiments conducted at Mie University in Japan in July 2019 to examine the combined effect of salinity and turbidity on development. Embryos were exposed for 3 h to 1 of 8 treatments that combined 2 levels of salinity and 4 levels of turbidity. After treatment, larvae were transferred to a controlled environment and monitored for 7 d. The survival rate of larvae was measured 5 d post-hatch. Standard errors of the means are provided in parentheses. NTU=nephelometric turbidity units.

Salinity	Turbidity (NTU)	Onset hatching time (h)	Hatching rate (%)	Percentage of abnormality (%)	Survival rate (%)	Total length (mm)	Yolk sac volume (mm^3)
18	100	40.6 (0.06)	91.0 (5.0)	15.4 (2.8)	70.0 (7.7)	1.63 (0.01)	0.098 (0.004)
	300	41.2 (0.12)	82.1 (2.6)	20.5 (3.2)	58.3 (6.0)	1.64 (0.01)	0.095 (0.005)
	500	41.4 (0.07)	80.8 (4.3)	25.6 (3.2)	55.0 (4.3)	1.65 (0.01)	0.089 (0.005)
	700	41.4 (0.15)	79.5 (4.3)	26.9 (4.8)	53.3 (4.9)	1.62 (0.02)	0.089 (0.005)
14	100	40.9 (0.12)	91.0 (3.1)	19.2 (3.3)	71.2 (3.1)	1.62 (0.02)	0.099 (0.003)
	300	41.3 (0.08)	83.3 (3.7)	26.9 (3.3)	53.3 (6.7)	1.61 (0.02)	0.093 (0.004)
	500	41.4 (0.07)	82.1 (4.7)	26.9 (4.3)	46.7 (6.7)	1.54 (0.02)	0.089 (0.003)
	700	41.4 (0.05)	78.2 (3.7)	28.2 (4.3)	48.3 (4.0)	1.53 (0.02)	0.087 (0.004)

significant effects of both salinity (F[3, 136]=18.653, P<0.05) and turbidity (F[3, 136]=3.441, P<0.05) on total length, with a significant interaction between these variables (F[3, 136]=3.156, P<0.05).

Discussion

Shallow coastal areas are some of the most vulnerable systems that will be affected by climate change (Phillippart et al., 2003). Findings from numerous studies indicate that fish in their early life stages were more susceptible than adults to fluctuations in environmental conditions and that they may be particularly sensitive to climate change (Pankhurst and Munday, 2011; Sugisaki and Murakami, 2018). However, the tolerance levels of marine fish in early developmental stages to changes in environmental conditions can vary among fish species (Wang et al., 2002; Shi et al., 2009). Torres et al. (2021) reported that organisms exposed to short-term fluctuations in environmental conditions may experience irreversible damage to body structures and eventually suffer mortality at higher rates if the range of variation is wider than the range of tolerance. In our study, simulating the sudden, short-term changes in salinity that occur after a rainstorm, we found that exposure to low salinity did not affect onset hatching time and hatching rate of eggs and did not affect survival rate of larvae after hatching. These findings are similar to those of our previous study, in which embryos of Japanese seabream (*Pagrus major*) were subjected to stress from low salinity (Phan et al., 2020).

Salinity tolerance of fish embryos has been reported to have improved with advancing development; for example, cleaving embryos were more sensitive to salinity change than blastulae, and blastulae were more sensitive to change in salinity than gastrulae (Farhana et al., 2019). Ord (2019) reported that embryos in the late developmental stages have more advanced osmoregulatory capacities. In the natural environment, coastal fish species are considered to be euryhaline. Therefore, their embryos can tolerate a wide range of salinities, as has been found for the European seabass (*Dicentrarchus labrax*) (Conides and Glamuzina, 2001), black sea bass (*Centropristis striata*) (Berlinsky et al., 2004), bastard halibut (Phan et al., 2019; Manuel et al., 2021), and Japanese seabream (Phan et al., 2020).

In our laboratory experiments with bamboo sole, short-term exposure to stress from turbidity significantly prolonged onset hatching time and decreased hatching rate of embryos and decreased survival rate of larvae after hatching. In nature, increased turbidity tends to coincide with decreases in dissolved oxygen, which could lead to lack of oxygen during development in individuals of many fish species (Mueller et al., 2017). In addition, turbidity impedes oxygen supply and the normal growth activity of embryos as kaolin clay coats egg membranes (Phan et al., 2020). Del Rio et al. (2019) revealed that oxygen significantly influenced the hatching process in fish embryos, in which low levels of oxygen led to delays in embryonic development and in the time of hatching as well as to a decrease in hatching success rate. Results of our study indicate that the percentage of larval bamboo sole that had abnormalities was higher when embryos were exposed to turbidity levels of 100–700 NTU than when embryos were exposed to no turbidity. The morphological abnormalities most commonly found in our study were notochord bending and tail-tip deformity. An increase in the proportion of larvae that were abnormal because of exposure to high turbidity has also been reported for other fish species, including the Pacific herring (Griffin et al., 2009), bastard halibut (Phan et al., 2019), climbing perch (*Anabas testudineus*) (Nurulnadia et al., 2020), and Japanese seabream (Phan et al., 2020). According to Cahu et al. (2003), such abnormalities are often associated with growth depression and

Table 4

Results from the 2-way analysis of variance in measurements of early stage development of bamboo sole (*Heteromycteris japonicus*) from laboratory experiments conducted at Mie University in Japan in July 2019 to examine the individual and combined effects of salinity (S) and turbidity (T) on development. Embryos were exposed to treatments with different levels of salinity and turbidity for 3 h and then monitored for 7 d. An asterisk (*) indicates that the means are significantly different ($P<0.05$) among treatments for that factor (or source of variability).

Variability source	df	Mean squares	*F*	*P*
Onset hatching time				
S	1	0.083	1.458	0.234
T	3	1.197	20.933	0.000*
S × T	3	0.056	0.972	0.416
Error	40	0.057		
Total	48			
Corrected total	47			
Hatching rate				
S	1	1.233	0.013	0.910
T	3	333.251	3.475	0.025*
S × T	3	4.520	0.047	0.986
Error	40	95.907		
Total	48			
Corrected total	47			
Percentage of abnormality				
S	1	123.274	1.488	0.230
T	3	249.836	3.016	0.041*
S × T	3	18.080	0.218	0.883
Error	40	82.840		
Total	48			
Corrected total	47			
Total length				
S	1	0.082	18.653	0.000*
T	3	0.015	3.441	0.019*
S × T	3	0.014	3.156	0.027*
Error	136	0.004		
Total	144			
Yolk sac volume				
S	1	2.025×10^{-5}	0.062	0.803
T	3	0.001	2.768	0.044*
S × T	3	1.582×10^{-5}	0.049	0.986
Error	136			
Total	144			
Survival rate				
S	1	208.333	1.096	0.301
T	3	1075.000	5.658	0.003*
S × T	3	52.778	0.278	0.841
Error	40	190.000		
Total	48			
Corrected total	47			

high mortality rates of late larvae and early juveniles due to impairments in prey capture and swimming behaviors.

Yolk sac volume plays an important role during the endogenous feeding period that serves as the major source of energy for larvae, providing protein, free amino acids, lipids, and carbohydrates for maintenance, differentiation, growth, and other activities (Subhan et al., 2020). The results of our study indicate a significant downward trend in yok sac volume of newly hatched larvae as turbidity increased, but no significant differences in volume were observed among salinity treatments or among treatments with different interactions between salinity and turbidity. Increased turbidity during the early developmental stages of embryos could decrease yolk sac volume, resulting in starvation of larvae before the mouth is fully formed for feeding and a high risk of mortality. Kamler (2008)

suggested that endogenous factors like yolk sac volume are one of the major causes of early mortality in fish. In addition, Subhan et al. (2020) reported that yolk sac volume is a main factor in determining the quality of larvae in the postlarval stage that is critical to adaptation in the natural environment.

Total length of newly hatched larvae is the only characteristic for which individual and combined effects of salinity and turbidity were found. Although stored energy is usually used for growth and organ maturation in normal conditions, under stressful conditions, such energy is reallocated to cope with stress instead of being used for development (Pérez-Robles et al., 2016). In our study, total length of newly hatched larvae decreased when embryos were exposed to combinations of low salinity and high turbidity, indicating that embryos in non-optimal salinities may be unable to maintain their osmoregulatory capacity because of decreasing availability of metabolic energy, thereby decreasing growth in development. Fish larvae with small sizes (<2.57 mm total length) at hatching have a lower chance of survival than larger larvae because they have fewer energy reserves, less feeding ability, and a slower, weaker response to predators (Garrido et al., 2015). Furthermore, larvae that are smaller than other larvae at hatching cannot grow and survive because of a lower metabolic rate and higher cost of development.

Conclusions

Results from analysis of all characteristics of embryos and larvae measured in this study indicate that, although embryos of bamboo sole are quite tolerant and are able to withstand conditions of low salinity, they are sensitive to stress from high turbidity. As the frequency of heavy rainfall events continues to increase, reductions in the hatching rate of embryos and the size and survival rate of larvae of bamboo sole could lead to detrimental effects at the population level.

Resumen

Las lluvias intensas pueden disminuir la salinidad y aumentar la turbidez del agua en las zonas costeras, lo que afecta negativamente al desarrollo de los organismos, especialmente durante sus primeras etapas de vida. En este estudio, se evaluaron los efectos de la salinidad y la turbidez en los embriones del lenguado bambú (*Heteromycteris japonicus*) para comprender mejor su tolerancia al cambio climático global. Se realizaron tres experimentos durante un periodo de 7 d. En el primer experimento, los embriones de lenguado bambú se expusieron durante 3 h a 1 de los 6 niveles de salinidad (14–34). Las longitudes totales de las larvas recién eclosionadas a niveles de salinidad bajos (14 y 18) fueron más pequeñas respecto al tamaño de las larvas en los tratamientos con mayores salinidades, aunque no se observaron diferencias significativas en las tasas de eclosión y de supervivencia de las larvas entre los tratamientos. En el segundo experimento, los embriones se expusieron a turbideces de 0, 100, 300, 500 y 700 unidades nefelométricas de turbidez durante 3 h. La turbidez disminuyó significativamente la tasa de eclosión, la tasa de supervivencia y la longitud total, y aumentó el tiempo de eclosión y el porcentaje de anormalidad. En el tercer experimento, los embriones se expusieron a diferentes combinaciones de salinidad y turbidez. El efecto de interacción de la salinidad y la turbidez sobre la longitud total de las larvas recién eclosionadas fue significativo. Estos resultados indican que el desarrollo embrionario del lenguado bambú se vio más afectado por los cambios de turbidez que por los de salinidad.

Acknowledgments

We would like to express our appreciation to all members of the Shallow Sea Aquaculture laboratory of Mie University for their kind assistance. We acknowledge the National Research Institute of Aquaculture in Mie, Japan, and its staff for providing the fertilized eggs of bamboo sole needed to carry out this study.

Literature cited

Allen, J. D., and J. A. Pechenik.
2010. Understanding the effects of low salinity on fertilization success and early development in the sand dollar *Echinarachnius parma*. Biol. Bull. 218:189–199.

Barange, M., G. Merino, J. L. Blanchard, J. Scholtens, J. Harle, E. H. Allison, J. I. Allen, J. Holt, and S. Jennings.
2014. Impacts of climate change on marine ecosystem production in societies dependent on fisheries. Nat. Clim. Change 4:211–216.

Baudron, A. R., C. L. Needle, A. D. Rijnsdorp, and C. T. Marshall.
2014. Warming temperatures and smaller body sizes: synchronous changes in growth of North Sea fishes. Glob. Change Biol. 20:1023–1031.

Berlinsky, D. L., J. C. Taylor, R. A. Howell, T. M. Bradley, and T. I. J. Smith.
2004. The effects of temperature and salinity on early life stages of black sea bass *Centropristis striata*. J. World Aquac. Soc. 35:335–344.

Bilotta, G. S., and R. E. Brazier.
2008. Understanding the influence of suspended solids on water quality and aquatic biota. Water Res. 42:2849–2861.

Bœuf, G., and P. Payan.
2001. How should salinity influence fish growth? Comp. Biochem. Physiol. C 130:411–423.

Boyd, C. E.
2015. Water quality: an introduction, 2nd ed., 357 p. Springer Int. Publ., Cham, Switzerland.

Brander, K.
2010. Impacts of climate change on fisheries. J. Mar. Syst. 79:389–402.

Cahu, C., J. Z. Infante, and T. Takeuchi.
2003. Nutritional components affecting skeletal development in fish larvae. Aquaculture 227:245–258.

Cheung, W. W. L., and M. A. Oyinlola.
2018. Vulnerability of flatfish and their fisheries to climate change. J. Sea Res. 140:1–10.

Conides, A. J., and B. Glamuzina.
2001. Study on the effects of rearing density, temperature and salinity on hatching performance of the European sea bass, *Dicentrarchus labrax* (Linnaeus, 1758). Aquac. Int. 9:217–224.

COSEWIC (Committee on the Status of Endangered Wildlife in Canada).
2015. COSEWIC assessment and status report on the Spotted Gar *Lepisosteus oculatus* in Canada, 32 p. COSEWIC, Ottawa, Canada. [Available from website.]

Del Rio, A. M., B. E. Davis, N. A. Fangue, and A. E. Todgham.
2019. Combined effects of warming and hypoxia on early life stage Chinook salmon physiology and development. Conserv. Physiol. 7:coy078.

Farhana, T., F. Haque, F. B. Amin, M. M. Zahangir, and M. S. Islam.
2019. Developmental pliability in zebrafish: an experimental enquiry of acute salinity stress on the early life of zebrafish. Aquac. Rep. 14:100189.

Fukuda, A., T. Tabata, K. Hiramatsu, and M. Harada.
2021. Analysis of salinity behavior in Hakata Bay after heavy rainfall using a three-dimensional σ-coordinate model. Jpn. Agric. Res. Q. 55:137–146.

Garrido, S., R. Ben-Hamadou, A. M. P. Santos, S. Ferreira, M. A. Teodósio, U. Cotano, X. Irigoien, M. A. Peck, E. Saiz, and P. Ré.
2015. Born small, die young: intrinsic, size-selective mortality in marine larval fish. Sci. Rep. 5:17065.

Gibson, R. N., R. D. M. Nash, A. J. Geffen, and H. W. van der Veer (eds.).
2015. Flatfishes: biology and exploitation, 2nd ed., 576 p. John Wiley and Sons, West Sussex, UK.

Gray, S. M., L. J. Chapman, and N. E. Mandrak.
2012. Turbidity reduces hatching success in threatened spotted gar (*Lepisosteus oculatus*). Environ. Biol. Fishes 94:689–694.

Griffin, F. J., E. H. Smith, C. A. Vines, and G. N. Cherr.
2009. Impacts of suspended sediments on fertilization, embryonic development, and early larval life stages of the Pacific herring, *Clupea pallasi*. Biol. Bull. 216:175–187.

Hasenbein, M., L. M. Komoroske, R. E. Connon, J. Geist, and N. A. Fangue.
2013. Turbidity and salinity affect feeding performance and physiological stress in the endangered delta smelt. Integr. Comp. Biol. 53:620–634.

Holsman, K. K., T. Essington, T. J. Miller, M. Koen-Alonso, and W. J. Stockhausen.
2012. Comparative analysis of cod and herring production dynamics across 13 northern hemisphere marine ecosystems. Mar. Ecol. Prog. Ser. 459:231–246.

Jawad, L. A.
2021. The importance of non-commercial and small-sized fish species: a proposal for an additional revenue to Iraq. *In* Tigris and Euphrates rivers: their environment from headwaters to mouth (L. A. Jawad, ed.), p. 1611–1623. Springer, Cham, Switzerland.

Kamler, E.
2008. Resource allocation in yolk-feeding fish. Rev. Fish Biol. Fish. 18:143–200.

Lehodey, P., J. Alheit, M. Barange, T. Baumgartner, G. Beaugrand, K. Drinkwater, J.-M. Fronmentin, S. R. Hare, G. Ottersen, R. I. Perry, et al.
2006. Climate variability, fish, and fisheries. J. Clim. 19:5009–5030.

Manuel, A. V., T. C. T. Phan, S. Yamamoto, N. Tsutsui, and T. Yoshimatsu.
2021. Effect of simulated sudden thunderstorm flood on the early stage development of Japanese flounder *Paralichthys olivaceus*. Aquac. Res. 52:6464–6471.

Mikhailenko, V. G.
2000. Salinity-stress-induced changes in the resistance of embryos of the White Sea herring *Clupea pallasi marisalbi* to freshwater. Russ. J. Mar. Biol. 26:370–372.

Mueller, J. S., T. B. Grabowski, S. K. Brewer, and T. A. Worthington.
2017. Effects of temperature, total dissolved solids, and total suspended solids on survival and development rate of larval Arkansas River shiner. J. Fish Wildl. Manag. 8:79–88.

Nakabo, T.
2002. Soleidae. *In* Fishes of Japan with pictorial keys to the species, English ed. (T. Nakabo, ed.), p. 1383–1387. Tokai Univ., Tokyo, Japan.

Nurulnadia, M. Y., A. B. Noradila, and G. Adiana.
2020. Turbidity effects of suspended bauxite in embryonic stage of climbing perch (*Anabas testudineus*) post fertilization. Egypt. J. Aquat. Res. 46:181–186.

Ord, J.
2019. Ionic stress prompts premature hatching of zebrafish (*Danio rerio*) embryos. Fishes 4:20.

Pankhurst, N. W., and P. L. Munday.
2011. Effects of climate change on fish reproduction and early life history stages. Mar. Freshw. Res. 62:1015–1026.

Pérez-Robles, J., F. Diaz, L. Ibarra-Castro, I. Giffard-Mena, A. D. Re, L. E. R. Ibarra, and J. A. I. Soto.
2016. Effects of salinity on osmoregulation during the embryonic development of the bullseye puffer (*Sphoeroides annulatus* Jenyns 1842). Aquac. Res. 47:838–846.

Phan, T. C. T., A. V. Manuel, N. Tsutsui, and T. Yoshimatsu.
2019. Impact of short-term salinity and turbidity stress on the early developmental stages of Japanese flounder, *Paralichthys olivaceus* (Temminck and Schlegel, 1846). Asian Fish. Sci. 32:93–103.

Phan, T. C. T., A. V. Manuel, N. Tsutsui, and T. Yoshimatsu.
2020. Impacts of short-term salinity and turbidity stress on the embryonic stage of red sea bream *Pagrus major*. Fish. Sci. 86:119–125.

Phillippart, C. J. M., H. M. van Aken, J. J. Beukema, O. G. Bos, G. C. Cadée, and R. Dekker.
2003. Climate-related changes in recruitment of the bivalve *Macoma balthica*. Limnol. Oceanogr. 48:2171–2185.

Poloczanska, E. S., C. J. Limpus, and G. C. Hays.
2009. Vulnerability of marine turtles to climate change. Adv. Mar. Biol. 56:151–211.

Shi, Z.-H., S.-M. Peng, Y.-Q. Yin, H.-Z. Luo, and M.-L. Ni.
2009. Morphological changes of embryo and yolk sac larvae of barred knifejaw (*Oplegnathus fascltus*) under salinity stress. Chin. J. Ecol. 28:471–476.

Subhan, U., Iskandar, Zahidah, and I. M. Joni.
2020. Efficiency yolk sac utilization of endogenous feeding larvae striped catfish (*Pangasianodon hypophthalmus*) in the environmentally rich fine bubbles (FBs). AIP Conf. Proc. 2219:090003.

Sugisaki, H., and K. Murakami.
2018. Impacts of climate change on the marine resources of Japan. *In* Climate change impacts on fisheries and aquaculture: a global analysis, vol. 1 (B. F. Phillips and M. Pérez-Ramírez, eds.), p. 121–128. John Wiley and Sons, Hoboken, NJ.

Thrush, S. F., J. E. Hewitt, V. J. Cummings, J. I. Ellis, C. Hatton, A. Lohrer, and A. Norkko.
2004. Muddy waters: elevating sediment input to coastal and estuarine habitats. Front. Ecol. Environ. 2:299–306.

Torres, G., K. Anger, and L. Giménez.
2021. Effects of short-term and continuous exposure to reduced salinities on the biochemical composition of larval lobster, *Homarus gammarus*. Zoology 144:125885.

Wang, H.-S., Q.-S. Fang, and L.-Y. Zheng.
2002. Effects of salinity on hatching rates and survival activity index of the larvae of *Epinephelus akaara*. J. Fish. China 26:344–350.

Yamamoto, M., and S. Katayama.
2013. Age, growth, and spawning period of bamboo sole *Heteromycteris japonica* in the Seto Inland Sea, Japan. Aquac. Sci. 61:359–365.

Zheng, L., Z. Qui, Y. Zhou, D. Sun, S. Wang, W. Wu, and W. Perrie.
2016. Comparisons of algorithms to estimate water turbidity in the coastal areas of China. Int. J. Remote Sens. 37:6165–6186.

Zhou, Z.-Z., T.-L. Huang, W.-X. Ma, Y. Li, and K. Zeng.
2015. Impacts of water quality variation and rainfall runoff on Jinpen Reservoir, in Northwest China. Water Sci. Eng. 8:301–308.

Acknowledgment of reviewers

The editorial staff of *Fishery Bulletin* would like to acknowledge the scientists who reviewed manuscripts in 2021–2022. Their contributions have helped ensure the publication of quality science.

Robert Ahrens
Scott Alford

Elizabeth Babcock
Henry Bart Jr.
Katherine Bemis
Lee Benaka
Florian Berg
Corinthia Black
Jesper Boje
Randy Brown

Matthew Campbell
Nick Caputi
J. Leonardo Castillo-Géniz
Brandon Chasco
Michael Courtney
Wendell Cropper

Evan D'Alessandro
Simon de Lestang
Lukas DeFilippo
Côme Denechaud
William Driggers III
Claude Dykstra

Jessica Farley
Jayde Ferguson
Lowell Fritz
Rainer Froese
Richard Fulford

Audrey Geffen
Jason Goldstein
Gretchen Grammer
Shane Griffiths
Jongkar Grinang
Benjamin Gutzler

Eric Hoffmayer
Edward Houde

James Ianelli
David Itano

George Jackson
Mattias Johansson
Matthew Johnson
Simon Jones

David Kerstetter
Jeff Kneebone

Tom Laidig
Richard Langton
Kari Lavalli
Cleridy Lennert-Cody

J. Fernando Márquez-Farías
Mary Elizabeth Matta
Richard McBride
Loren McClenachan
Richard Merrick

Richard Methot
Michael Murphy

Lisa Natanson

Krista Oke

Michelle Passerotti
Andrew Pershing
Mark Peterson
John Piatt
Gregg Poulakis
André Punt

Joseph Quattro

Paul Rudershausen
Brendan Runde

Joseph Serafy
Carrie Simmons
Christoph Stransky

Eric Taylor
James Tolan

John Waldman
John Walter III
Phoebe Woodworth-Jefcoat

Fishery Bulletin

Guidelines for authors

Contributions published in *Fishery Bulletin* describe original research in marine fishery science, fishery engineering and economics, and marine environmental and ecological sciences (including modeling). Preference will be given to manuscripts that examine processes and underlying patterns. Descriptive reports, surveys, and observational papers may occasionally be published but should appeal to an audience outside the locale in which the study was conducted.

Although all contributions are subject to peer review, responsibility for the contents of papers rests upon the authors and not on the editor or publisher. *Submission of an article implies that the article is original and is not being considered for publication elsewhere.*

All submissions are subject to a double-blind review to remove the identity of author and reviewer during the review process.

Plagiarism and double publication are considered serious breaches of publication ethics. To verify the originality of the research in papers and to identify possible previous publication, manuscripts may be screened with plagiarism-detection software.

Manuscripts must be written in English; authors whose native language is not English are strongly advised to have their manuscripts checked by English-speaking colleagues before submission.

Once a paper has been accepted for publication, online publication takes approximately 2 weeks.

There is no cost for publication in *Fishery Bulletin*.

Types of manuscripts accepted by the journal

Articles generally range from 20 to 30 double-spaced typed pages (12-point font) and describe an original contribution to fisheries science, engineering, or economics. Tables and figures are not included in this page count, but the number of figures should not exceed 1 figure for every 4 pages of text. Articles contain the following divisions: abstract, introduction, methods, results, discussion, and conclusions.

Notes are generally less than 10 double-spaced typed pages (12-point font), including the Literature cited section. Like articles, notes describe an original contribution to fisheries science. They follow a format similar to that for articles: abstract, introduction, methods, results, and discussion, but the results and discussion sections may be combined and a conclusions section should not be included. They should include no more than 2 figures or tables (2 of each would be too many). They are distinguished from full articles in that they report a noteworthy new observation or discovery—such as the first report of a new species, a unique finding, condition, or event that expands our knowledge of fisheries science, engineering, or economics—and do not require a lengthy discussion. Manuscripts on range extensions will not be considered.

Companion articles should be submitted together and are published together as a scientific contribution. Both articles should address a closely related topic and may be articles that result from a workshop or conference.

Review articles of exceptional quality may be considered occasionally for publication on a case-by-case basis. They address a timely topic that is relevant to aspects of fisheries science. They should include an abstract, but the format of the article, per se, will be up to the author. Please contact the scientific editor to discuss your ideas regarding a potential review article before embarking on such a project.

Perspective essays generally are less than 5 double-spaced typed pages (12-point font) and provide clarification of misused terms or misunderstood topics in fisheries science. Essays are accepted at the discretion of the scientific editor. Opinion pieces on policy will not be considered. They should include an abstract and a list of the literature cited, but no other sections should divide the article. Please contact the scientific editor to discuss your idea before making a submission.

Preparation of manuscript

Title page should include authors' full names, affiliations, mailing addresses, and the senior author's email address.

Abstract should be limited to 200 words (one-half typed page), state the main scope of the research, and emphasize the authors' conclusions and relevant findings. Do not review the methods of the study or list the contents of the paper. Because abstracts are circulated by abstracting agencies, it is important that they represent the research clearly and concisely.

General text must be typed in 12-point Times New Roman font throughout. A brief introduction should convey the broad significance of the paper; the remainder of the paper should be divided into the following sections: Materials and methods, Results, Discussion, Conclusions, and Acknowledgments. Headings within each section must be short, reflect a logical sequence, and follow the rules of subdivision (i.e., there can be no subdivision without at least 2 subheadings). The entire text should be intelligible to interdisciplinary readers; therefore, all acronyms, abbreviations, and technical terms should be written out in full and defined the first time they are mentioned. Abbreviations should be used sparingly because they are not carried over to indexing databases and slow readability for those readers

outside a discipline. They should never be used for the main subject (e.g., species or method) of a paper.

For general style, follow the U.S. Government Publishing Office *Style Manual* (2016, available at website) and *Scientific Style and Format: the CSE Manual for Authors, Editors, and Publishers* (2014, 8th ed.) published by the Council of Science Editors. For scientific nomenclature, use the current edition of the American Fisheries Society's (AFS) *Common and Scientific Names of Fishes from the United States, Canada, and Mexico* and its companion volumes (*Crustaceans, Mollusks, Cnidaria and Ctenophora*, and *World Fishes Important to North Americans*). For species not found in the previously mentioned AFS publications and for more recent changes in nomenclature, use the Integrated Taxonomic Information System (ITIS, available at website), or, secondarily, the California Academy of Sciences *Catalog of Fishes* (available at website) for species names not included in ITIS. Common (vernacular) names of species should be lowercase. Citations must be given for the identification of specimens. For example, "Fish species were identified according to Collette and Klein-MacPhee (2002); sponges were identified according to Stone et al. (2011)."

Dates should be written as follows: 11 November 2018. Measurements should be expressed in metric units, for example, "58 metric tons (t);" if other units of measurement are used, please make this fact explicit to the reader. Use numerals, not words, to express whole and decimal numbers in the general text, tables, and figure captions (except at the beginning of a sentence). For example, "We considered 3 hypotheses. We collected 7 samples in this location." Use American spelling. Refrain from using the shorthand slash (/), an ambiguous symbol, in the general text.

Cite all software, special equipment, and chemical solutions used in the study within parentheses in the general text, including the version number, company name, and the city and state (or nation) of the company headquarters, for example, "SAS, vers. 9.4 (SAS Institute Inc., Cary, NC)."

Word usage and grammar that may be useful are the following:

- *Aging*
  For our journal, the word *aging* is used to mean both age determination and the aging process (senescence). Authors should make clear which meaning is intended where ambiguity may arise.

- *Fish and fishes*
  The plural of the word fish (a collective noun that implies individuals without regard to species) is *fish*.
  Example: The *fish* were collected by trawl net.
  Example: The numbers of *fish* collected that season were less than the numbers from previous years.

  The plural for *fish species* is *fishes* (a contrived plural used by taxonomists to mean several or more *fish species*) or one can use *fish species* (which is preferred in this journal for clarity across disciplines).
  Example: The *fishes* of Puget Sound [biodiversity is implied] or
  Example: The *fish species* of Puget Sound [preferred plural for clarity across disciplines].

- *Crab and crabs, squid and squids, etc.*
  The plural of the word *crab* (i.e., many individuals without regard to species) is *crab*.
  Example: The crab were sorted by weight.
  Example: Many red king *crab* were dying [Many individuals of one species of crab.]

  The plural of *crab species* is *crabs* (a word used by taxonomists) or *crab species* (the latter is preferred in this journal for clarity).
  Example: These *crabs* were selected for treatment. [Different crab species are implied.]
  Example: These *crab species* were selected for treatment. [Preferred word choice for clarity.]
  Example: Snow *crabs* are found throughout the North Pacific Ocean and Bering Sea. [There are 2 species of snow crab; therefore the word *crabs* can be used here.]
  Example: *Two species* of snow *crab* are found throughout the North Pacific Ocean and Bering Sea. [Preferred usage for clarity.]
  Example: Three crabs were selected for treatment. [3 species of crab are implied.]
  Example: Three crab species were selected for treatment. [Preferred word choice for clarity.]

- We use *fisherman* and *fishermen*, not *fisher* and *fishers*, in this journal. One can always use crew member, vessel operator, and angler (the latter for recreational fishing).

- *The definite article with common names of species*
  When the singular common name of a species represents the entire class or group to which it belongs, use the definite article.
  Example: Only one species of the genus *Salmo* is found in the Atlantic Ocean—*the* Atlantic salmon (*Salmo salar*).
  Example: The sonic emissions of *the* bottlenose dolphin are complex.

  For plural common names, this rule does not apply.
  Example: Chinook salmon are found throughout the Pacific Ocean.
  Example: Bottlenose dolphins are found in temperate and tropical waters.

- *Sex*
  For the meaning of male and female, use the word *sex*, not *gender*. Do not write, "fish were sexed." Write, "sex was determined."

- *Participles*
  As adjectives, participles must modify a specific noun or pronoun.
  Example: Using mark-recapture methods, these scientists determined the size of the population. [Correct. The participle *using* modifies the word *scientists*.]

Example: These scientists, based on the collected data, concluded that the mortality rate of these fish had increased. [Incorrect. The scientists were not based on the collected data.]

Example: These scientists concluded, on the basis of collected data, that the mortality rate of these fish had increased. [Correct. The offending participle has been eliminated and an adverbial phrase modifies the verb *concluded*.]

Equations and mathematical symbols should be set from a standard mathematical program (MathType or Equation Editor). Equations formatted in LaTex are not acceptable. For mathematical symbols in the general text (α, χ^2, π, $\pm$, etc.), use the symbols provided by the MS Word program and italicize all variables, except those variables represented by Greek letters and the superscript and subscript parts of variables and expressions. Do not use photo mode when creating these symbols in the general text, and do not cut and paste equations, letters, or symbols from a different software program.

Number equations (if there are more than one) for future reference by scientists; place the number within parentheses at the end of the first line of the equation.

Literature cited section comprises published works and those accepted for publication (in press) in peer-reviewed journals. Follow the name and year system for citation format in this section (i.e., citations should be listed alphabetically by the authors' last names, and then by year if there is more than one citation by the same author. A list of abbreviations for citing journal titles can be found on our website.

Authors are responsible for the accuracy and completeness of all citations. Avoid the use of multiple citations when a single citation sufficiently supports a statement; cite the work that first reported the information that supports a statement, not all of the subsequent works. Literature citation format: Authors (last name, followed by initials for first name and, if given, middle name of first author; then list names of additional authors with initials before last names). Year. Title of article. Abbreviated title of the journal in which it was published. Always include either the range of page numbers (for a journal article) or a total number of pages (for a book or other type of publication). List a sequence of citations in the general text chronologically, for example, "(Smith, 1932; Green, 1998; Smith and Jones, 2015)."

Acknowledgments should be no more than 6 lines of text. Only those who have contributed in an outstanding way should be acknowledged by name. For recognition of other persons or groups, use a general term, such as *crew*, *observers*, or *research coordinators*, and do not include names with these terms.

Digital object identifier (doi) code ensures that a publication has a permanent location online. A doi link (which may include a doi code) should be included at the end of citations of published literature. Authors are responsible for submitting accurate doi links. Faulty links will be deleted at the page-proof stage.

Footnotes are used for all documents that have not been formally peer reviewed and for observations and personal communications, but these types of references should be cited sparingly in manuscripts submitted to the journal.

All reference documents, administrative reports, internal reports, progress reports, project reports, contract reports, personal observations, personal communications, unpublished data, manuscripts in review, and council meeting notes are footnoted in 10-point font and placed at the bottom of the page on which they are first cited. Footnote format is the same as that for formal literature citations. A link to the online source (e.g., [Available from http://www..., accessed July 2017.]), or the mailing address of the agency or department holding the document, should be provided so that readers may obtain a copy of the document.

Tables are often overused in scientific papers; it is seldom necessary to present all the data associated with a study. Tables should not be excessive in size and must be cited in numerical order in the text. Headings should be short but ample enough to allow the table to be intelligible on its own.

All abbreviations and unusual symbols must be explained in the table legend. Other incidental comments may be footnoted with numeral footnote markers. Use asterisks only to indicate significance in statistical data. Do not put a table legend on a page separate from the table; place the legend above the table. *Do not submit tables in photo mode.*

- Note probability with a capital, italic *P*.
- Provide a zero before all decimal points for values less than one (e.g., 0.07).
- Round all values to 2 decimal points.
- Use a comma in numbers of 5 digits or more (e.g., 13,000 but 3000).

Figures must be cited in numerical order in the text. Graphics should aid in the comprehension of the text, but they should be limited to presenting patterns rather than raw data. The number of figures should not exceed 1 figure for every 4 pages of text.

Figure legends should explain all symbols and abbreviations seen in the figure and should be double spaced on a separate page at the end of the manuscript.

Line art and halftone figures should be saved at resolutions >600 dots per inch (dpi) and >300 dpi, respectively. Color is allowed in figures to show morphological differences among species (for species identification), to show stain reactions, to show gradations (such as those of temperature and salinity within maps), and to distinguish

between numerous lines and symbols in graphs. Figures approved for color should be saved in CMYK format.

All figures must be submitted as PDF, TIFF, or EPS files.

- Capitalize only the first letter of the first word and proper nouns in all labels within figures.
- Do not use overly large font sizes for labels in maps and for axis labels in graphs.
- Use the same point size for all labels, except for panel labels (e.g., **A**), which should be slightly larger than other labels (e.g., 11 point versus 8 point).
- Use a sans serif font for all labels. Panel labels (e.g., **A**), however, should be in Times New Roman font.
- Do not use bold fonts or bold lines in figures. Do not use italic fonts. Exceptions include use of italic fonts for labels of bodies of water in maps and a bold font for panel labels (e.g., **A**).
- Do not place outline rules around graphs.
- Do not include vertical and horizontal lines in the background of graphs. Ticks for values on the x-axis and y-axis will suffice.
- Place a north arrow and label degrees latitude and longitude (e.g., 170°E) in all maps. If scale of map requires more than degrees, use degrees minutes, not decimal degrees.
- Place panel labels (e.g., **A**, **B**, **C**) within the upper-left area of each graph or photo in a multi-panel figure, from left to right, then top to bottom. If the letter is not visible against a dark background, put a white box behind it. Do not use white labels.
- Avoid placing labels vertically or diagonally. Y-axis labels can be vertical. Words in horizontal labels can be stacked vertically to fit.
- Use symbols, shading, or patterns (not clip art) in maps and graphs.
- For scale bars in maps, use kilometers. Use the label *km* or *kilometers* (lowercased).

Supplementary materials that are considered essential, but are too large or impractical for inclusion in a paper (e.g., metadata, figures, tables, videos, and websites), may be provided at the end of an article. These materials are subject to the editorial standards of the journal. A URL to the supplementary material and a brief explanation for including such material should be sent at the time of initial submission of the paper to the journal.

- **Metadata, figures, and tables** should be submitted in standard digital format (MS Word or PDF file) and should be cited in the general text, for example, as ". . . was determined (Suppl. Table 3, Suppl. Fig. 1)."
- **Websites** should be cited with a URL in the general text.
- **Videos** must not be larger than 30 MB to allow a swift technical response for viewing the video. Authors should consider whether a short video uniquely captures what text alone cannot capture for the understanding of a process or behavior under examination in the article. Supply an online link to the location of the video.

Copyright law does not apply to *Fishery Bulletin*, which falls within the public domain. However, if an author reproduces any part of an article from *Fishery Bulletin*, reference to source is considered correct form (e.g., Source: Fish. Bull. 117:105).

Failure to follow these guidelines and failure to correspond with editors in a timely manner will delay publication of a manuscript.

Submission of manuscript

Submit a manuscript online at the ScholarOne Manuscripts website for *Fishery Bulletin*. Commerce Department authors must provide proof of internal clearance of their manuscripts with either a completed and signed NOAA Form 25-700 or a copy of the clearance email from the Research Publication Tracking System. For further details on electronic submission, please contact the associate editor, Cara Mayo, at

cara.mayo@noaa.gov.

When requested, the text and tables should be submitted in MS Word format. Each figure should be sent as a separate PDF, TIFF, or EPS file. Send a copy of a figure in the original software if conversion to any of these formats yields a degraded version of the figure.

Questions? If you have questions regarding these guidelines, please contact the managing editor, Kathryn Dennis, at

kathryn.dennis@noaa.gov.

Questions regarding manuscripts under review should be addressed to Associate Editor Cara Mayo.

Fishery Bulletin

Subscription form

Superintendent of Documents **Publications** Order Form

*5178

☐ YES, please send me the following publications:

____ Subscriptions to *Fishery Bulletin*
for $32.00 per year ($44.80 foreign)

The total cost of my order is $ _____ . Prices include regular domestic postage and handling and are subject to change.

_____
(Company or Personal Name) (Please type or print)

_____
(Additional address/attention line)

_____
(Street address)

_____
(City, State, ZIP Code)

_____
(Daytime phone including area code)

_____
(Purchase Order No.)

Charge your order. IT'S EASY!

VISA

MasterCard

Please Choose Method of Payment:

☐ Check payable to the Superintendent of Documents
☐ GPO Deposit Account ☐☐☐☐☐☐☐–☐
☐ VISA or MasterCard Account
☐☐☐☐☐☐☐☐☐☐☐☐☐☐☐☐
☐☐☐☐ (Credit card expiration date)

To fax your orders (202) 512-2104

_____
(Authorizing Signature)

Mail to: Superintendent of Documents
P.O. Box 979050, St. Louis, Missouri 63197
Tel. no. (U.S. callers): 866-512-1800
Tel. no. (International callers): 1-202-512-1800

Thank you for your order!

Also available online at
https://bookstore.gpo.gov/products/fishery-bulletin
email: ContactCenter@gpo.gov